Electronic Thesis and Dissertation Repository

8-31-2018 10:00 AM

The Periglacial Landscape of Mars: Insight into the 'Decameter-scale Rimmed Depressions' in Utopia Planitia

Arya Bina
The University of Western Ontario

Supervisor
Osinski, Gordon R
The University of Western Ontario

Graduate Program in Geology
A thesis submitted in partial fulfillment of the requirements for the degree in Master of Science
© Arya Bina 2018

Recommended Citation

Abstract

Currently, Mars appears to be in a 'frozen' and 'dry' state, with the clear majority of the planet's surface maintaining year-round sub-zero temperatures. However, the discovery of features consistent with landforms found in periglacial environments on Earth, suggests a climate history for Mars that may have involved freeze and thaw cycles. Such landforms include hummocky, polygonised, scalloped, and pitted terrains, as well as ice-rich deposits and gullies, along the mid- to high-latitude bands, typically with no lower than 20° N/S. The detection of near-surface and surface ice via the Phoenix lander, excavation of ice via recent impact cratering activity as monitored by High Resolution Imaging Science Experiment (HiRISE), Context Camera (CTX), and Compact Reconnaissance Imaging Spectrometer (CRISM), complemented by interpreted results from the SHAllow RADar (SHARAD) instrument, further unveil a landscape enriched in water/ice. Studies of the orbital behaviour of Mars have equally inferred that climate-forcing, triggered by cyclic shifts in the obliquity of Mars, controls the atmospheric stability of water-ice on the surface, allowing the mid- to high-latitudes to host a, so-called, periglacial environment. Still, there is much debate regarding just how 'wet' the paleoclimate of Mars has been, with concurrent water-related and 'dry' hypotheses having been put forth to explain the landscape evolution of the planet. We advocate that, considering the current limitations in studying Mars, geomorphological analysis is a reliable avenue in inferring the genetic nature of a landscape. As such, via a geomorphologic survey, we report on the landscape analysis of a region within Utopia Planitia. This region hosts a diverse abundance of potential periglacial features, including an intriguing 'rimmed' feature found within our study area. This feature, which we have dubbed 'Decameter-scale Rimmed Depression', serves as a valuable stratigraphic marker for rebuilding the geologic history of Utopia Planitia within the recent late Amazonian period, as it is both relatively young and potentially periglacial in nature. Ultimately, our aim is to unveil an additional piece to the periglacial 'puzzle' of Mars, via focusing on the prevalent process(es), responsible in shaping the landscape in question, and suggest a scenario for the late-Amazonian climate history, specific to Utopia Planitia.

Keywords

Dedication

In the summer of 2001, at the age of 8, I wrote a short story about a baby rabbit who dreamed of becoming an astronaut. I then turned the short story into a hand-written 'book', with the hopes of selling it to my family and friends. I even tried to make my 'book' marketable, and among other things, included a copyrights page, a table of contents, and a soft cover made from two stapled A4 sheets of paper that contained a bizarrely hand-drawn picture in the front, and an abstract of the story and the selling price, equivalent to 10 cents, on the back. I did not sell a single copy. Not until my grandfather found out about my book. He read it, and he was interested to purchase a copy, but it had to be free of spelling mistakes. So, we agreed that I would return an edited copy to him, for which he gave me the equivalent to 10 dollars in advance. Unfortunately, he passed away shortly after, before I had a chance to fulfil my end of our agreement.

I dedicate my work here to my grandfather, Hossein, in hopes that it satisfies the promise that I made to him long ago. May we meet again at the gates of Elysium.

Co-Authorship Statement

The concept behind this thesis grew as a discussion with Drs. Gordon R. Osinski and Richard Soare, with both providing initial guidance. Dr. Gordon R. Osinski continued advising for the entirety of this thesis, providing comments and editing, as well as suggesting Devon Island as an ideal analogue site on Earth for comparison. Dr. Etienne Godin provided the Factor Analysis of Mixed Data (FAMD) with respect to the landscape survey presented in chapter 2, as well as providing comments and edits for the same chapter. Polygonization on Decameter-scale Rimmed Depressions (DRDs), presented in Figure 2.11, and Lake Orbiter LiDAR image, presented in Figures 2.12l & 3.2, were initially brought to my attention by Jordan E. Hawkswell, a fellow MSc. student; Drs. Michael Zanetti and Antero Kukko were responsible for obtaining this Lake Orbiter LiDAR image. The remainder of all data collection and analysis was done by Arya Bina.

Acknowledgements

Thank you to my unparalleled father, Hamid, who taught me kindness, patience, humility, and without whom I would not have understood the essence of love in every aspect of life; you are and will always be the greatest man I have ever known. To my incomparable mother, Manijeh, who taught me how to fight for my goals, and who laid the foundation for where I am today and my path in life. I love you both, and owe you an unpayable debt of gratitude, for sacrificing the quality of your life since my birth, to better the quality of mine.

A sincere and heartfelt thank you to my advisor, Dr. Gordon R. Osinski, for firstly accepting me as his MSc student, taking a chance on me under precarious circumstances, and secondly doing so despite his multitude of prior commitments; neither of which affected the flawless level of guidance, constructive criticism, and encouragement he provided me with. I would not have dreamt of doing an MSc under your supervision 2 years ago, and without exaggeration, it has been a true honour to be your student.

To my partner in life, Chantal, who through the thick and thin, has always been by my side to provide me with support, in every form possible. Your kindness and passion resemble an ash-covered eternal fire, not always visible, yet catering endless warmth during cold periods of time in my life.

Lastly, to my uniquely benevolent cats, Athena and Phoenix, for waking me up and providing me with the drive to go to school every morning, and for the loyal company when I return from it. A man could not ask for better companions; you, both, colour my life with the chaos of trouble.

Epigraph

"*We have uncovered wonders undreamt by our ancestors who first speculated on the nature of those wandering lights in the night sky. We have probed the origins of our planet and ourselves. By discovering what else is possible, by coming face to face with alternative fates of worlds more or less like our own, we have begun to better understand the Earth. Every one of these worlds is lovely and instructive.*

When Voyager 1 scanned the Solar System from beyond the outermost planet, it saw, just as Copernicus and Galileo had said we would, the Sun in the middle and the planets in concentric orbits about it. Far from being the center of the Universe, the Earth is just one of the orbiting dots. No longer confined to a single world, we are now able to reach out to others and determine decisively what kind of planetary system we inhabit.

During the Viking robotic mission, beginning in July 1976, in a certain sense I spent a year on Mars. I examined the boulders and sand dunes, the sky red even at high noon, the ancient river valleys, the soaring volcanic mountains, the fierce wind erosion, the laminated polar terrain, the two dark potato-shaped moons. We have just begun to search. We can't help it. Life looks for life. Maybe life is hiding on Mars or Jupiter, Europa or Titan. Maybe the Galaxy is filled with worlds as rich in life as ours. Maybe we are on the verge of making such discoveries."

- Carl Sagan, Pale Blue Dot

Table of Contents

List of Tables

Chapter 2:

List of Figures

List of Abbreviations

2D	Two-Dimensional
CCF	Concentric crater fill
CRISM	Compact Reconnaissance Imaging Spectrometer for Mars
CTX	Context Camera
DEM	Digital elevation model
DRD	Decameter-scale Rimmed Depression
ESRI	Environmental Systems Research Institute
FAMD	Factor Analysis of Mixed Data
FGI	Finnish Geospatial Institute
GRS	Gamma-Ray Spectrometer
HCP	High-Centre Polygon
HRSC	High Resolution Stereo Camera
HiRISE	High Resolution Imaging Science Experiment
IRF	Ice-Rich Fill (CCF/LDA/LVF)
ISIS	Integrated Software for Imagers and Spectrometers
JMARS	Java Mission-planning and Analysis for Remote Sensing
JPL	Jet Propulsion Laboratory
KLS	Kinematic mobile LiDAR Scanner
LCP	Low-Centre Polygon
LDM	Latitude-dependent mantle
LVF	Lineated valley fill
LiDAR	Light Detection And Ranging
MGS	Mars Global Surveyor
MOLA	Mars Orbiter Laser Altimeter
MRO	Mars Reconnaissance Orbiter
MRRD	Mesoscale Raised Rim Depression
mSM	Mobile Scene Modeling
MSSS	Malin Space Science Systems

Myr	Million years
NASA	National Aeronautics and Space Administration
NGT	Neo-Geographic Toolkit
NN	Nearest Neighbour
PDS	Planetary Data Systems
SHARAD	Shallow Radar
TES	Thermal Emission Spectrometer
THEMIS	Thermal Emission Imaging Spectrometer (infrared subsystem)
USGS	United States Geological Survey

Chapter 1: Background & Literature Review

1.1 Introduction

The discovery of landform features such as valley networks, outflow channels [*Baker et al.*, 1983], lakes [*Newsom et al.*, 1996], and deltas [*Moore et al.*, 2003] on the Martian landscape, suggest that liquid water was a factor in its development. However, the answers to questions with respect to the abundance of water in both early and modern Mars, and the significance of water in the landscape evolution of Mars are still heavily debated. A number of concurrent hypotheses have been put forth, with some workers suggesting 'warm' and 'wet' geoclimatic conditions in early Mars [e.g., *Craddock & Howard*, 2002; *McKay*, 1997; *Pollack et al.*, 1987*]*, while others have challenged the veracity of such proposals with a 'cold' and 'dry' scenario [e.g., *Fairén*, 2010*; Head*, 2012]. Resolutely, in efforts to reconstruct the paleoenvironmental conditions on Mars, as means to understand the lineage of water on the planet and informing the extent and magnitude of its role in Martian landscape evolution today, geomorphological analysis is an essential aid. More specifically, considering the limitations involved with studying Mars, the responsiveness of periglacial landforms to changes in geoclimatic conditions, prove them to be reliable paleoenvironmental markers [*Karte*, 1983], fit for reporting on the past climate history of Mars. Importantly, the presence of potential periglacial landscapes on Mars is a recurring hypothesis with previous workers having identified scalloped depressions [*Costard & Kargel*, 1995], a variety of patterned ground (e.g., polygons) [*French*, 2013], and gullies [*Malin & Edgett*, 2000]; extending from the mid to high latitudes with none lower than 20º N/S. The presence of such features on Earth, would unequivocally indicate a periglacial environment, and is an indicator of the presence of water in the terrain, at a past and/or present time [*Carr*, 2006; *French*, 1993; *Greeley*, 1994; *Gurney*, 1998; *Lucchitta*, 1981; *Mackay*, 1979, 1998]. In addition, the history of obliquity shifts of Mars within the past 10 Myrs [*Laskar et al.*, 2004], which control the latitudinal range of water-ice stability, further confirms that the mid-latitudes on Mars periodically hosted a periglacial landscape. Moreover, the presence of an ice-rich terrain is suggested in association with the interpreted results from the SHAllow RADar (SHARAD) instrument aboard the Mars Reconnaissance Orbiter (MRO) satellite [*Bramson et al.*, 2015; *Stuurman et al.*, 2016], periodic excavation of subsurface ice via recent impact cratering activity monitored by the Context Camera (CTX), High Resolution Imaging Science Experiment

(HiRISE), and Compact Reconnaissance Imaging Spectrometer for Mars (CRISM) instruments (also onboard MRO) [*Byrne et al.*, 2009; *Dundas & Byrne*, 2010], and experiments carried out by the Phoenix lander [*Smith & the Phoenix Science Team*, 2009], complementing the identification of periglacial features.
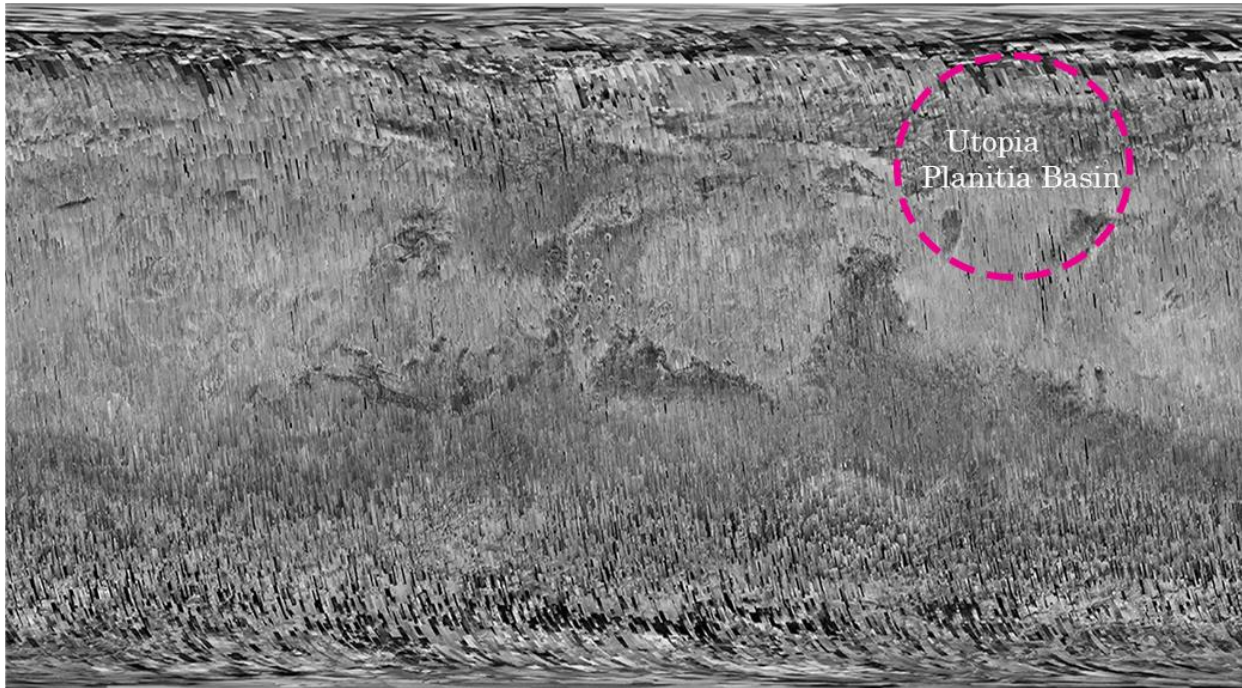
Figure 1.1: Global coverage as of March 2017 by the Context Camera (CTX) instrument, aboard the Mars Reconnaissance Orbiter (MRO) satellite. *Image credit: NASA/JPL-Caltech/MSSS.*

In search of periglacial landforms on Mars, Utopia Planitia is a striking region for the aggregation of such features. This region contains the highest and most diverse instances of periglacial features, suggested to contain the largest concentration of scalloped depressions [e.g., *Costard & Kargel*, 1995; *Soare et al.*, 2008, 2012, 2013], as well as accounting for a sizable cluster of gullies present in the northern hemisphere, with at least one instance that remains active to date [*Dundas et al.*, 2015]. Moreover, the age of these landforms is believed to be young (i.e., 10–20 Myrs), with Utopia Planitia being a mildly to moderately cratered region (see section 1.4 in this chapter), and containing abundant satellite imagery coverage (Figure 1.1) [e.g., *Costard & Kargel*, 1995; *Lefort et al.*, 2009; *Soare et al.*, 2008]. Morphological analysis is a reliable step when uncertain about the genetic nature of a landscape [*Komatsu*, 2007]; thus, Utopia Planitia is an ideal study area to investigate further the claims on the climate history and

landscape evolution of Mars, specifically within the Late Amazonian period,.

In this chapter, we review the morphological characteristics of dominantly recurring landscape features in the so-called periglacial landscape of Mars, their relationships to one another, as well as undertaking a comparative analysis with similar periglacial features found on Earth. In addition, we will review a summary of the geologic history of Utopia Planitia, a region on Mars with a high concentration in periglacial features discussed in this chapter. Lastly, we discuss an underreported feature observed in Utopia Planitia, which we believe will provide additional information in assessing the paleoclimate of this supposed periglacial environment. Through this, we aim to 1. consolidate claims for the presence of a periglacial landscape on Mars (specifically with respect to Utopia Planitia), 2. outline the key region-wide process or set of processes responsible for the formation of such a landscape, and 3. determine how such process or set of processes could be used to infer formation mechanism with respect to other underreported or highly debated landform features found within this landscape. To set the stage, we will begin with a summary of the climate history of Mars in the following section.

1.2 Climate History of Mars

The geologic history of Mars is principally divided into three broad periods: 1. Noachian, 2. Hesperian, and 3. Amazonian [*Carr & Head*, 2010; *Head*, 2012]. In absence of ground-truth data (with the exception of rover/lander findings) and having thus far been unable to explore the Martian geology at depth, the current geologic timescale is highly dependent on surface morphology of the planet, largely thanks to the science of crater counting and morphologic mapping.

The Noachian period, extending from ~4.1 Ga to ~3.8 Ga [*Carr & Head*, 2010; *Head*, 2012], marked one of the most dynamic times in both the climate and geologic history of Mars. During this time, the 'heavy bombardment' event rapidly changed the planetary surface with impact craters, alongside systematic formation of valley networks carving the landscape with features such as rivers, deltas, lakes, and possibly oceans, triggering open system weathering [*Carr*, 2006; *Carr & Head*, 2010; *Clifford*, 2001; *Di Achille & Hynek*, 2010; *Hartmann & Neukum*, 2001; *Head & Wilson*, 2011; *Moore et al.*, 2003; *Tanaka*, 1986; *Tanaka & Kolb*, 2001]. In addition, periodic volcanic eruptions resulting in extensive lava flows that resurfaced large regions of Mars [*Carr*, 1973, 2006; *Carr & Head*, 2010; *Tanaka*, 1986]. Though, there is no

clear time transition to the Hesperian period (~ 3.7–3.1 Ga) [*Carr & Head*, 2010; *Hartmann & Neukum*, 2001; *Head*, 2012; *Tanaka*, 1986], it is generally believed that the volcanic activity progressed well into this period, infilling many of the large basins created due to impact events, frequency of which had been greatly reduced as the Late Heavy Bombardment had been subdued [*Carr*, 2006; *Carr & Head*, 2010; *Gomes et al.*, 2005; *Head & Wilson*, 2011; *Morbidelli et al.*, 2005; *Tanaka*, 1986; *Thomson & Head*, 2001; *Tsiganis et al.*, 2005]. Concurrently, water surface run-off had largely restricted to ephemeral bodies, resulting in the formation of outflow channels and perhaps subsurface flows [*Barlow*, 2010; *Carr*, 2006; *Carr & Head*, 2010; *Clifford*, 1993; *Head & Wilson*, 2011]. The Amazonian period (~ 3.1 Ga–Present) encompassed remnants of the aqueous landscape with comparatively minimal flow activity in its early years, possibly largely limited to sub-surface water; as well as volcanism that continued, in lower capacity, to as recent as 2 Ma [*Carr & Head*, 2010; *Fuller*, 2002; *Neukum et al.*, 2004; *Vaucher et al.*, 2009]. However, as far as our understanding of Mars geoclimatic history goes, this period is of more significance in terms of its part in shaping the proposed periglacial landscape of Mars. Unlike Earth, the obliquity shift of Mars has a high range, from 0 to 60°, and the extent of this shift has been fully exploited at least twice within the last 10 Ma (Figure 1.2) [*Laskar et al.*, 2004; *Mischna*, 2003]. These shifts have a paramount influence on the climate of Mars, as they control the surface water/ice stability, and represent potential cycles of ice migration that can form planet-wide formation of ice-cover that extend from poles to the low latitudes [*Levrard et al.*, 2004; *Mischna*, 2003]. Additionally, the repetitive and frequent shifts in the obliquity of Mars has produced up to 20 shifts, with obliquities <30°, throughout the past few million years, while it currently resides at an obliquity like that of Earth at ~ 25° [*Laskar et al.*, 2004; *Mischna*, 2003].
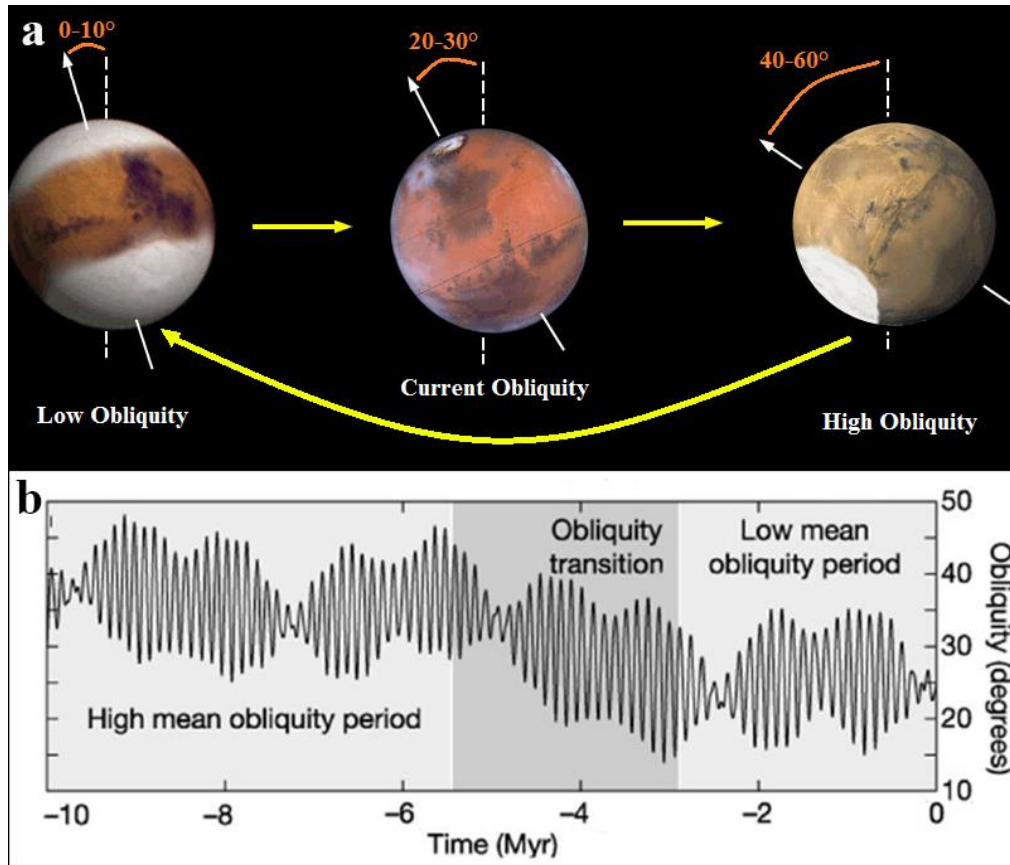
Figure 1.2: **(a)** Demonstration of redistribution of surface ice on Mars with shifts in obliquity, modified from an image by NASA/JPL-Caltech, **(b)** graph depicting the magnitude in degrees of changes in the obliquity of Mars within the past 10 Myr. From Levrared et al. [2004].

The evidence for this cyclic migration of ice is believed to have remained in the shallow substrate and has been detected via various means. The Gamma-Ray Spectrometer (GRS) aboard the Mars Odyssey satellite, capable of detecting neutron concentrations within a metre depth of the surface, has provided proof for the existence of oxygen-bound hydrogen (suggested to be water-ice) throughout regions of the mid-latitudes [*Boynton*, 2002; *Feldman et al.*, 2004]. With the launch the MRO satellite, the SHARAD instrument, through measuring the dielectric response at the decameter-scale [*Bramson et al.*, 2015; *Stuurman et al.*, 2016], alongside CRISM, further supported the GRS observations [*Byrne et al.*, 2009; *Dundas & Byrne*, 2010]. Presently, the high-resolution imaging instruments aboard the MRO, CTX and HiRISE, frequently image recent impact sites in the mid-latitudes, revealing the excavation of water-ice [e.g., *Byrne et al.*, 2009; *Dundas & Byrne*, 2010].

In conjunction with satellite data, the Phoenix lander reported confirmation of shallow-subsurface ice at its landing site in Vastitas Borealis on Mars [*Smith & the Phoenix Science Team*, 2009]. The obtained high-resolution satellite imagery (e.g., HiRISE, CTX), have additionally revealed morphologies that are suggested to be expressive of a periglacial landscape and confirm the initial claim of the presence of water-rich terrain at the present (or past) time. The noteworthy mentions include Concentric Crater Fills (CCF) [*Squyres*, 1979], Lineated Valley Fills (LVF) [*Squyres*, 1979], Lobate Debris Aprons (LDA) [*Squyres*, 1979], Latitude Dependent Mantle (LDM) [*Head et al.*, 2003], polygonised terrain [*French*, 2013; *Levy, Head, Marchant, et al.*, 2009], past and present-day gully activity [e.g., *Dundas et al.*, 2015; *Malin & Edgett*, 2000], and scalloped depressions [*Costard & Kargel*, 1995]. The potential of such features to support the idea of a 'water-rich' climate and geologic history, at least specific to the mid-latitudes of Mars, is associated with periglacial feature's high sensitivity to environmental changes (e.g., hydrologic, thermal) [*French*, 2013; *Karte*, 1983; *Nelson et al.*, 2002]. In the following section, we discuss the morphology, geographic distribution, and the relationships of the prevalent periglacial landforms on Mars.

1.3 The Periglacial Landscape of Mars

A periglacial environment is a landscape with cold climate conditions that encompasses an spectrum of geologic processes and landform features, irrespective of their spatial or temporal ties to a glacier [*French*, 1996]. While glacial regions constitute cold, freezing conditions; a periglacial environment allows for seasonal thaw and subsequent freezing [*French*, 1980, 2013; *Pidwirny*, 2006; *Slaymaker*, 2011]. The influence of this cyclic process on the affected region, results in the production of geomorphologic landform features, and ultimately a landscape, indicative of the presence of water within the associated environment, at a past or present time [*Carr*, 2006; *French*, 1993; *Greeley*, 1994; *Gurney*, 1998; *Lucchitta*, 1981; *Mackay*, 1979, 1998]. Such a scenario on Earth, may not be deemed unconventional, with liquid water being present in abundance throughout the planet. In contrast, on Mars, given that current atmospheric conditions do not allow the long-term sustenance of liquid water on the surface, the presence of a periglacial landscape has significant implications with regard to the geoclimatic history and landscape evolution of the planet. With the launch of NASA's Mariner program in the early 1960's, the first evidence for a periglacial landscape on Mars was observed on the resulting imagery

[*Belcher et al.*, 1971]. Still, studies on the landscape of Mars were limited, until recent high-resolution data was made available through subsequent missions (e.g., Mars Odyssey, MGS, MRO). Today, the potential periglacial landscape on Mars remains an active area of research, as, in respect to past or present suitability of the planet for life, it suggests that liquid water was and may still be a factor in shaping the planet.

Nearly all of these potentially periglacial landforms are found, latitudinally restricted, in the mid- to high-latitudes of Mars. Albeit, the global distribution of these periglacial landforms is not homogenous within the mid- to high-latitudes. Instead, regions on Mars host an aggregation of these features, with Utopia Planitia being an epicentre of a diverse concentration of such features. In the following section, we will examine the prevalent landform features of the suggested periglacial landscape of Mars, followed by providing a synopsis of Utopia Planitia.

1.3.1 Latitude Dependent Mantle

The so-called Latitude Dependent Mantle (LDM) is believed to be a depositional ice-rich 'apron' that partially shields the surface of Mars, in mid- to high- latitude regions [*Kreslavsky & Head*, 2000; *Mustard et al.*, 2001]. This layer covers ~23% of the surface of the planet, discontinuously between 30-50°, and completely at ≥50°, in either hemisphere [*Head et al.*, 2003; *Kreslavsky & Head*, 2000]. LDM is suggested to be metres-thick and, at least at locations where partial-coverage allows for direct comparison between LDM and the underlying units, it exhibits a smoothing cover of the underlying terrain [*Head et al.*, 2003; *Kreslavsky & Head*, 2000, 2002]. The LDM average thickness is believed to vary between 10–20 metres, though it is suggested to increase as high as 40 metres in some areas [*Head et al.*, 2003; *Kreslavsky & Head*, 2000]. Furthermore, in places where the dissected edges of LDM are visible (Figure 1.3), workers have noted that internal layering at a metre-scale can be observed, indicative of episodic emplacement [*Dickson et al.*, 2015; *Kreslavsky & Head*, 2002; *Milliken*, 2003; *Schon et al.*, 2009]. In fact, the formation of this layer has been attributed to atmospheric deposition of ice, derived by changes in obliquity; subsequently cemented together with aeolian by-products available on the surface [*Kreslavsky & Head*, 2002; *Mustard et al.*, 2001]. As such, the internal layering of LDM is believed to be suggestive of some numerous successive episodes of atmospheric deposition on million-year timescales [*Kreslavsky & Head*, 2002; *Mustard et al.*, 2001; *Schon et al.*, 2009].
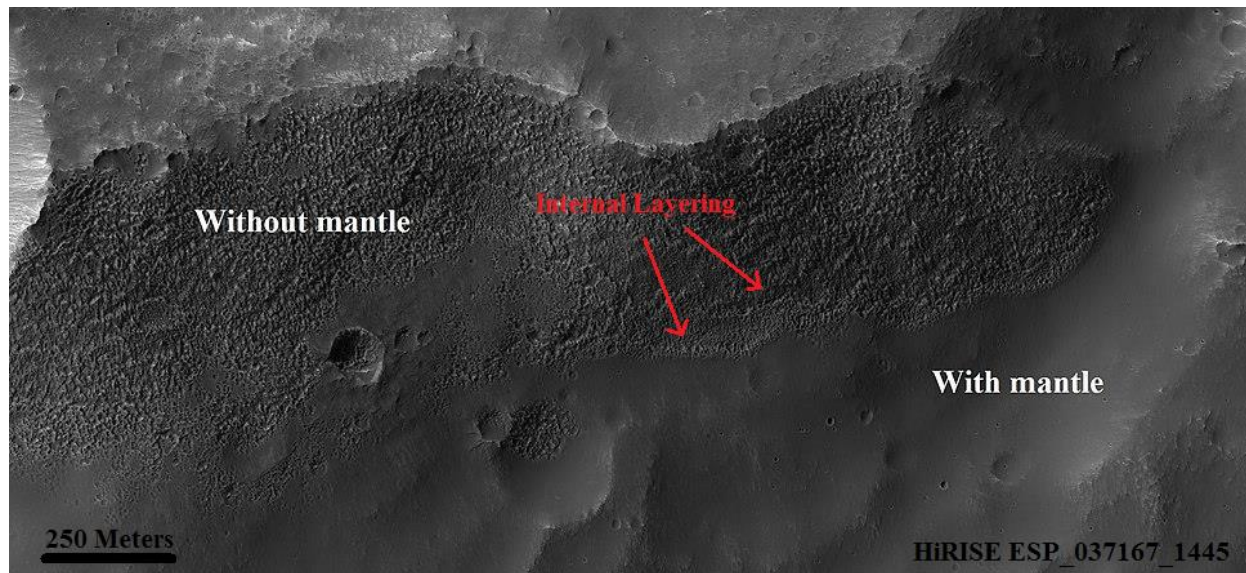
Figure 1.3: Sample image outlining the smooth surfaces containing LDM coverage, while in areas this layer has been dissected exposing a portion of the underlying deposits. Note the layering visible on boundaries between LDM coverage and dissected terrain, suggesting an episodic deposition. Portion of HiRISE ESP_037167_1445. *Image credit: NASA/JPL/University of Arizona.*

As the name suggests, LDM coverage is controlled by latitude, thus both its thickness and morphology vary with latitude. The classification of morphology and erosional patterns of LDM (Figure 1.4) [*Milliken & Mustard*, 2003; *Zanetti et al.*, 2010], is thought to be representative of a direct relationship between LDM preservation state and latitude. That is, with a decrease in latitude, LDM appears generally more dissected/weathered and only shows partial coverage of the terrain with areas displaying complete removal (~30º to 50º N/S) [*Milliken & Mustard*, 2003; *Mustard et al.*, 2001; *Zanetti et al.*, 2010]. Conversely, with an increase in latitude, the erosional patterns become more continuous, displaying 'knobby & wavy' (~30º to 55º N/S) and eventually 'scalloped' (~40º to 65º N/S) textures (see section 1.3.2 in this chapter). Ultimately, at high latitudes (i.e., >50º N/S) LDM coverage becomes fairly consistent exhibiting polygonization (see section 1.3.3), with terms such as 'dragon-scale' or 'basketball' textures having been used to describe its morphology [*Head et al.*, 2003; *Kreslavsky & Head*, 2002].

Despite the suggested formation mechanism and previous characterization of LDM, it remains a poorly understood landscape feature, with key questions either remaining unanswered or heavily debated. For instance, how exactly did changes in obliquity and/or atmospheric

deposition result in ground ice? Do these deposits contain a dust/debris matrix or is ice the responsible medium for the cementation processes? Subsequent scientific research, derived by the insight produced from future planetary missions to Mars, will allow these questions to be answered with a high degree of certainty, and provide a better understanding of the nature of LDM.
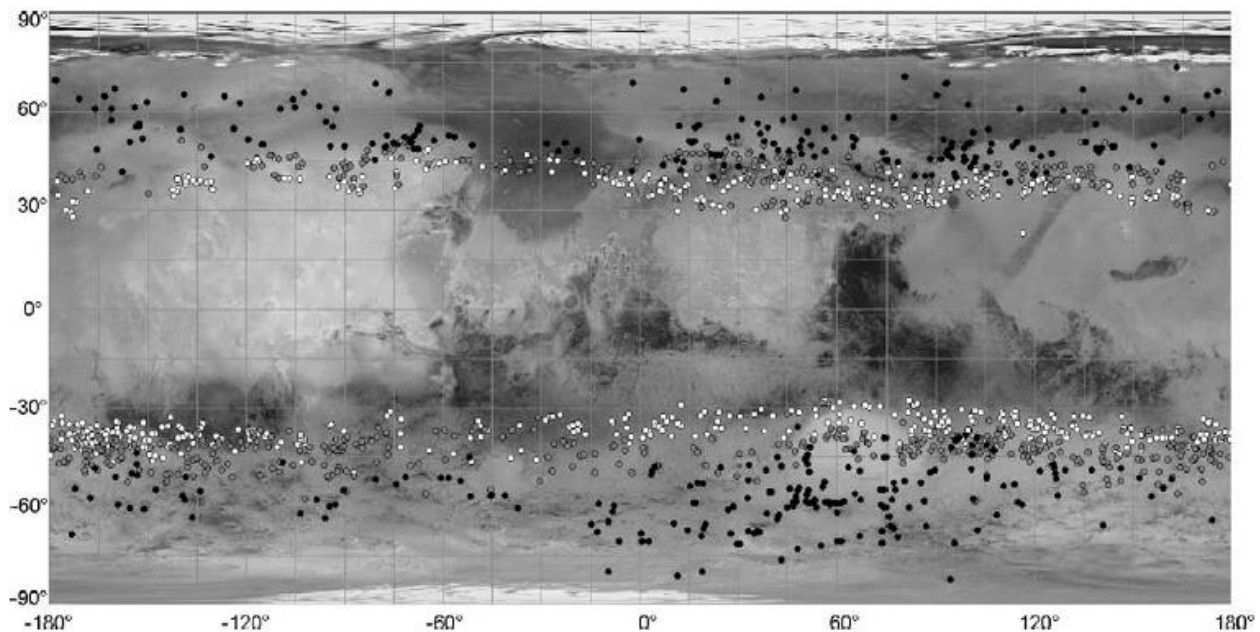
Figure 1.4: Distribution pattern of LDM dissection and erosional patterns as initially created by Milliken and Mustard [2001], and subsequently modified by Zanetti et al. [2010]. White dots represent heavily dissected terrain with instances of complete removal, grey dots displaying locations of gradual erosion with 'knobby & wavy' textures, and black dots are samples of mantled regions with 'scalloped' textures. From Zanetti et al. [2010]. *Basemap image credit: NASA/JPL/ESA/PDS Geosciences.*

1.3.2 Scalloped Depressions

Scalloped depressions are morphologic landscape features, appearing as circular to elliptical rimless depressions, with relatively flat floors and an asymmetric North-South profile. Their overall size, measured by the diameter of a best-fit circle, can be highly variable from tens of metres to tens of kilometres, at times coalescing, with relatively small depth-to-diameter ratio ranging from a few metres to tens of metres [*Costard & Kargel*, 1995; *Morgenstern et al.*, 2007; *Séjourné et al.*, 2011; *Soare et al.*, 2007].

Their irregular profile consists of a more degraded and flattened equator-facing wall, relative to their pole-facing counterparts [*Lefort et al.*, 2009; *Morgenstern et al.*, 2007; *Soare et al.*, 2007; *Ulrich et al.*, 2010]. Like gullies, some equator-facing walls exhibit morphology consistent with alcoves, which are, at times, accompanied by etched forms, similar to channels, downstream [*Costard*, 2002; *Malin & Edgett*, 2000]. On the pole-facing wall, semicircular terraces/bright-rings can be observed, propagating perpendicular to the equator-facing wall (Figure 1.5). The occurrence of terraces/bright-rings has a positive relationship with the size of depressions; that is, in small depressions, no rings are discernible, while the number of detected rings increases in large depressions [*Costard & Kargel*, 1995; *Morgenstern et al.*, 2007; *Séjourné et al.*, 2011]. As well, their elongation also appears to be in direct correlation to their size. As reported by Séjourné et al. [2011], small depressions generally depict a more circular form, while with an increase in size, the circumference of the depressions transforms to more elongate shapes. The exception to this observation is the coalescence of depressions, which is a common occurrence in Utopia Planitia.
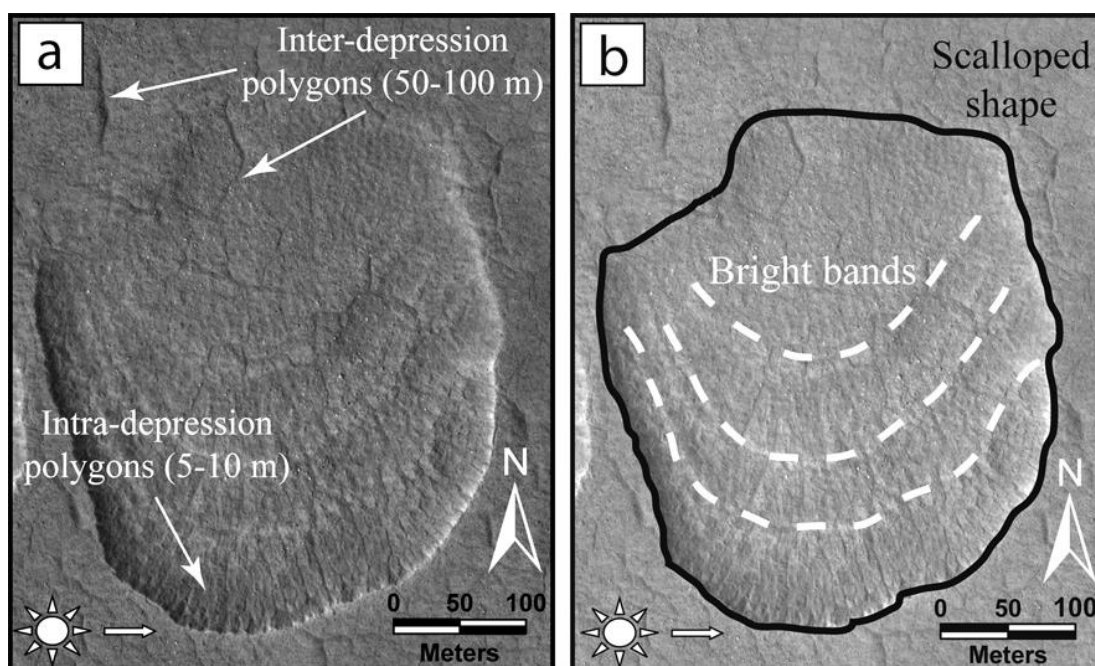
Figure 1.5: **(a)** close-up of an scalloped depression in Utopia Planitia, with outlined equator-facing heavily subsided wall, and pole-facing steep-sloped wall, **(b)** Outlined bright bands concentric to the pole-facing wall. From Séjourné et al. [2011]. *Image credit: NASA/JPL/University of Arizona.*

The formation mechanism for these landforms remains debated, with prominent hypotheses involving a differential solar insulation model [*Lefort et al.*, 2009, 2010; *Morgenstern et al.*, 2007; *Plescia*, 2003], or conversely thermokarst thaw lakes [*Costard & Kargel*, 1995; *Soare et al.*, 2007, 2008]. As discussed previously (see section 1.3.1 in this chapter), the occurrence of scalloped depressions is believed to be tied to the presence of LDM, frequenting between ~40° to 65° in either hemisphere. The differential solar insolation model builds on this theory, proposing undulating topography causing changes in solar insolation and therefore selective sublimation of interstitial subsurface ice, resulting in the formation of scalloped depressions. The higher solar insolation received by equator-facing walls relative to pole-facing walls results in a higher net-sublimation and subsequently a smoother, gradational slope [*Morgenstern et al.*, 2007; *Plescia*, 2003]. Alternatively, the formation of thermokarst lakes is attributed to the collapse of ice-rich terrain, initiated by melting of either interstitial or massive ground ice. Sequentially, the meltwater would occupy the depression and a lake basin would form as a result, leaving episodic concentric bands of water-height marks upon evaporation, sublimation, and/or infiltration (Figure 1.5b) [*Soare et al.*, 2007, 2008].

Similar to LDM, the hypotheses put forth for the formation mechanism of scalloped depressions are not without challenges. Production of thermokarst lakes on Earth requires the presence of regions with reasonably massive ground ice, where thermal/physical breach of the insulating cover has taken place [*Anderson & Anderson*, 2010]. How was this scenario replicated on Mars? Given that the atmospheric conditions of Mars do not support the long-term sustainment of liquid water on the planet's surface, how was such large quantity of water sustained on the surface? Regardless, the presence of an ice-rich terrain, and therefore the potential for the existence of a periglacial landscape, is a requirement in both of these scalloped depression hypotheses [e.g., *Costard & Kargel*, 1995; *Lefort et al.*, 2009; *Morgenstern et al.*, 2007; *Soare et al.*, 2007, 2008]. This is with the assumption that either one or the other of these suggested scenarios is in fact the correct hypothesis.

1.3.3 Polygons

Polygons are a morphological classification of patterned ground, often exhibited by striking symmetrical geometric patterns, in this case, polygonal in shape, that occupy surfaces of landscapes that undergo recurrent freeze-thaw cycles (Figure 1.6) [*French*, 1993; *Washburn*,

1956]. On Earth, the most readily observed type of polygonised terrain is thermal-contraction polygons found in periglacial environments [*French*, 2013; *Lachenbruch*, 1962]. Put simply, the expansion and contraction of a water-rich ground through repeated episodes of freezing and thawing results in the formation of fractures and crevices [*French*, 1993, 2013; *Lachenbruch*, 1962; *Washburn*, 1956]. Subsequently, the infilling of these fissures by a variety of different material such as water (i.e., Ice-wedge polygons) or loess to coarse-grained sand (i.e., sand-wedge polygons) further evolves the landscape into polygonised terrain [*French*, 1993, 2013; *Lachenbruch*, 1962; *Washburn*, 1956]. In comparison, on Mars, polygons are a common landform observed throughout regions of mid- to high-latitudes [e.g., *Lefort et al., 2009; Morgenstern et al.*, 2007; *Seibert & Kargel*, 2001; *Soare et al.*, 2008]. While ice-, sand-, and composite-wedge polygons have been proposed to exist on Mars, given that liquid water is not sustainable on the surface due to current climate conditions of Mars, polygons resulting from the sublimation of ice have also been suggested [e.g., *Levy et al.,* 2010, 2011; *Marchant & Head*, 2007]. Morphometrically, two classes of polygonised terrain have been thus far identified on Mars: polygons 5 to 10 metres in best-fit-circle diameter, specific to scalloped depressions [*Lefort et al.*, 2009; *Levy, Head, Marchant, et al.*, 2009; *Morgenstern et al.*, 2007; *Séjourné et al.*, 2011; *Soare et al.*, 2008], and polygons few tens of metres to 100 metres in best-fit-circle diameter, occurring elsewhere [*Lefort et al.*, 2009; *Morgenstern et al.*, 2007; *Seibert & Kargel*, 2001; *Soare et al.*, 2008]. Along with their diversity in size, polygons have also been suggested to morphologically vary on Mars. Two types of morphologically distinct polygons have been identified [*Séjourné et al.*, 2011]: low-centre polygons that exhibit a depressed centre with distinctive outer ridges, and high-centre polygons that are flat or exhibit a pronounced convex-like cross profile. At times, the border between polygons ~<50 metres in best-fit diameter, appears as a circular to elongate incision 10's to few 100's of metres in length [*Lefort et al.*, 2009; *Morgenstern et al.*, 2007; *Soare et al.*, 2005, 2012]. These features have been previously referred to as 'polygon-junction pits' [*Séjourné & Soare*, 2014], with an extension of their long-axis dominantly parallel to the North-South direction [*Morgenstern et al.*, 2007].

Figure 1.6: **(a)** Desiccation pattern polygons as observed on Earth, **(b)** polygonised terrain on Mars. *Image credit: NASA/JPL/University of Arizona/Google.*

On Earth, a water/ice-rich terrain is a requirement for the production of patterned ground, and similarly on Mars they are suggested to be spatially tied to LDM. Specifically, within scalloped depressions, low-centre polygons typically occupy the floor and pole-facing walls; while high-centre polygons mainly occur on the equator-facing wall [e.g., *Lefort et al.*, 2009; *Levy et al.*, 2009; *Morgenstern et al.*, 2007; *Séjourné et al.*, 2011; *Soare et al.*, 2008]. That being said, similar to the polygon-junction pits, the polygons occurring in scalloped terrain, have a long-axis that is dominantly parallel to the North-South direction [e.g., *Lefort et al.*, 2009; *Levy et al.*, 2009; *Morgenstern et al.*, 2007; *Séjourné et al.*, 2011; *Soare et al.*, 2008]. Additionally, some gully systems have also been reported to be stratigraphically linked to polygons [e.g., *Levy et al.*, 2009]. In these scenarios, it's suggested that polygonised terrain behaves as a reserve of ice, and upon melting it gives way to the channelized transport of liquid water on high-sloping terrain and therefore the formation of gullies.

1.3.4 Gullies

Gully is a term used to describe a channel incision, etched by flow from surface-runoff,

and/or interflow, typically occurring on sloping terrain [*Malin & Edgett*, 1999]. The morphology of gullies typically consists of a source alcove, accompanied with one or more downstream channels, followed by a depositional apron (Figure 1.7) [*Balme et al.*, 2006; *Harrison et al.*, 2015; *Heldmann et al.*, 2007; *Heldmann & Mellon*, 2004; *Kneissl et al.*, 2010; *Malin & Edgett*, 1999]. The highest point of a gully channel, referred to as the flow front, is usually the widest part of the channel; which decreases in width downstream [*Iverson et al.*, 1997]. However; more often than not, the coalescence of gully channels, or the flow front part of the channel, can make their distinction difficult [*Iverson et al.*, 2010]. The morphological characteristics of these channels can vary in association with different terrain properties. For instance, in rough terrain, gully channels form levees; and depending on the mixture of sediment present in the terrain, they can form thinner and longer channels [*Iverson et al.*, 2010].
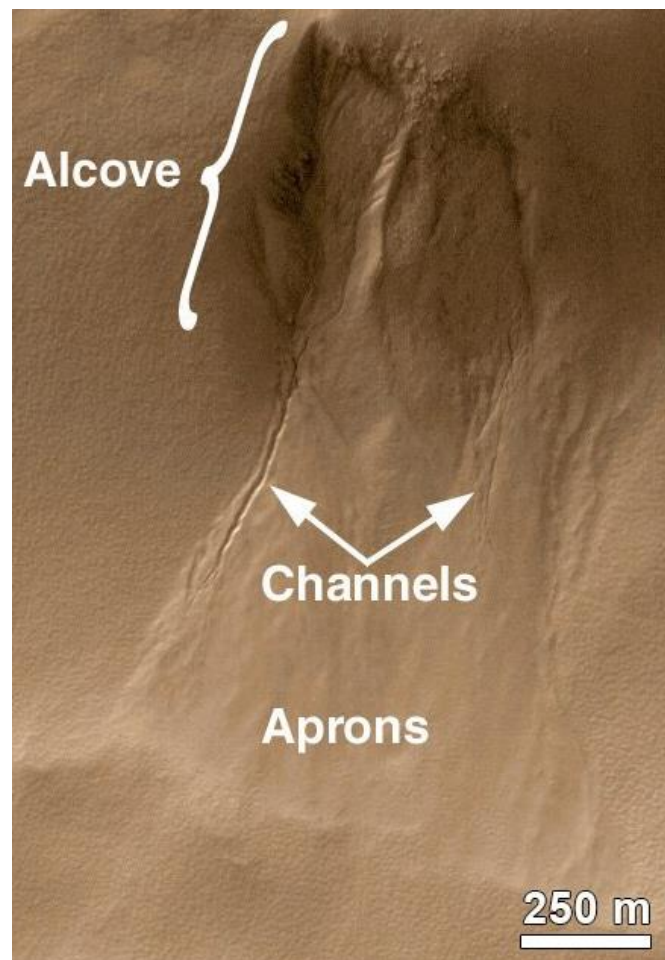
Figure 1.7: Gully on a crater wall on Mars with its main morphological break-down outlined. Note the placement of the alcove, followed by carved channel(s) and the depositional apron. *Image credit: NASA/JPL-Caltech/MSSS.*

On Mars, gullies are abundant in a variety of preservation states in both hemispheres (Figure 1.8). They are observed on slopes of valleys, massifs, central peaks, and dunes, with the vast majority of them appearing on crater walls (>80%) [*Harrison et al.*, 2015; *Heldmann et al.*, 2007; *Kneissl et al.*, 2010]. Consequently, present-day gullies have been reported in multiple regions of Mars, with at least one present-day gully activity observed and reported in Utopia (58.7^{o}N, 82.3^{o}E) [*Dundas et al.*, 2015]. Generally, gully frequency decreases with increasing latitude; however, in the southern hemisphere, gullies reach a minimum at ~60° and increase in numbers poleward [*Harrison et al.*, 2015; *Heldmann & Mellon*, 2004]. In the northern hemisphere, they extend from ≥28° to ≤76.6^o; while the southern hemisphere hosts much greater numbers from ≥27° to ≤83° [*Balme et al.*, 2006; *Bridges & Lackner*, 2006; *Harrison et al.*, 2015; *Heldmann et al.*, 2007; *Heldmann & Mellon*, 2004; *Kneissl et al.*, 2010; *Malin & Edgett*, 1999]. Moreover, in the northern hemisphere, gullies indicate a preference for poleward-facing slopes until ~40°, where this preference shifts to equator-facing slopes up to ~50°, beyond which they are equally distributed on either slope [*Harrison et al.*, 2015; *Heldmann et al.*, 2007; *Kneissl et al.*, 2010]. The same behaviour is observed in the southern hemisphere, where this transition is observed at ~45°, and shifted back to pole-facing preference at ~58° [*Balme et al.*, 2006; *Harrison et al.*, 2015; *Heldmann & Mellon*, 2004].
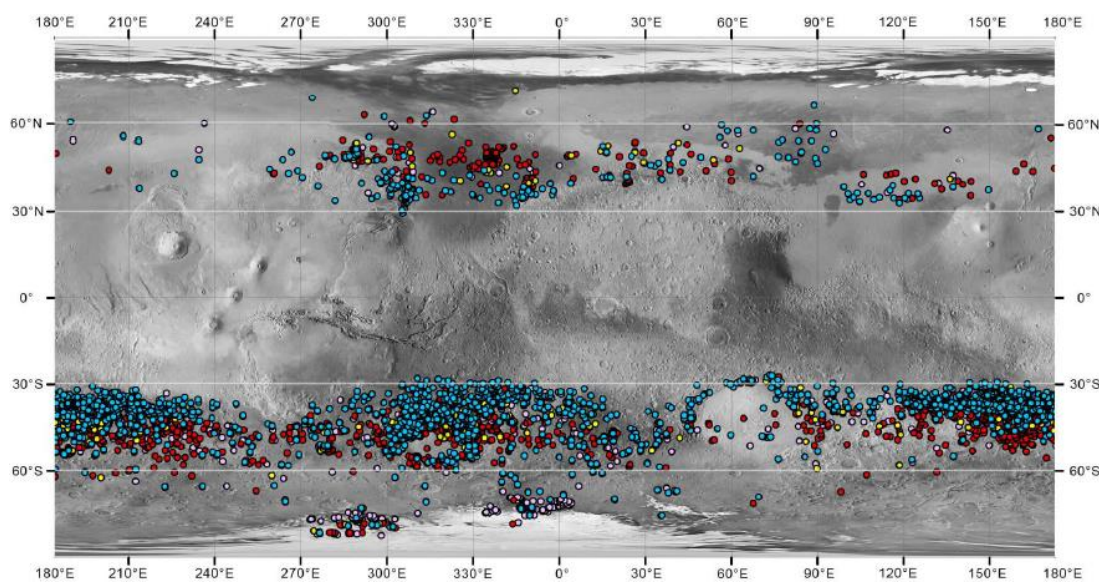
Figure 1.8: Global distribution of gullies on Mars based on mapping by Harrison et al. [2015]. Colours signify the orientation of gullies at the respective site with **red**: equator-facing, **blue**: pole-facing, **yellow**: east-/west-facing, and **purple**: no preference. From Harrison et al. [2015]. *Basemap image credit: NASA/JPL-Caltech/MSSS.*

Gullies on Mars are spatially correlated with CCFs/LVFs/LDAs (see section 1.3.5 in this chapter) and LDM (including scalloped depressions and polygons). These landforms, assuming a feasible atmospheric and climate condition, are, based on their suggested hypotheses, sources of liquid water upon melt; and liquid water is what terrestrial gullies on Earth are initiated by. Respectively, the frequency of gullies on Mars appear highest in locations where LDM is most dissected [*Balme et al.*, 2006; *Bridges & Lackner*, 2006; *Harrison et al.*, 2015; *Head et al.*, 2003; *Heldmann et al.*, 2007; *Heldmann & Mellon*, 2004; *Kneissl et al.*, 2010; *Malin & Edgett*, 1999]. LDM dissection reaches a maximum at ~40° S/N (see Figure 3 of Head et al. [2003]), which roughly corresponds to the gully frequency maximum (see Figure 2 of Dundas et al. [2015] or Figure 2.5 of Harrison et al. [2015]). In fact, it has been suggested that, in some examples, gullies appear dissecting the LDM coverage (see Figure 2 of Dickson et al. [2013]).

Gullies on Earth are not restricted to periglacial environments; however, this may not be the case on Mars. As discussed here, there is a strong correlation between gullies and latitude, and landforms proposed to be suggestive of an ice-rich terrain (e.g., LDM, CCFs/LDAs/LVFs). While there are proposed 'dry' gully formation mechanism [e.g., *Treiman,* 2003], the majority of gully formation hypotheses put forth involve the presence of water (e.g., groundwater: Malin and Edgett [2000], snowmelt: Christensen [2003], ground ice: Costard et al. [2002], H_2O or CO_2 frost: Kossacki and Markiewicz [2004], Dundas et al. [2010]). As such, the significance of the co-location between gullies and ice-rich terrains on Mars, is that a periglacial landscape would potentially provide the meltwater required for, at least initial, gully formation. In comparison, however, while water flow is a requirement for the initiation of gullies on Earth, their further development can result from 'dry' processes such as rock avalanches or dry debris flows. Therefore, it's important to note that active or 'young' gully systems on Mars, do not necessarily correspond to a connection with water under current conditions [*Harrison*, 2016]. Instead, they are suggested to have been initially incised by water and may have morphologically evolved with or without the presence of water.

1.3.5 Concentric Crater Fill, Lineated Valley Fill, and Lobate Debris Aprons

Concentric Crater Fill (CCF), Lineated Valley Fill (LVF), and Lobate Debris Aprons (LDAs) are terms used to describe genetically concurrent landform morphologies, believed to represent by-products of glacial flow, in the form of debris-covered ice-rich deposits found in

low lying land or scarps [*Carr*, 2006; *Kress & Head*, 2008; *Squyres*, 1979]. For the sake of simplicity, when referring to these landforms collectively, we will use the term 'ice-rich fills' (IRFs) going forward. In the case of LDAs, its morphology appears as convex-shaped, stemming outward from a higher elevation into a low-lying land downslope (e.g., from crater wall to crater floor) [*Carr*, 2006; *Squyres*, 1979]. LDAs exhibit pronounced lateral termination, distinctly separating them from the underlying material (Figure 1.9b) [*Carr*, 2006; *Kress & Head*, 2008; *Squyres*, 1979]. Texturally, the fill itself is heavily dissected, or 'fretted', at finer scales; however, an overview of the apron reveals lineations, at times chaotic, 'etched' into the surface [*Carr*, 2001; *Squyres*, 1978, 1979]. Alternatively, IRFs that cover the floor of an impact crater, with similar etched lineations observed in LDAs, concentric to the crater walls, are referred to as CCFs [*Squyres*, 1979]. Crater fills are most commonly found in degraded small craters in Utopia Planitia, as a fill covering the floor with distinct undulations that appear 'hacked' or 'carved' into the surface (Figure 1.9a) [*Carr*, 2006; *Squyres*, 1979]. IRFs found restricted to, alternatively, a channelized stream or valley, with lineations parallel to the direction of channel elongation are known as LVFs (Figure 1.9c) [*Carr*, 2006; *Squyres*, 1979].
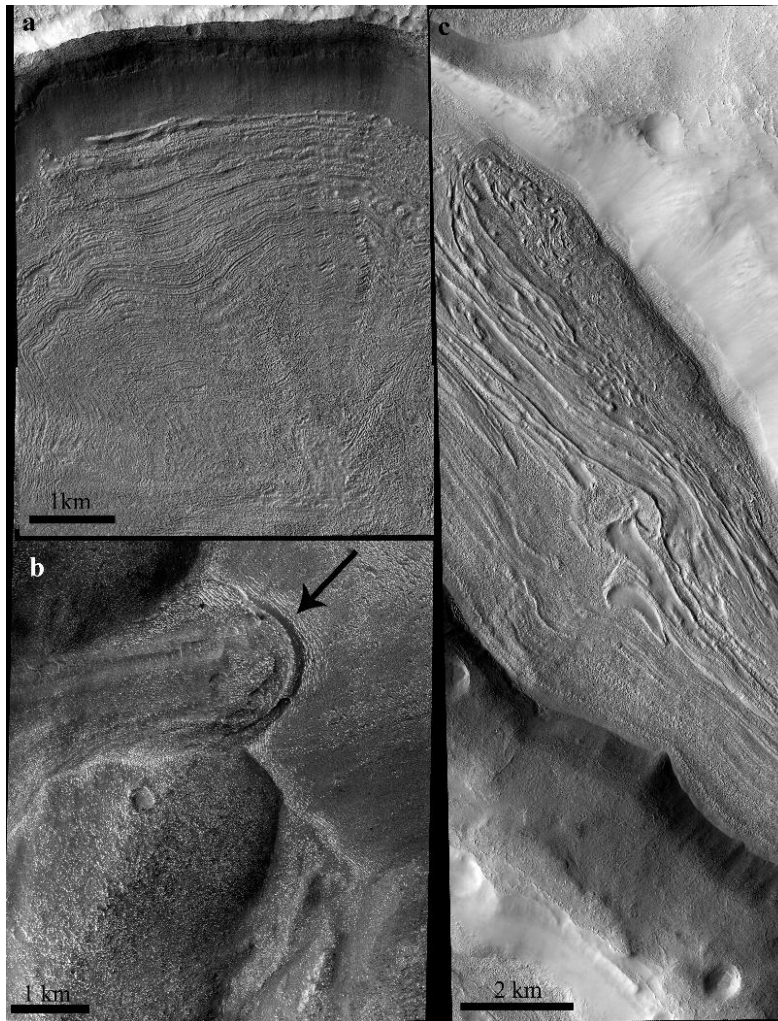
Figure 1.9: **(a)** Concentric Crater Fill (CCF) with undulations concentric to crater walls (HiRISE ESP_046622_1365), **(b)** Lobate Debris Apron (LDA) with the black arrow pointing out the termination edge (HiRISE ESP_023497_1395), **(c)** Lineated Valley Fill (LVF) occupying a valley floor with distinctly hacked ridges within the fill (HiRISE PSP_009033_2155). *Image credit: NASA/JPL/University of Arizona.*

Like all landform features previously discussed in this chapter, IRFs exhibit latitudinal restrictions. Altogether, within the mid-latitudes, they occur from 29° to 59° N/S, while they are most widespread between ~30° to ~60° N/S [*Fastook & Head*, 2014; *Squyres*, 1979]. However, the distribution pattern of IRFs are not uniform, and alter with longitudinal changes as well (Figure 1.10) [e.g., *Levy et al.*, 2014]. That is to say, similar to the case of gullies, differential solar insolation, as well as atmospheric conditions, are believed to both be key factors in determining where IRFs aggregated on Mars. While genetically different, IRFs and LDM are

similar in that, they are landform features believed to represent debris-covered ice-deposits, though they remain controversial and poorly understood. Moreover, the possibility that IRFs represent glacial features (e.g., rock glaciers), rather than periglacial features, should not be ignored. All the same, regardless of their specific genetics, based on the current leading hypothesis, they represent an ice-rich feature.
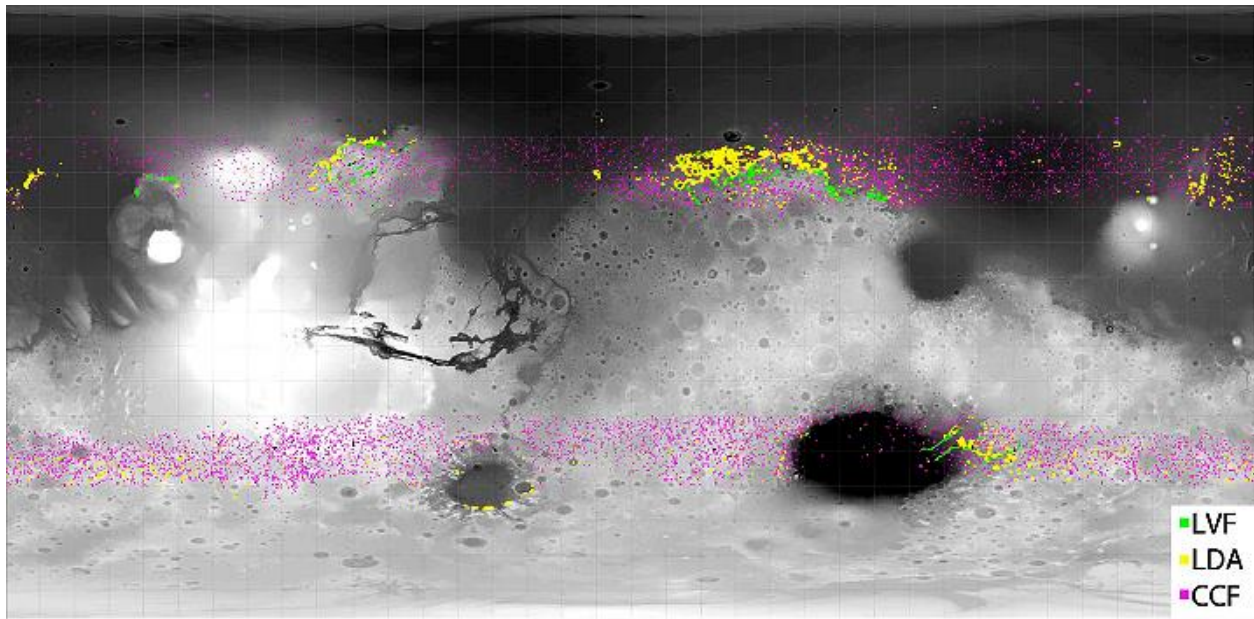
Figure 1.10: Global distribution of Ice-rich Fills (IRFs) based on Levy et al. [2014]. Modified from an image by Levy et al. [2014]. *Basemap image credit: NASA-Goddard Flight Center/JPL/MOLA Science Team/USGS.*

1.4 Utopia Planitia

Utopia Planitia is a 3,300-km diameter basin, situated in the northern plains of Mars at 49.7°N, 118.0°E (Figure 1.11) [*McGill*, 1989; *Thomson & Head*, 2001]. The basement of Utopia is believed to have been formed by a large impact, early in the Noachian period of Mars, which has been subsequently infilled to form the present-day Utopia [*McGill*, 1989; *Thomson & Head*, 2001]. Volcanic infilling of this basin began in Early Hesperian and periodically continued, possibly, as late as the Late Amazonian [*Thomson & Head*, 2001; *Werner*, 2009]. As well, sedimentation from outflow channels in the Late Hesperian, forming the Vastitas Borealis Formation, are also believed to have aided in the infilling of this basin [*Thomson & Head*, 2001]. During the past 10 Ma (i.e., in the Late Amazonian), large obliquity shifts up to 60° [*Laskar et*

al., 2004], as well as ≥ 15 shifts < 30º during the past 2.1–2.5 Ma [*Laskar et al.*, 2004; *Mischna*, 2003], are believed to have resulted in atmospheric deposition in this region [*Head et al.*, 2003]. The relatively young infilling material of the Late Amazonian in Utopia is believed to include mainly an ice-rich dust mixture, derived by the migration of ice from the poles to mid-latitudes [*Levrard et al.*, 2004; *Madeleine et al.*, 2009]. At least a portion of the ice-rich terrain of Utopia is believed to have been preserved in the shallow subsurface to the present-day [*Clifford*, 1993, 2001]. Evidence of this includes the excavation of the terrain carried-out by the Phoenix lander, resurfacing of ice from recent impacts, present-day gully activity in Utopia, and interpreted results from the SHARAD instrument aboard the MRO satellite [*Byrne et al.*, 2009; *Hess et al.*, 1977; *Kress & Head*, 2008; *Stuurman et al.*, 2016].
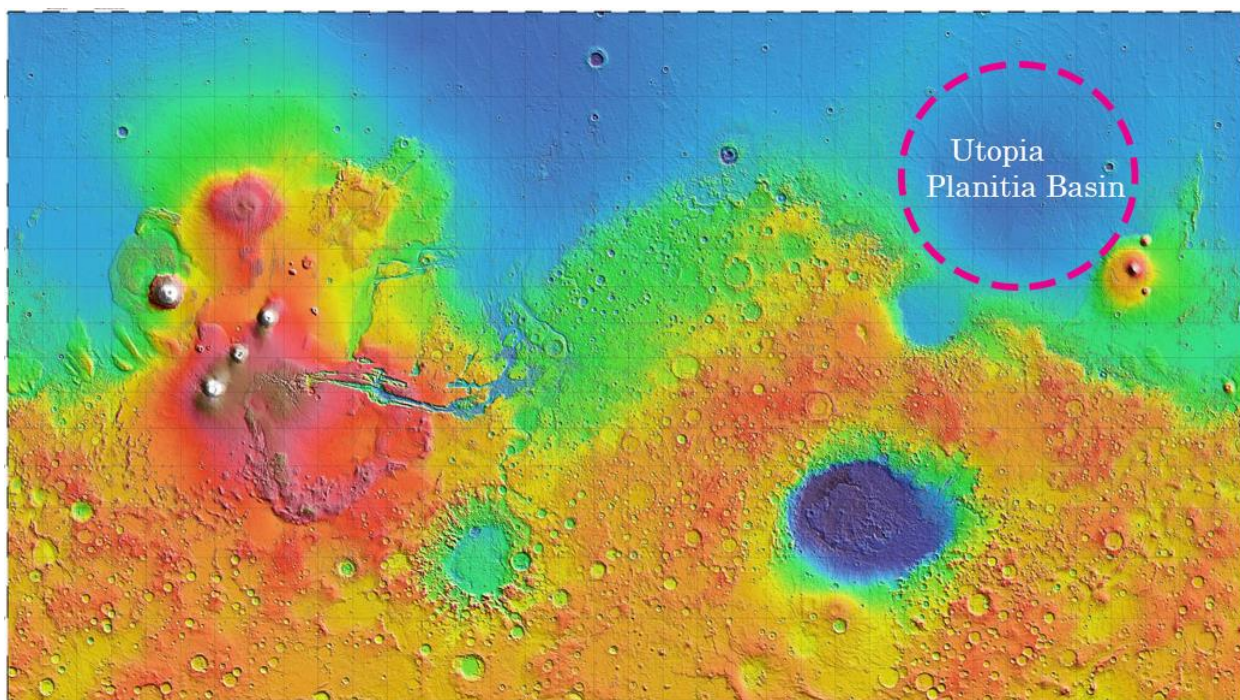
Figure 1.11: Mars Orbiter Laser Altimeter (MOLA) colourized global elevation mosaic with the Utopia Planitia region outlined in the pink dashed line top-right corner. *Basemap image credit: NASA-Goddard Flight Center/JPL/MOLA Science Team/USGS.*

While the current diurnal air temperatures vary significantly in this region, by approximately 50–60º C [*Hess et al.*, 1977], sub-zero temperatures are sustained year-round [*Mellon et al.*, 2004]. The most recent ice-age, occurring between 2.1 to 0.4 Myr ago (Figure 1.2b) [*Head et al.*, 2003; *Levrard et al.*, 2004], is a testament to the comparatively 'young' landscape of Utopia,,

geologically categorized as Amazonian in age, as its morphology, in contrast to Mars as a whole, has not undergone vast reworking and degradation. Moreover, under Utopia's cold climatic conditions, identified landscape features such as latitude-dependent mantle (LDM) and scalloped depressions, a variety of patterned ground, gullies, and IRFs suggest that this region did not always maintain a frozen state in its recent past. Still, there exist hypotheses, put forth by previous workers, that suggest both a 'wet' and a 'dry' periglacial history in Utopia Planitia (e.g., see section 1.3.4).

1.4.1 Introduction to Thesis

Decameter-scale Rimmed Depressions (DRDs) are landform features, observed in Utopia Planitia, that appear as small-scale (i.e., decameter-scale) depressions contained by thin rims (Figure 1.12). The rims of the feature stand at higher elevation relative the surrounding terrain, while the interior of the feature is commonly in-sync with the elevation of the surrounding terrain outside of the enclosing walls. From a bird's-eye perspective, DRDs are generally quasi-circular, but like scalloped depressions they can coalesce, at times forming more complex labyrinthine patterns. Coalescence of DRDs are typically linked with low-lying and relatively flat terrain (e.g., crater floors); while in other cases, they do not show this topographic limitation. Aside from the instances where DRDs coalesce, their separation from one another can range from chaotic assortments, at times clustered or spread out, to near uniform spacing. Similar to polygons, within a confined locality (e.g., a crater) and/or stratigraphic layer, individual DRDs can appear similar, both morphometrically and orientationally (i.e., long-axis direction). Spatially, DRDs exhibit a close link with the presence of polygons. In fact, in every HiRISE image where we have observed DRDs, polygonised terrain was detected as well. Additionally, DRDs appear to favour proximity to ice-rich terrain, such as LDM and IRFs; while they stratigraphically superpose both of these landforms (including scalloped depressions).
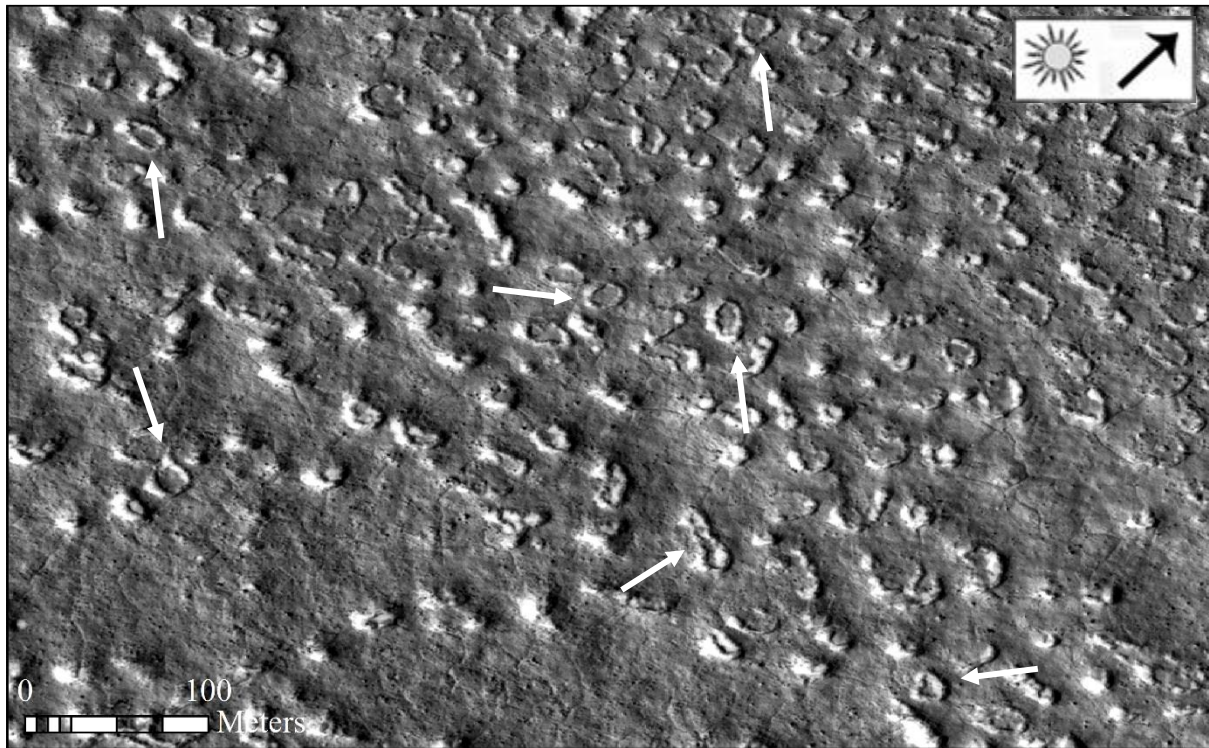
Figure 1.12: Terrain dominated by Decameter-scale Depressions (DRDs) on Mars, with the white arrows pointing to several distinct individual DRDs (HiRISE ESP_037223_2235). *Image credit: NASA/JPL/University of Arizona.*

The goal of this thesis is to provide an additional piece to the periglacial 'puzzle' of Mars, via identifying the prevalent process(es), responsible in the evolution of this so-called periglacial landscape, found on the Northern Plains of Mars. In the following chapter, we introduce our study area within Utopia Planitia, via which we conduct a thorough landscape survey based on available HiRISE imagery. Through this, we will describe the morphology, morphometrics, and distribution patterns observed with respect to DRDs. Subsequently, we will compare and contrast DRDs in relation to the periglacial landscape features discussed in this chapter. Ultimately, we will discuss the specific relationships of these potentially periglacial features to DRDs and use this as a framework upon which we will infer the formation mechanism for DRDs, as well as proposing a scenario for the Late Amazonian history of Utopia Planitia.

1.5 References

Anderson, R. S., & Anderson, S. P. (2010). Geomorphology: the mechanics and chemistry of landscapes. Cambridge University Press.

Baker, V. R., Boothroyd, J. C., Carr, M. H., Cutts, J. A., Komar, P. D., Laity, J. E., … Patton, P. C. (1983). Channels and valleys on Mars. *Bulletin of the Geological Society of America*, *94*(9), 1035–1054. http://doi.org/10.1130/0016-7606(1983)94<1035:CAVOM>2.0.CO;2

Balme, M. R., Mangold, N., Baratoux, D., Costard, F. M., Gosselin, M., Masson, P., … Neukum, G. (2006). Orientation and distribution of recent gullies in the southern hemisphere of Mars: Observations from High Resolution Stereo Camera/Mars Express (HRSC/MEX) and Mars Orbiter Camera/Mars Global Surveyor (MOC/MGS) data. *Journal of Geophysical Research E: Planets*, *111*(5). http://doi.org/10.1029/2005JE002607

Barlow, N. G. (2010). What we know about Mars from its impact craters. *Bulletin of the Geological Society of America*, *122*(5–6), 644–657. http://doi.org/10.1130/B30182.1

Belcher, D., Veverka, J., & Sagan, C. (1971). Mariner photography of Mars and aerial photography of Earth: Some analogies. *Icarus*, *15*(2), 241–252. http://doi.org/10.1016/0019-1035(71)90078-9

Boynton, W. V. (2002). Distribution of Hydrogen in the Near Surface of Mars: Evidence for Subsurface Ice Deposits. *Science*, *297*(5578), 81–85. http://doi.org/10.1126/science.1073722

Bramson, A. M., Byrne, S., Putzig, N. E., Sutton, S., Plaut, J. J., Brothers, T. C., & Holt, J. W. (2015). Widespread excess ice in Arcadia Planitia, Mars. *Geophysical Research Letters*, *42*(16), 6566–6574. http://doi.org/10.1002/2015GL064844

Bridges, N. T., & Lackner, C. N. (2006). Northern hemisphere Martian gullies and mantled terrain: Implications for near-surface water migration in Mars' recent past. *Journal of Geophysical Research*, *111*(E9). http://doi.org/10.1029/2006JE002702

Byrne, S., Dundas, C. M., Kennedy, M. R., Mellon, M. T., McEwen, A. S., Cull, S. C., … Seelos, F. P. (2009). Distribution of Mid-Latitude Ground Ice on Mars from New Impact Craters. *Science*, *325*(5948), 1674–1676, doi:http://doi.org/10.1126/science.1175307.

Carr, M. H. (1973). Volcanism on Mars, *Journal of Geophysical Research, 78*(20), 4049–4062.

Carr, M. H. (2001). Mars Global Surveyor observations of Martian fretted terrain. *Journal of Geophysical Research: Planets*, *106*(E10), 23571–23593.

http://doi.org/10.1029/2000JE001316.

Carr, M. H. (2006). Ice. In *The Surface of Mars* (Vol. 6, pp. 173-191). Cambridge University Press.

Carr, M. H., & Head, J. W. (2010). Geologic history of Mars. *Earth and Planetary Science Letters*, *294*(3–4), 185–203. http://doi.org/10.1016/j.epsl.2009.06.042

Clifford, S. M. (1993). A model for the hydrologic and climatic behavior of water on Mars. *Journal of Geophysical Research*, *98*(E6), 10973. http://doi.org/10.1029/93JE00225

Clifford, S. M. (2001). The Evolution of the Martian Hydrosphere: Implications for the Fate of a Primordial Ocean and the Current State of the Northern Plains. *Icarus*, *154*(1), 40–79. http://doi.org/10.1006/icar.2001.6671

Costard, F. M. (2002). Formation of Recent Martian Debris Flows by Melting of Near-Surface Ground Ice at High Obliquity. *Science*, *295*(5552), 110–113. http://doi.org/10.1126/science.1066698

Costard, F. M., & Kargel, J. S. (1995). Outwash plains and thermokarst on Mars. *Icarus*, *114*(1), 93–112.

Craddock, R. A., & Howard, A. D. (2002). The case for rainfall on a warm, wet early Mars. *Journal of Geophysical Research: Planets*, *107*(E11), 21–36. http://doi.org/10.1029/2001JE001505

Di Achille, G., & Hynek, B. M. (2010). Ancient ocean on Mars supported by global distribution of deltas and valleys. *Nature Geoscience*, *3*(7), 459–463. http://doi.org/10.1038/ngeo891

Dickson, J. L., Head, J. W., & Barbieri, L. (2013). Martian gullies as stratigraphic markers for latitude-dependent mantle emplacement and removal. In *44th Lunar and Planetary Science Conference* (Abstract# 1012).

Dickson, J. L., Head, J. W., Goudge, T. A., & Barbieri, L. (2015). Recent climate cycles on Mars: Stratigraphic relationships between multiple generations of gullies and the latitude dependent mantle. *Icarus*, *252*, 83–94. http://doi.org/10.1016/j.icarus.2014.12.035

Dundas, C. M., & Byrne, S. (2010). Modeling sublimation of ice exposed by new impacts in the martian mid-latitudes. *Icarus*, *206*(2), 716–728. http://doi.org/10.1016/j.icarus.2009.09.007

Dundas, C. M., Diniega, S., & McEwen, A. S. (2015). Long-term monitoring of martian gully formation and evolution with MRO/HiRISE. *Icarus*, *251*, 244–263. http://doi.org/10.1016/j.icarus.2014.05.013

Fairén, A. G. (2010). A cold and wet Mars. *Icarus*, *208*(1), 165–175. https://doi.org/10.1016/j.icarus.2010.01.006

Fastook, J. L., & Head, J. W. (2014). Amazonian mid- to high-latitude glaciation on Mars: Supply-limited ice sources, ice accumulation patterns, and concentric crater fill glacial flow and ice sequestration. *Planetary and Space Science*, *91*, 60–76. http://doi.org/10.1016/j.pss.2013.12.002

Feldman, W. C., Prettyman, T. H., Maurice, S., Plaut, J. J., Bish, D. L., Vaniman, D. T., … Tokar, R. L. (2004). Global distribution of near-surface hydrogen on Mars. *Journal of Geophysical Research E: Planets*, *109*(9). http://doi.org/10.1029/2003JE002160

French, H. M. (1980). Periglacial geomorphology and permafrost. *Progress in Physical Geography*, *4*(2), 254–261.

French, H. M. (1993). Cold-climate processes and landforms. In *Canada's Cold Environments* (pp. 271–290). McGill University Press.

French, H. M. (1996). The Periglacial Domain. In *The Periglacial Environment* (p. 3). London Longman.

French, H. M. (2013). Surface Features of Permafrost. In *The Periglacial Environment* (Third Ed., pp.116-127). Wiley. http://doi.org/10.1002/9781118684931

Fuller, E. R. (2002). Amazonis Planitia: The role of geologically recent volcanism and sedimentation in the formation of the smoothest plains on Mars. *Journal of Geophysical Research*, *107*(E10), 1–25. http://doi.org/10.1029/2002JE001842

Gomes, R., Levison, H. F., Tsiganis, K., & Morbidelli, A. (2005). Origin of the cataclysmic Late Heavy Bombardment period of the terrestrial planets. *Nature*, *435*(7041), 466.

Greeley, R. (1994). Gradation. In *Planetary landscapes* (Second Ed., pp. 56-68). Chapman & Hall.

Gurney, S. D. (1998). Aspects of the genesis and geomorphology of pingos: perennial permafrost mounds. *Progress in Physical Geography*, *22*(3), 307–324.

Harrison, T. N. (2016). Martian Gully Formation and Evolution: Studies From the Local to Global Scale. *Electronic Thesis and Dissertation Repository*, Paper 3980. Retrieved from http://ir.lib.uwo.ca/etd/3980

Harrison, T. N., Osinski, G. R., Tornabene, L. L., & Jones, E. (2015). Global documentation of gullies with the Mars Reconnaissance Orbiter Context Camera and implications for their

formation. *Icarus*, *252*, 236–254. http://doi.org/10.1016/j.icarus.2015.01.022

Hartmann, W. K., & Neukum, G. (2001). Cratering chronology and the evolution of Mars. *Space Science Reviews*, *96*(1–4), 165–194. http://doi.org/10.1023/A:1011945222010

Head, J. W. (2012). Mars climate history: A geological perspective. In *43rd Lunar and Planetary Science Conference* (Abstract# 2582).

Head, J. W., Mustard, J. F., Kreslavsky, M. A., Milliken, R. E., & Marchant, D. R. (2003). Recent ice ages on Mars. *Nature*, *426*(6968), 797–802. http://doi.org/10.1038/nature02114

Head, J. W., & Wilson, L. (2011). The Noachian-Hesperian Transition On Mars: Geological Evidence For A Punctuated Phase Of Global Volcanism As A Key Driver In Climate And Atmospheric Evolution. In *42nd Lunar and Planetary Science Conference* (Abstract# 1214).

Heldmann, J. L., Carlsson, E., Johansson, H., Mellon, M. T., & Toon, O. B. (2007). Observations of martian gullies and constraints on potential formation mechanisms: II. The northern hemisphere. *Icarus*, *188*(2), 324–344. http://doi.org/10.1016/j.icarus.2006.12.010

Heldmann, J. L., & Mellon, M. T. (2004). Observations of martian gullies and constraints on potential formation mechanisms. *Icarus*, *168*(2), 285–304. http://doi.org/10.1016/j.icarus.2003.11.024

Hess, S. L., Henry, R. M., Leovy, C. B., Ryan, J. A., & Tillman, J. E. (1977). Meteorological results from the surface of Mars: Viking 1 and 2. *Journal of Geophysical Research*, *82*(28), 4559–4574. http://doi.org/10.1029/JS082i028p04559

Iverson, R. M., Logan, M., LaHusen, R. G., & Berti, M. (2010). The perfect debris flow? Aggregated results from 28 large-scale experiments. *Journal of Geophysical Research*, *115*(F3). http://doi.org/10.1029/2009JF001514

Iverson, R. M., Reid, M. E., & LaHusen, R. G. (1997). Debris-flow mobilization from landslides. *Annual Review of Earth and Planetary Sciences*, *25*(1), 85–138.

Karte, J. (1983). Periglacial phenomena and their significance as climatic and edaphic indicators. *GeoJournal*, *7*(4), 329–340.

Kneissl, T., Reiss, D., van Gasselt, S., & Neukum, G. (2010). Distribution and orientation of northern-hemisphere gullies on Mars from the evaluation of HRSC and MOC-NA data. *Earth and Planetary Science Letters*, *294*(3–4), 357–367. http://doi.org/10.1016/j.epsl.2009.05.018

Komatsu, G. (2007). Rivers in the Solar System: Water Is Not the Only Fluid Flow on Planetary Bodies. *Geography Compass*, *1*(3), 480–502. http://doi.org/10.1111/j.1749-8198.2007.00029.x

Kreslavsky, M. A., & Head, J. W. (2000). Kilometer-scale roughness of Mars: Results from MOLA data analysis. *Journal of Geophysical Research: Planets*, *105*(E11), 26695–26711.

Kreslavsky, M. A., & Head, J. W. (2002). Mars: Nature and evolution of young latitude-dependent water-ice-rich mantle. *Geophysical Research Letters*, *29*(15), 14-1-14–4. http://doi.org/10.1029/2002GL015392

Kress, A. M., & Head, J. W. (2008). Ring-mold craters in lineated valley fill and lobate debris aprons on Mars: Evidence for subsurface glacial ice. *Geophysical Research Letters*, *35*(23). http://doi.org/10.1029/2008GL035501

Lachenbruch, A. H. (1962). *Mechanics of thermal contraction cracks and ice-wedge polygons in permafrost* (Vol. 70). Geological Society of America.

Laskar, J., Correia, A. C. M., Gastineau, M., Joutel, F., Levrard, B., & Robutel, P. (2004). Long term evolution and chaotic diffusion of the insolation quantities of Mars. *Icarus*, *170*(2), 343–364. http://doi.org/10.1016/j.icarus.2004.04.005

Lefort, A., Russell, P. S., & Thomas, N. (2010). Scalloped terrains in the Peneus and Amphitrites Paterae region of Mars as observed by HiRISE. *Icarus*, *205*(1), 259–268. http://doi.org/10.1016/j.icarus.2009.06.005

Lefort, A., Russell, P. S., Thomas, N., McEwen, A. S., Dundas, C. M., & kirk, R. L. (2009). Observations of periglacial landforms in Utopia Planitia with the high resolution imaging science experiment (HiRISE). *Journal of Geophysical Research: Planets*, *114*(E4).

Levrard, B., Forget, F., Montmessin, F., & Laskar, J. (2004). Recent ice-rich deposits formed at high latitudes on Mars by sublimation of unstable equatorial ice during low obliquity. *Nature*, *431*(7012), 1072.

Levy, J. S., Fassett, C. I., Head, J. W., Schwartz, C., & Watters, J. L. (2014). Sequested glacial ice contribution to the global Martian water budget. *Journal of Geophysical Research: Planets*, (1), 2–10. http://doi.org/10.1002/2014JE004685

Levy, J. S., Head, J. W., & Marchant, D. R. (2011). Gullies, polygons and mantles in Martian permafrost environments: Cold desert landforms and sedimentary processes during recent Martian geological history. *Geological Society, London, Special Publications, 354*(1),

167–182. http://doi.org/10.1144/SP354.10

Levy, J. S., Head, J. W., Marchant, D. R., Dickson, J. L., & Morgan, G. A. (2009). Geologically recent gully-polygon relationships on Mars: Insights from the Antarctic Dry Valleys on the roles of permafrost, microclimates, and water sources for surface flow. *Icarus*, *201*(1), 113–126. http://doi.org/10.1016/j.icarus.2008.12.043

Levy, J. S., Marchant, D. R., & Head, J. W. (2010). Thermal contraction crack polygons on Mars: A synthesis from HiRISE, Phoenix, and terrestrial analog studies. *Icarus*, *206*(1), 229–252. http://doi.org/10.1016/j.icarus.2009.09.005

Lucchitta, B. K. (1981). Mars and Earth: Comparison of cold-climate features. *Icarus*, *45*(2), 264–303. http://doi.org/10.1016/0019-1035(81)90035-X

Mackay, J. R. (1979). Pingos of the Tuktoyaktuk peninsula area, Northwest territories. *Géographie Physique et Quaternaire*, *33*(1), 3–61.

Mackay, J. R. (1998). Pingo growth and collapse, Tuktoyaktuk Peninsula area, western Arctic coast, Canada: A long-term field study. *Géographie Physique et Quaternaire*, *52*(3), 271–323.

Madeleine, J.-B., Forget, F., Head, J. W., Levrard, B., Montmessin, F., & Millour, E. (2009). Amazonian northern mid-latitude glaciation on Mars: A proposed climate scenario. *Icarus*, *203*(2), 390–405. http://doi.org/10.1016/j.icarus.2009.04.037

Malin, M. C., & Edgett, K. S. (1999). Oceans or seas in the Martian northern lowlands: High resolution imaging tests of proposed coastlines. *Geophysical Research Letters*, *26*(19), 3049–3052. http://doi.org/10.1029/1999GL002342

Malin, M. C., & Edgett, K. S. (2000). Evidence for recent groundwater seepage and surface runoff on Mars. *Science*, *288*(5475), 2330–2335. http://doi.org/10.1126/science.288.5475.2330

Marchant, D. R., & Head, J. W. (2007). Antarctic dry valleys: Microclimate zonation, variable geomorphic processes, and implications for assessing climate change on Mars. *Icarus*, *192*(1), 187–222.

McGill, G. E. (1989). Buried topography of Utopia, Mars: Persistence of a giant impact depression. *Journal of Geophysical Research*, *94*(B3), 2753–2759. http://doi.org/10.1029/JB094iB03p02753

McKay, C. P. (1997). The search for life on Mars. In *Planetary and Interstellar Processes*

Relevant to the Origins of Life (pp. 263-289), Springer, Dordrecht.

Mellon, M. T., Feldman, W. C., & Prettyman, T. H. (2004). The presence and stability of ground ice in the southern hemisphere of Mars. *Icarus*, *169*(2), 324–340. http://doi.org/10.1016/j.icarus.2003.10.022

Milliken, R. E. (2003). Viscous flow features on the surface of Mars: Observations from high-resolution Mars Orbiter Camera (MOC) images. *Journal of Geophysical Research*, *108*(E6). http://doi.org/10.1029/2002JE002005

Milliken, R. E., & Mustard, J. F. (2003). Erosional morphologies and characteristics of latitude-dependent surface mantles on Mars. In *6th International Conference on Mars*.

Mischna, M. A. (2003). On the orbital forcing of Martian water and CO2 cycles: A general circulation model study with simplified volatile schemes. *Journal of Geophysical Research*, *108*(E6). http://doi.org/10.1029/2003JE002051

Moore, J. M., Howard, A. D., Dietrich, W. E., & Schenk, P. M. (2003). Martian Layered Fluvial Deposits: Implications for Noachian Climate Scenarios. *Geophysical Research Letters*, *30*(24). http://doi.org/10.1029/2003GL019002

Morbidelli, A., Levison, H. F., Tsiganis, K., & Gomes, R. (2005). Chaotic capture of Jupiter's Trojan asteroids in the early Solar System. *Nature*, *435*(7041), 462.

Morgenstern, A., Hauber, E., Reiss, D., van Gasselt, S., Grosse, G., & Schirrmeister, L. (2007). Deposition and degradation of a volatile-rich layer in Utopia Planitia and implications for climate history on Mars. *Journal of Geophysical Research: Planets*, *112*(E6).

Mustard, J. F., Cooper, C. D., & Rifkin, M. K. (2001). Evidence for recent climate change on Mars from the identification of youthful near-surface ground ice. *Nature*, *412*(6845), 411–414. http://doi.org/10.1038/35086515

Nelson, F. E., Anisimov, O. A., & Shiklomanov, N. I. (2002). Climate change and hazard zonation in the circum-arctic permafrost regions. *Natural Hazards*, *26*(3), 203–225. http://doi.org/10.1023/A:1015612918401

Neukum, G., Jaumann, R., Hoffmann, H., Hauber, E., Head, J. W., Basilevsky, A. T., … the HRSC Co-Investigator Team. (2004). Recent and episodic volcanic and glacial activity on Mars revealed by the High Resolution Stereo Camera. *Nature*, *432*, 971. http://dx.doi.org/10.1038/nature03231

Newsom, H. E., Brittelle, G. E., Hibbitts, C. A., Crossey, L. J., & Kudo, A. M. (1996). Impact

crater lakes on Mars. *Journal of Geophysical Research E: Planets*, *101*(E6), 14951–14955. http://doi.org/10.1029/96JE01139

Pidwirny, M. (2006). Periglacial Processes and Landforms. In *Fundamentals of Physical Geography* (2nd ed.). http://www.physicalgeography.net/fundamentals/10ag.html

Plescia, J. B. (2003). Amphitrites-Peneus Paterae/ Malea Planum geology. In *34th Lunar and Planetary Science Conference* (Abstract# 1478).

Pollack, J. B., Kasting, J. F., Richardson, S. M., & Poliakoff, K. (1987). The case for a wet, warm climate on early Mars. *Icarus*, *71*(2), 203–224.

Schon, S. C., Head, J. W., & Milliken, R. E. (2009). A recent ice age on Mars: Evidence for climate oscillations from regional layering in mid-latitude mantling deposits. *Geophysical Research Letters*, *36*(15). http://doi.org/10.1029/2009GL038554

Seibert, N. M., & Kargel, J. S. (2001). Small-scale Martian polygonal terrain: Implications for liquid surface water. *Geophysical Research Letters*, *28*(5), 899–902.

Séjourné, A., Costard, F. M., Gargani, J., Soare, R. J., Fedorov, A., & Marmo, C. (2011). Scalloped depressions and small-sized polygons in western Utopia Planitia, Mars: A new formation hypothesis. *Planetary and Space Science*, *59*(5–6), 412–422. http://doi.org/10.1016/j.pss.2011.01.007

Séjourné, A., & Soare, R. J. (2014). Polygon-Junction Pits. In *Encyclopedia of Planetary Landforms* (pp. 21). Springer, New York. http://doi.org/10.1007/978-1-4614-9213-9_274-1

Slaymaker, O. (2011). Criteria to distinguish between periglacial, proglacial and paraglacial environments. *Quaestiones Geographicae*, *30*(1), 85–94.

Smith, P. H., & the Phoenix Science Team. (2009). Water at the Phoenix landing site. In *40th Lunar and Planetary Science Conference* (Abstract #1329). http://doi.org/10.1029/2004GL021326

Soare, R. J., Burr, D. M., & Wan Bun Tseung, J.-M. (2005). Possible pingos and a periglacial landscape in northwest Utopia Planitia. *Icarus*, *174*(2), 373–382.

Soare, R. J., Conway, S. J., Pearce, G. D., Dohm, J. M., & Grindrod, P. M. (2013). Possible crater-based pingos, paleolakes and periglacial landscapes at the high latitudes of Utopia Planitia, Mars. *Icarus*, *225*(2), 971–981.

Soare, R. J., Costard, F. M., Pearce, G. D., & Séjourné, A. (2012). A re-interpretation of the recent stratigraphical history of Utopia Planitia, Mars: Implications for late-Amazonian

periglacial and ice-rich terrain. *Planetary and Space Science*, *60*(1), 131–139. http://doi.org/10.1016/j.pss.2011.07.007

Soare, R. J., Kargel, J. S., Osinski, G. R., & Costard, F. M. (2007). Thermokarst processes and the origin of crater-rim gullies in Utopia and western Elysium Planitia. *Icarus*, *191*(1), 95–112.

Soare, R. J., Osinski, G. R., & Roehm, C. L. (2008). Thermokarst lakes and ponds on Mars in the very recent (late Amazonian) past. *Earth and Planetary Science Letters*, *272*(1), 382–393.

Squyres, S. W. (1978). Martian fretted terrain: Flow of erosional debris. *Icarus*, *34*(3), 600–613. http://doi.org/10.1016/0019-1035(78)90048-9

Squyres, S. W. (1979). The distribution of lobate debris aprons and similar flows on Mars. *Journal of Geophysical Research: Solid Earth*, *84*(B14), 8087–8096. http://doi.org/10.1029/JB084iB14p08087

Stuurman, C., Osinski, G. R., Holt, J. W., Levy, J. S., Brothers, T. C., Kerrigan, M. C., & Campbell, B. A. (2016). SHARAD detection and characterization of subsurface water ice deposits in Utopia Planitia, Mars. *Geophysical Research Letters*, *43*(18), 9484–9491. http://doi.org/10.1002/2016GL070138

Tanaka, K. L. (1986). The stratigraphy of Mars. *Journal of Geophysical Research*, *91*(B13), E139–E158. http://doi.org/10.1029/JB091iB13p0E139

Tanaka, K. L., & Kolb, E. J. (2001). Geologic history of the polar regions of Mars based on Mars Global survey data. I. Noachian and Hesperian Periods. *Icarus*, *154*(1), 3–21. http://doi.org/10.1006/icar.2001.6675

Thomson, B. J., & Head, J. W. (2001). Utopia Basin, Mars: Characterization of topography and morphology and assessment of the origin and evolution of basin internal structure. *Journal of Geophysical Research*, *106*(E10), 23209–23230. http://doi.org/10.1029/2000JE001355

Tsiganis, K., Gomes, R., Morbidelli, A., & Levison, H. F. (2005). Origin of the orbital architecture of the giant planets of the Solar System. *Nature*, *435*(7041), 459.

Ulrich, M., Morgenstern, A., Günther, F., Reiss, D., Bauch, K. E., Hauber, E., … Schirrmeister, L. (2010). Thermokarst in Siberian ice-rich permafrost: Comparison to asymmetric scalloped depressions on Mars. *Journal of Geophysical Research: Planets*, *115*(E10).

Vaucher, J., Baratoux, D., Mangold, N., Pinet, P., Kurita, K., & Grégoire, M. (2009). The volcanic history of central Elysium Planitia: Implications for martian magmatism. *Icarus*,

204(2), 418–442.

Washburn, A. L. (1956). Classification of patterned ground and review of suggested origins. *Geological Society of America Bulletin*, *67*(7), 823–866.

Werner, S. C. (2009). The global martian volcanic evolutionary history. *Icarus*, *201*(1), 44–68. http://doi.org/10.1016/j.icarus.2008.12.019

Zanetti, M., Hiesinger, H., Reiss, D., Hauber, E., & Neukum, G. (2010). Distribution and evolution of scalloped terrain in the southern hemisphere, Mars. *Icarus*, *206*(2), 691–706. http://doi.org/10.1016/j.icarus.2009.09.010

Chapter 2: Observation of Decameter-scale Rimmed Depressions, their inferred formation mechanism, and implications for the late Amazonian geologic history of Utopia Planitia

2.1 Introduction

Currently, Mars appears to be in a 'frozen' and dry state, with the clear majority of the planet's surface maintaining year-round sub-zero temperatures [*Arvidson et al.*, 1989; *Hess et al.*, 1977]. Together with the low pressure of the thin atmosphere of Mars, climate conditions do not accommodate the formation or long-term sustainment of liquid water on its surface [*Carr*, 1983; *Martínez & Renno*, 2013]. However, the Mariner missions gave birth to hypotheses that suggested the Martian climate had a much 'wetter' past, with the discovery of morphologies such as valley networks, tributary channels and delta deposits, and patterned ground including hummocky, polygonised, scalloped, and pitted terrain, closely resembling those found in periglacial environments on Earth [*Balme et al.*, 2009; *Gallagher et al.*, 2011; *Levy, Head, Marchant, et al.*, 2009; *Mangold*, 2005; *Séjourné et al.*, 2011]. The evidence for the potential periglacial landscape of Mars lies in these landform morphologies that extend from the mid to high latitudes, typically with none lower than 20º N/S [*Balme et al.*, 2009; *Gallagher et al.*, 2011; *Mellon et al.*, 2009]. Their distribution characteristic is suggested to reflect the nature of the obliquity shift of Mars, having a range from 0–60º, with the extent of this range having been fully exploited at least two times within the last 10 Ma (i.e., late Amazonian) [*Laskar et al.*, 2004; *Mischna*, 2003]. These shifts have a paramount influence on the climate of Mars, as they control the surface water/ice stability, and results in cycles of ice migration that form planet-wide formation of ice-cover that can extend from poles to the low latitudes [*Levrard et al.*, 2004; *Madeleine et al.*, 2009]. Additionally, the repeated changes in the obliquity of Mars has produced up to 20 shifts, with obliquities <30º, throughout the past few million years (i.e., 2.0– 2.5 Ma), while it currently resides at an obliquity like that of Earth at ~ 25º [*Laskar et al.*, 2004; *Mischna*, 2003].

The high-resolution satellite imagery from the surface of Mars, via instruments including High Resolution Imaging Science Experiment (HiRISE), and Context Camera (CTX) instruments aboard the Mars Reconnaissance Orbiter (MRO) satellite, commonly monitor excavation of surface ice by impact cratering activity. In conjunction, the Phoenix lander

reported shallow-subsurface ice at its respective landing site in Vastitas Borealis on Mars [*Hess et al.*, 1977; *Mellon et al.*, 2009; *Smith*, 2013]. Data from the Mars Odyssey satellite, equipped with the Gamma Ray Spectrometer (GRS), has provided substantial evidence for the presence of oxygen-bound hydrogen, within the upper metre of the mid-latitude regions [*Boynton*, 2002; *Dundas & Byrne*, 2010; *Mellon et al.*, 2004]. With the launch of the MRO satellite, the Shallow Radar (SHARAD) instrument, through measuring the dielectric response at the decameter scale, alongside Compact Reconnaissance Imaging Spectrometer for Mars (CRISM), further solidified the GRS observations [*Mustard et al.*, 2008; *Smith et al.*, 2013]. Moreover, the potential of such features provides evidence of a 'water-rich' climate and geologic history, at least specific to the mid-latitudes of Mars, based on their high sensitivity to environmental changes (e.g., hydrologic, thermal, etc.) [*French*, 2013; *Nelson et al.*, 2002]. The spatial analysis and relative stratigraphy of these features is key to understanding climate change on Mars. While these potentially periglacial landforms can be ubiquities across the planet, their clustering in certain regions of Mars has attracted the attention of the scientific community. For this reason, Utopia Planitia, amongst the regions situated in the northern plains of Mars, in conjunction with increase in availability of high-resolution imagery thanks to the HiRISE and CTX instruments, has been a great region of interest to researchers [e.g., *Kerrigan*, 2013; *Lefort et al.*, 2009; *Séjourné et al.*, 2011; *Soare et al.*, 2005].

We recognize and advocate that morphological analysis is a reliable step when uncertain about the genetic nature of a landscape [cf. *Komatsu*, 2007]. As such, in an attempt to investigate further the claims on the climate history and landscape evolution of the Martian northern plains within the Late Amazonian period, we have studied an area in Utopia Planitia. We begin with a thorough morphologic and morphometric description of an underreported feature in Utopia Planitia, which we have dubbed 'Decameter-scale Rimmed Depressions' (DRDs). Subsequently, we describe the spatial and stratigraphic relationship of DRDs to the most relevant landscape features (i.e., those potentially periglacial in nature). Previous workers have identified morphologically similar landscape features, such as 'brain coral' [*Williams et al.*, 2008], 'brain coral terrain' [*Noe Dobrea et al.*, 2007], and 'brain terrain' [*Levy et al.*, 2009]; however, these features continue to be an active area of research, and thus the relationship (if any) between the previously studied features and DRDs will be investigated in this study. We believe DRDs serve as valuable stratigraphic markers, similar to those utilized in prior studies (e.g., scalloped

depressions) [*Soare et al.*, 2012]; via which we will suggest a late Amazonian geologic history of Utopia Planitia and consolidate our claims.

2.2 Methods

Our study area contains 105 HiRISE images providing local coverage, and 229 CTX images providing complete coverage of the study region. Due to significant overlap in the available CTX imagery, and to narrow down the CTX selection and fine-tune georeferencing, the Mars Orbiter Laser Altimeter (MOLA) global mosaic [*Albee et al.*, 2001; *Smith et al.*, 2001] was used as a base layer. Subsequently, day infra-red imagery from THermal EMission Imaging System (THEMIS Day IR), at a resolution of 100m per pixel [*Christensen et al.*, 2004] was used to create a mosaic of the study area, georeferenced to MOLA, to bridge the gap between MOLA and CTX resolutions. Finally, the production of the CTX mosaic followed the same procedures as the THEMIS Day IR mosaic, but instead using the THEMIS Day IR mosaic as the base-layer for georeferencing purposes, as opposed to MOLA. In both of these mosaics, while full coverage of the study area is available, there are data gaps within our created mosaic, specifically in regard to CTX. This is because the mosaic sorting order was adjusted to prioritize imagery with regard to; 1. Lowest emission angle; 2. Least difference in emission angle relative to overlapping/neighbouring images; 3. Least difference in time of captured imagery relative to overlapping/neighbouring images; and 4. Least difference in band statistics relative to overlapping/neighbouring images. This ensured that imagery with high emission angles or with a high difference in emission angle to their neighbouring images did not result in a skewed or unaligned mosaic. As well, the similarity in the time the image was taken and band statistics assured that the consistency in terms of lighting and seasonal conditions was maintained and that post-processing colour-corrections, which may increase overall error, were not needed. In cases where an image contained significant data gaps, or vastly differed in the variables discussed above from its neighbouring images, it was discarded from the mosaic.

Within some places within our study area (e.g., the large impact craters), seasonal monitoring via the HiRISE instrument had taken place. This means that multiple images covering the same locality, with difference in time and image parameters, were available. In these cases, we chose the image with the most similarity in image parameters and time of day/year, relative to the rest of our HiRISE images in our database, provided that, such an image

had no errors/artefacts and showcased good visibility (e.g., no atmospheric haze). From 105 HiRISE images, 26 containing DRDs were selected as summarized in Table 2.1. Within the locality of each available HiRISE image utilized in our study, we classified the DRDs into 3 different type of distribution classes: 1. Cluster, 2. Random, 3. Dispersed. These classes were based on using a 500 x 500-metre moving window, within a HiRISE image, to analyze the nearest neighbour ratio of DRDs within each window using the geostatistical analyst toolbox of ArcGIS 10.5 (Figure 2.2). The term 'moving window' refers to the statistical method of data analysis, whereby a 'window' of pre-determined size is moved across the data, in this case HiRISE images, to reveal spatial variability. The location of individual DRDs (represented by red dots in Figure 2.2), were manually mapped and inputted into the 'Nearest Neighbour Average' tool available through ArcMap 10.5. The program then measured the separation between a point to its nearest neighbour, for every point in the 'window'. Within one 'window', the average of these nearest neighbour distances was then compared to an arbitrary random distribution, where an average lesser than the arbitrary random distribution was considered clustered, while a value greater would have been considered dispersed [*Ebdon*, 1985; *Mitchel*, 2005]. The value of the arbitrary random distribution is simply the expected average nearest neighbour distance, calculated based on the number of points within the sample (in this case DRDs) and the total sampling area (in this case 'window') [*Ebdon*, 1985; *Mitchel*, 2005]. The nearest neighbour ratio, as reported in Figure 2.2, is the numeric representation of the observed average nearest neighbour distance being divided by the expected average nearest neighbour distance [*Ebdon*, 1985; *Mitchel*, 2005]. The assumption here was that there were no topographic or stratigraphic barriers that controlled the location of where DRDs appeared [c.f. *Ebdon*, 1985; *Mitchel*, 2005]. This is also another reason why a moving 'window' was used to calculate the nearest neighbour ratios, as opposed to calculating the nearest neighbour ratio for the entirety of a HiRISE image at once. That is, we used smaller subsamples to minimize the error in our calculation due to changes in elevation or structural barriers. Furthermore, the p-value and the z-score reported represent the possibility of error in the calculated nearest neighbour ratio. The p-value represents the probability that the observed distribution is random, where a small p-value would indicate a low likeliness for randomness, while the z-score reports the standard deviation [*Ebdon*, 1985; *Mitchel*, 2005]. In simple terms, a low p-value in combination with a high z-score (either negative or positive), suggests that it is highly unlikely for the results to be random.

In combination, ISIS3 [*Anderson et al.*, 2013], an open-source planetary image processing software provided by USGS, and 'StereoPipeline'[*Shean et al.*, 2016], an open-source tool as part of NASA's Neo-Geographic Toolkit (NGT), were used to generate two DEM products that were utilized in geometric data collection (e.g., height, aspect, etc.). The tools, and their explanation, used to produce these DEM products, using ISIS3, are summarized, in respective order, as follows (for the detailed explanation see Shean et al. [2016]):

1. 'hiedr2mosaic.py'
   a. Transformation of HiRISE .IMG to ISIS .cub format
   b. Calibration using spacecraft imaging parameters
   c. Arranging channels from instrument sensors to assemble the whole image
   d. Fine-tuning alignment of channels and reducing noise or 'jitter'
   e. Mosaicking the two stereo images into a single file
2. 'cam2map4stereo'
   a. Determines minimum overlap between stereo-pair images
   b. Determines worst common resolution between stereo-pair images
   c. Map-projects the two stereo-pair images to identical overlap and resolution
3. 'stereo'
   a. Preprocessing of stereo-pairs
   b. Disparity map creation between stereo-pairs
   c. Sub-pixel refinements
   d. Filling holes in the point cloud and discarding outliers
   e. Triangulation of the point cloud
4. 'point2dem'
   a. Production of DEM from point cloud
   b. .tif file output with header files

HiRISE Image ID	Resolution/Pixel	Longitude (+E)	Latitude (+N)
ESP_027610_2205	25	125	40.1
PSP_010679_2205	50	120.1	40.3
PSP_006249_2210	25	116.6	40.6
PSP_006908_2215	25	124.1	41.1
ESP_026041_2215	50	118.4	41.4
PSP_005972_2220	25	120.6	41.7
ESP_046032_2225	25	116.8	42.2
ESP_025632_2225	50	122.7	42.2
ESP_036366_2235	50	115.4	43
ESP_037223_2235	50	115.8	43
ESP_028929_2240	50	117	43.5
ESP_027821_2245	25	124.7	43.9
PSP_006882_2245	25	112	44
ESP_045610_2245	25	118.5	44.2
ESP_026621_2250	25	123	44.4
ESP_026410_2250	50	123.3	44.5
ESP_026265_2250	25	122.2	44.7
PSP_006618_2250	25	120.9	44.8
ESP_027808_2255	25	119.2	45
ESP_028072_2255	50	111.5	45.4
ESP_034164_2260	25	110.8	45.5
ESP_027650_2275	50	112.2	46.5
ESP_026450_2270	50	110.9	46.8
ESP_046757_2270	50	122.7	46.9
ESP_035614_2280	50	122.3	47.6

Table 2.1: Summary of HiRISE images containing DRDs within our study area.
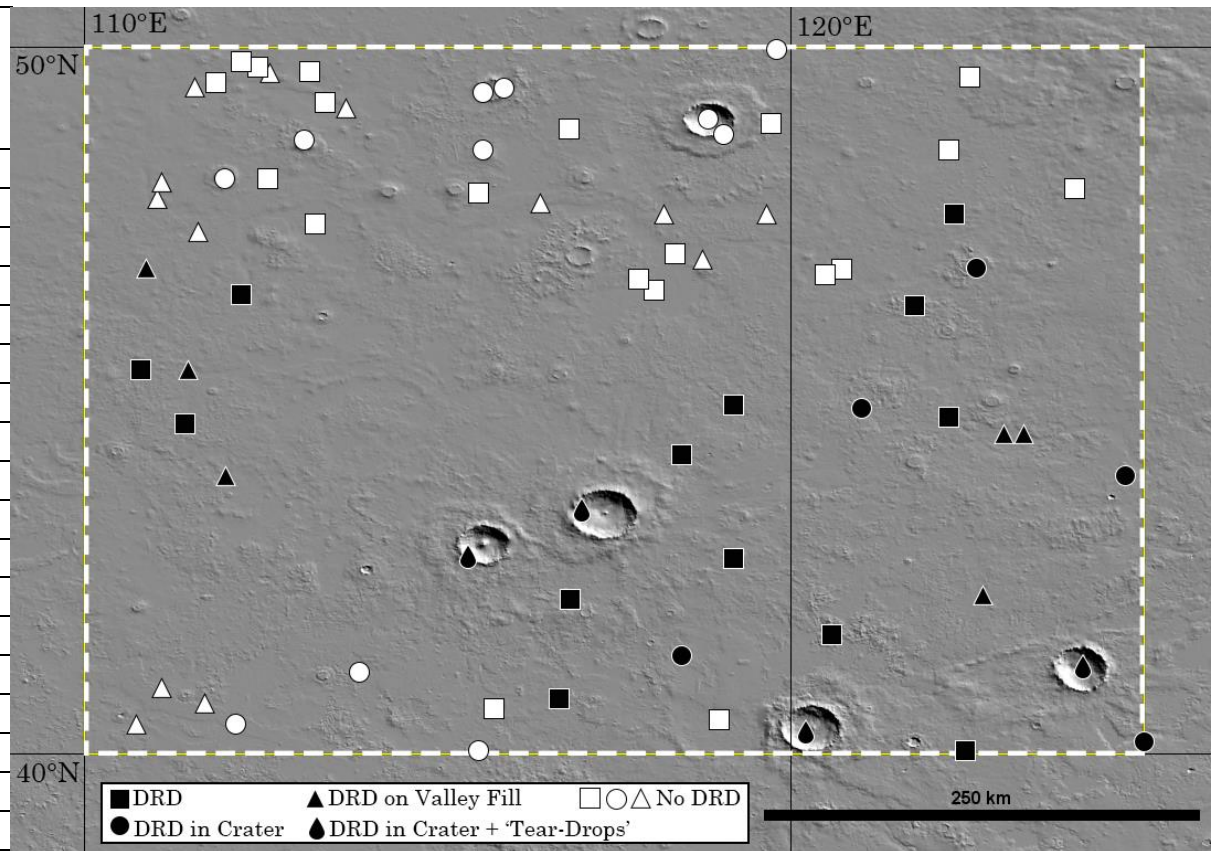
Figure 2.1: Overview of the study area, indicated by the white dotted rectangle. The points represent locations of available HiRISE imagery, with the colour black outlining observations of DRD, while the white ones indicate no DRD presence. Basemap image *credit: NASA-Goddard Flight Center/JPL/MOLA Science Team/USGS/JMARS.*
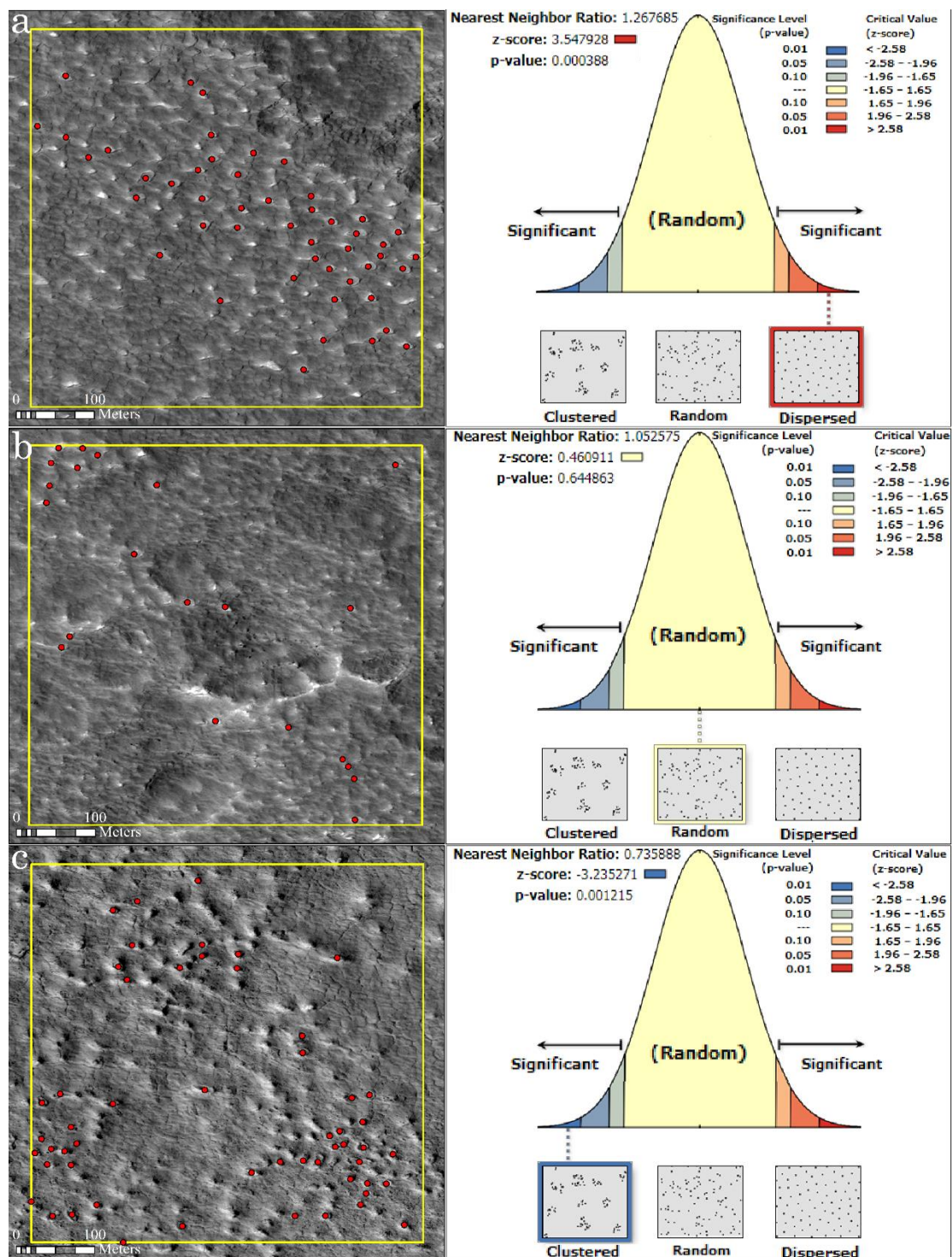
Figure 2.2: Examples of Nearest Neighbour (NN) analysis. The box in each sub-image outlines the 500 x 500-metre moving window, while the dots outline the centre of each individual DRD within the moving window. The nearest neighbour analysis result of each sub-image, **(a)** Dispersed, **(b)** Random, and **(c)** Cluster, is displayed to its right. *Credit: NASA/JPL/University of Arizona/ESRI.*

2.3 Observations and Results

The term Decameter-scale Rimmed Depression is only used to describe the morphologic nature of the feature, and not to infer any geologic process(es). These features are small-scale basins surrounded by a thin rim or wall, no more than few metres in width, that stands at a higher elevation relative to the terrain surrounding the feature. The height of these rims extends from less than 1 metre, in degraded instances, to no higher than a few metres, in well-preserved examples (e.g., Figure 2.3). The interior depth of these features is similar to the local elevation surround the feature, and depending on preservation state is no lower than a few metres measured from the top of the feature's rims. While the overall aerial-view of DRDs is generally quasi-circular, their shape can highly vary when these features coalesce. As such, we have classified their morphology into two different categories: Ellipse, (Figure2.4) and Labyrinth (Figure 2.4). The ellipse morphology exhibits a clear separation between individual DRDs with flatter terrain between the features. Ellipse morphologies observed on the steep slopes of crater walls, commonly lack a completely enclosing rim (Figure 2.4c) and are 'tear-drop' shaped. Morphologically, they bear similarity to the apron of gullies, where the 'U' shaped enclosure of the apron faces towards the down-slope direction. For clarity, in this study we specifically consider 'ellipse morphologies' (e.g., Figures 1.12 and 2.4a) as DRDs; while 'labyrinth morphologies' (e.g., Figure 2.4b) and 'tear-drops' (e.g., Figure 2.4c) are reported only as an extension, or morphologic transitions, of DRDs.
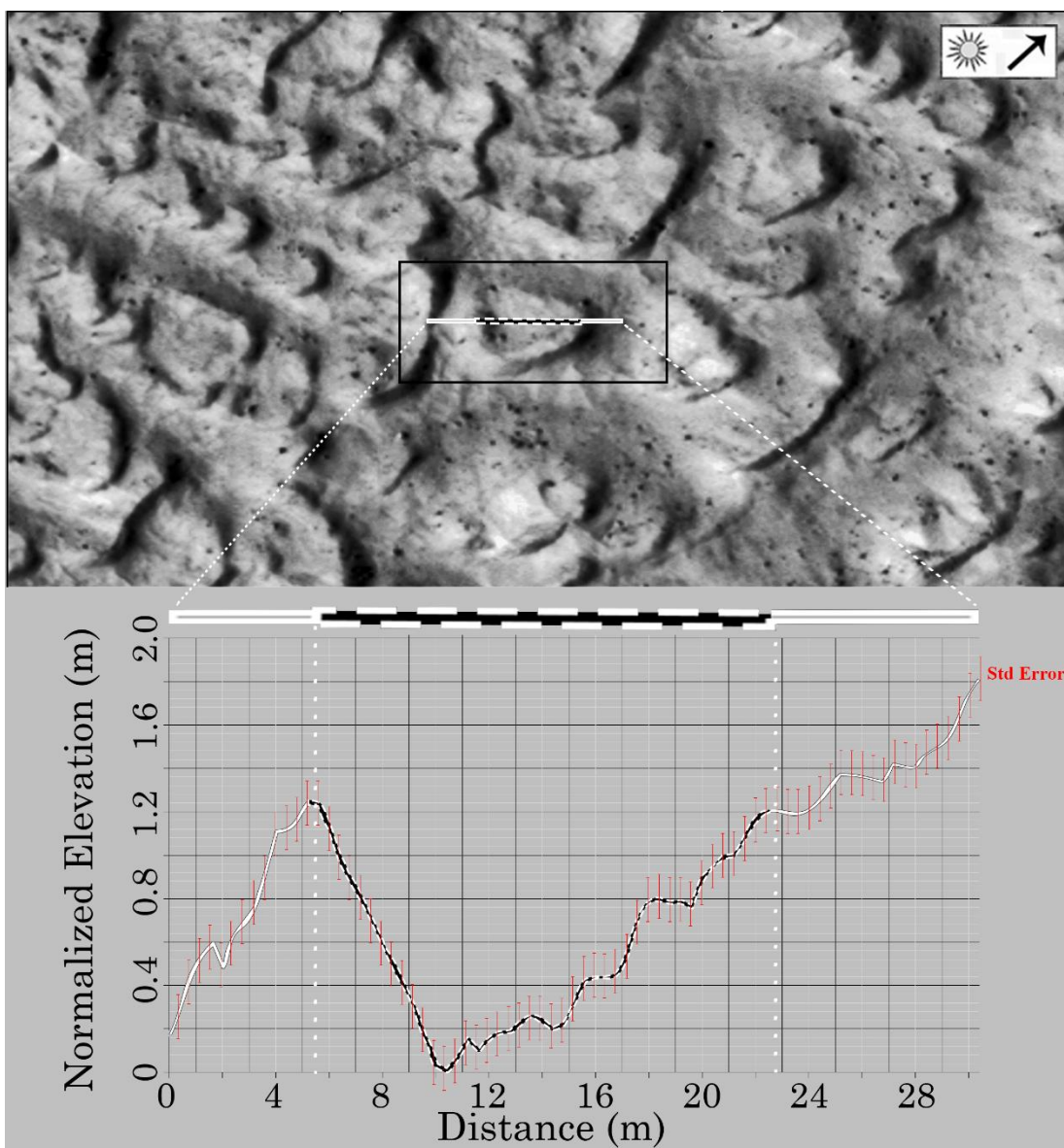
Figure 2.3: An example of a 2D vertical profile graph used to calculate the vertical and horizontal displacement of a DRD, in this case, an ellipse morphology. The white line in the image corresponds to the white profile line in the graph, while the dotted black line portion is equivalent to the long-axis length of the feature measured by rim to rim separation. This is a normalized elevation profile, assuming an elevation of 0 at the interior floor of the feature. Portion of HiRISE image PSP_001528_2210. *Image Credit: NASA/JPL/University of Arizona*.
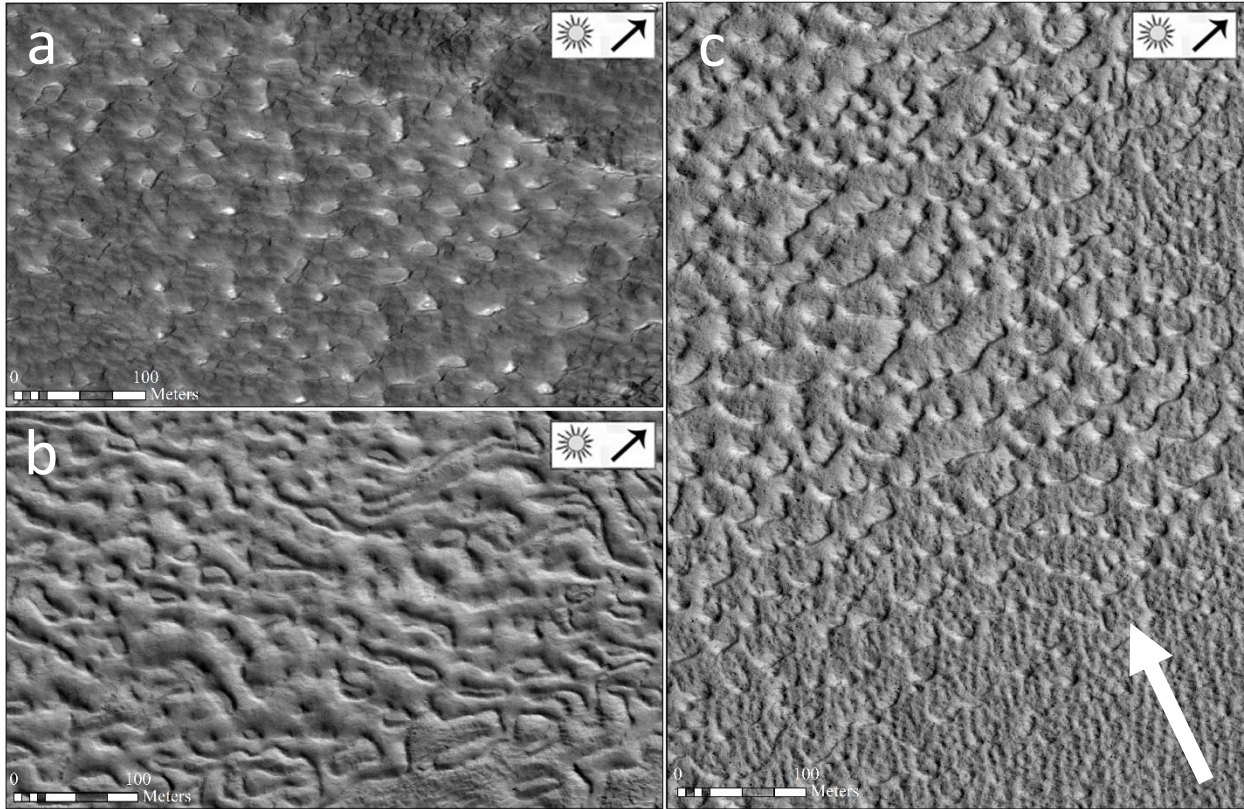
Figure 2.4: **(a)** Ellipse DRDs on relatively flat terrain (HiRISE ESP_026450_2270), **(b)** Labyrinth DRDs on a flat valley floor (HiRISE PSP_005972_2220), **(c)** Ellipse DRDs on high-sloping crater wall. The white arrow points downhill and there is a net elevation change of ~40 metres from bottom to top (HiRISE PSP_006908_2215). *Image credit: NASA/JPL/ University of Arizona.*

Alternatively, the labyrinth morphology is composed of coalescing DRDs, that are directly adjacent to one another, sharing rims, and often shaping complex sinuous channels which form a maze-like overview (Figure 2.4b). These types of morphologies are strictly found in low-lying, relatively flat terrain, and never observed on slopes. Within our observations, ~28% were found on crater floors, while the remaining were observed on some type of locally low-lying topography, in between scarps, on etched out or dissected pockets in the landscape, at times within continuous ejecta of mantled impact craters (Figure 2.5). In fact, in many examples, the transition from labyrinth to ellipse morphologies can be observed, for instance, morphing from the slopes of crater walls to the crater floor (Figure 2.6).
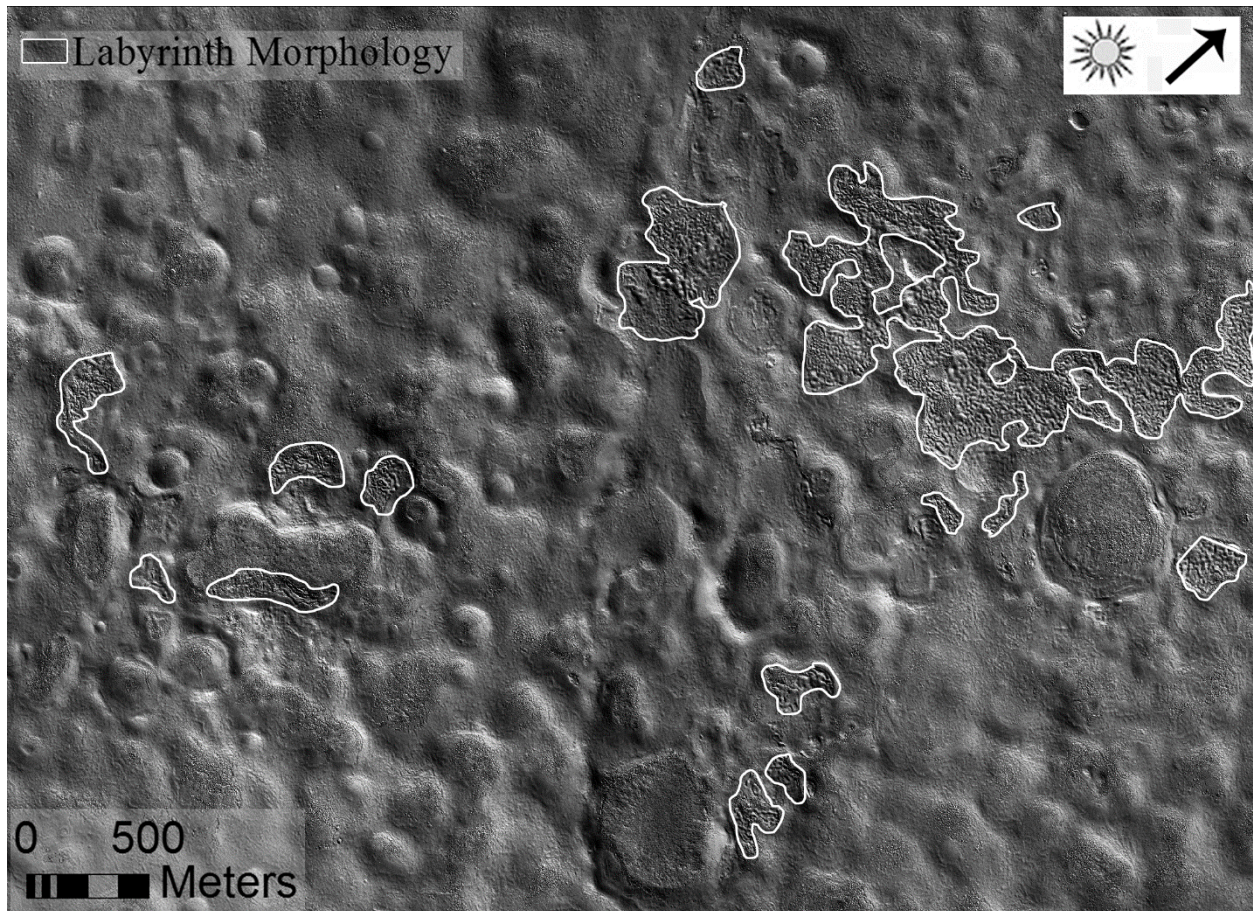
Figure 2.5: An example of the distribution of labyrinth morphologies that are not restricted to crater floors, where the white lines outline the labyrinth morphologies. (HiRISE PSP_006249_2210). *Image credit: NASA/JPL/University of Arizona.*
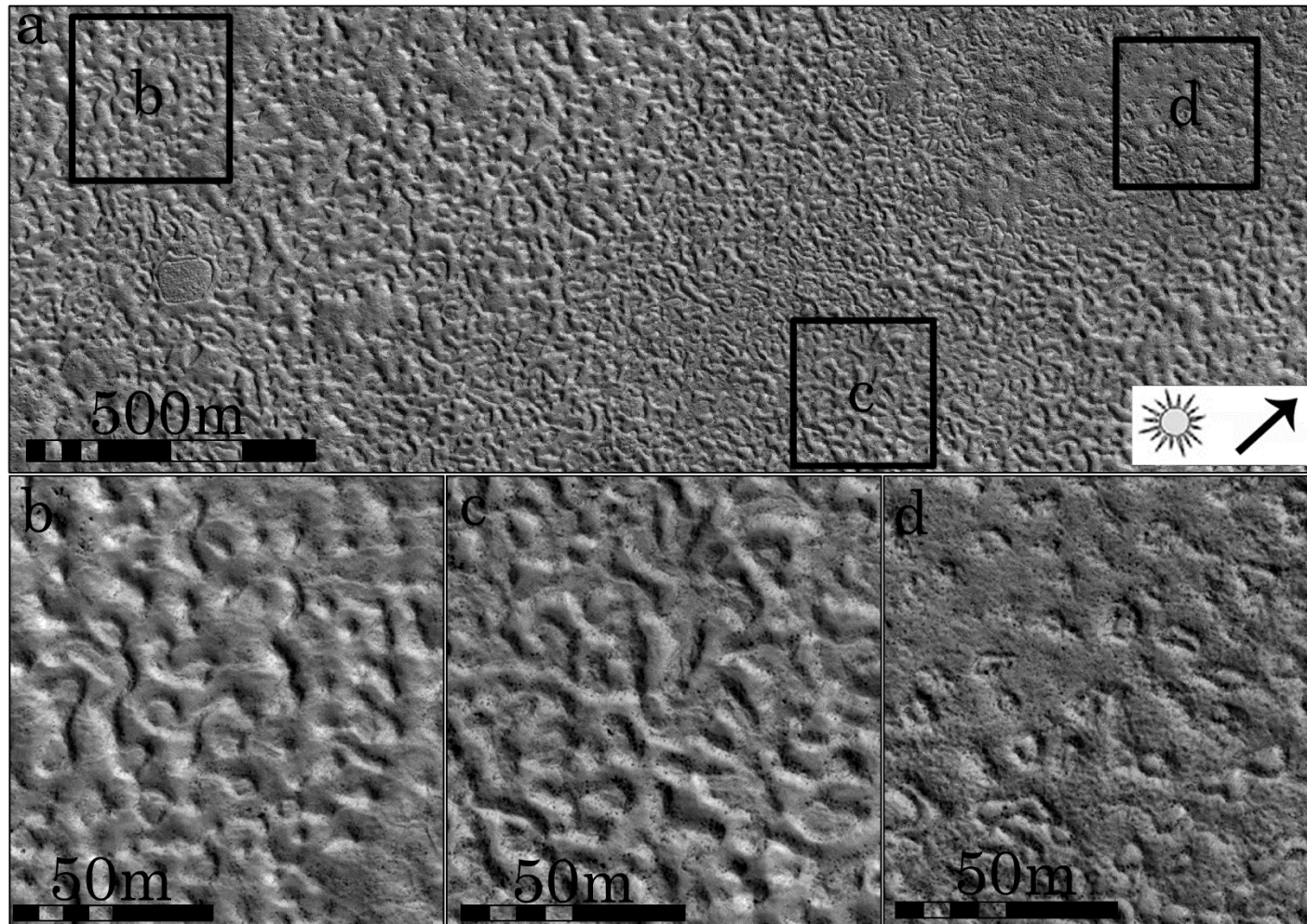
Figure 2.6: **(a)** Overview of a section of HiRISE PSP_006882_2245 showing an example of the transition between labyrinth and ellipse morphologies. **(b)** and **(c)** show changes in labyrinth morphology and transition to **(d)** ellipse morphology. *Image credit: NASA/JPL/University of Arizona.*

Geographically, no DRDs were found north of 48°N within our study area, with their maxima appearing at ~44°N (Figures 2.1 and 2.7). In terms of their spatial distribution within individual HiRISE images, one image could contain all three distribution classes (i.e., cluster, random, dispersed). In dispersed distributions, DRDs appear in near uniform spacing from one another, while in clustering distributions the distance between individual DRDs is variable, typically forming multiple groups of closely-spaced DRD's within a moving window. In random distributions, the number of DRDs within the statistical moving window is comparatively sparse with large and variable separations between individual DRDs (Figure 2.2). That being said, a Factor Analysis of Mixed Data (FAMD) on the type of distribution(s) found within each HiRISE image revealed that with increasing latitude, random distribution becomes more dominant, while dispersed and cluster distributions became prevalent with decreasing latitude (Figure 2.7). Having said that, dispersed distributions remained the dominant pattern observed for DRDs within the entirety of our study area.
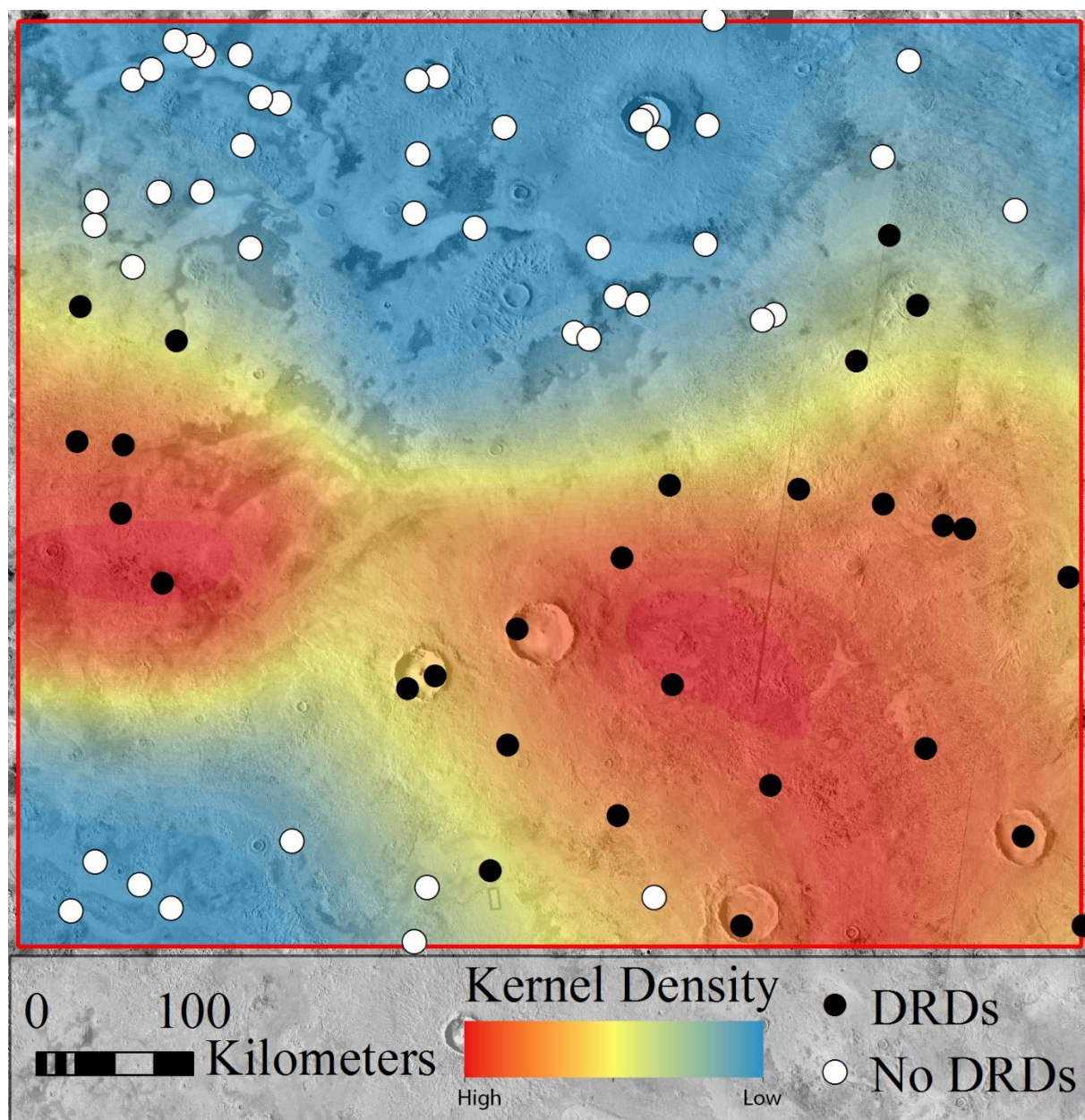
Figure 2.7: A kernel smoothened layer overlaying the extent of our study area. The red regions correspond to the highest concentration of DRDs found, as well as correlating with the maxima of cluster and dispersed distributions. Conversely, the shift of the colour ranges from red to blue depicts the transition of DRD distributions to random and outlining regions where DRDs were not observed in HiRISE images. The dots showcase the location of the available HiRISE imagery within our study area, where the colour black is appointed to imagery that contained DRDs. A mosaic created from the Thermal Emission Imaging System (THEMIS) Day Infra-red (IR) imagery is used for the base map in this image. *Basemap image credit: NASA/JPL/Arizona State University/USGS/JMARS.*

For any geometric measurement carried out within our study, except for height and elevation measurements, we limited our sampled DRDs to ellipse morphology. This is because in labyrinth morphologies, coalescence of DRDs are quite common and, therefore, the delineation of individual DRDs for geometric measurement proved difficult. To this end, we used a sample of 50 randomly chosen DRDs per HiRISE image for all of the measurements reported here. Put simply, the random sampling of DRDs were done via executing the 'RAND' function on a table, containing a list of mapped DRDs within an image, in Microsoft Excel. As such, with an average long- to short-axis ratio of 2/1; the long-axes, measured by rim to rim separation, ranged from 5 to 48 m, while their short-axis ranged from 3 to 24 m. Moreover, the average DRD measures ~18 by 9 m in length (Figure 2.8). As well, in all instances where the ellipse morphology is observed, the orientation of the long-axis of individual DRDs, on a local-scale (i.e., per HiRISE image), are roughly parallel in direction, which broadly extends from South-East to North-West (Figure 2.9).
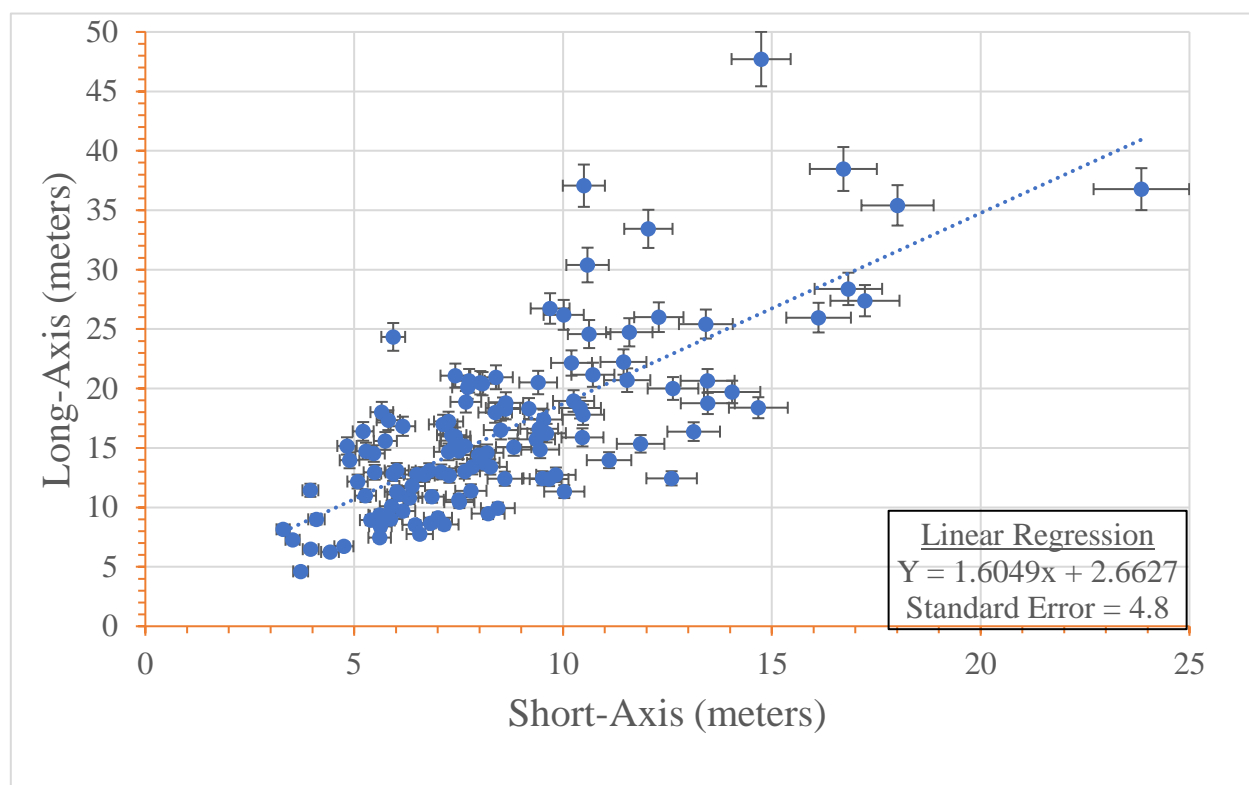
Figure 2.8: Long- and short-axis measurements example from a sample of 125 DRDs. This sub-sample was selected as the representative of the results from the entire measured sample of 1300 DRDs, for better visualization. Note the line-of-best-fit for both the long- and short-axes, which was used to estimate the ratio (i.e., the trend of their overall shape).
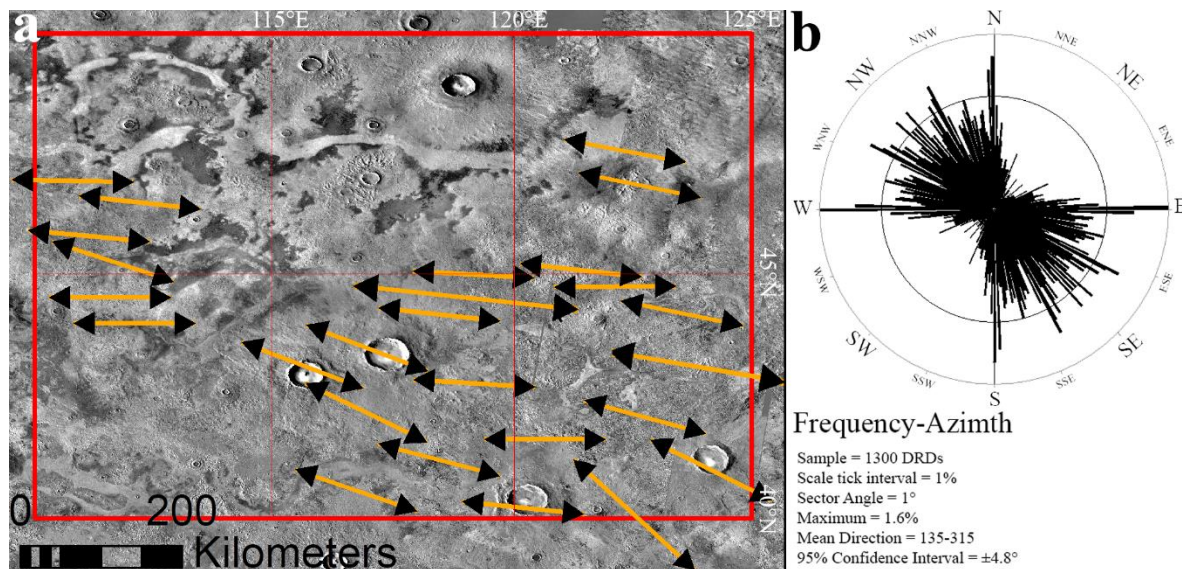
Figure 2.9: **(a)** The average long-axis orientation of DRDs, generalized based on 50 DRDs within each individual HiRISE image that was identified to contain DRDs. (b) Rose diagram showing the long-axis orientation data from 1300 DRDs. A mosaic created from the Thermal Emission Imaging System (THEMIS) Day Infra-red (IR) imagery is used for the base map in this image. *Basemap image credit: NASA/JPL/Arizona State University/USGS/JMARS.*

A thorough landscape survey within our study area, via the help of the available HiRISE imagery, as well as custom-made CTX and THEMIS Day-IR mosaics, revealed 5 dominantly occurring features that appear in spatial correlation with DRDs (summarized in Table 2.2). This survey included the dissection of LDM, an ice-rich depositional 'apron' [e.g., *Kreslavsky & Head, 2002*]; Scalloped Depression bearing terrain, rimless degradational by-products of LDM [e.g., *Mustard et al., 2001*]; IRFs (i.e., CCF/LVF/LDA), debris-covered ice-rich glacial flow deposits [e.g., *Squyres, 1979*]; LCP and HCP, polygonal patterned ground [e.g., *Drew & Tedrow, 1962*]; and gullies, channel incisions on high-sloping terrain [e.g., *Malin & Edgett, 2000*].

Image ID	Res/Pixel	Lat.	Long.	Distribution	Morphology	LCP	HCP	Gully	Scallop	LDM	CCF/LVF/LDA
ESP_027610_2205	25	125	40.1	C + R	E	N	Y	N	N	Y	Y
PSP_010679_2205	50	120.1	40.3	C + D	E (Tear Drops) + L	Y	Y	Y	N	Y	Y
PSP_006249_2210	25	116.6	40.6	C + D + R	E + L	N	Y	N	Y	N	Y
PSP_006908_2215	25	124.1	41.1	C + D	E (Tear Drops) + L	Y	Y	Y	Y	Y	Y
ESP_026041_2215	50	118.4	41.4	C + D	E + L	N	Y	N	N	Y	Y
PSP_005972_2220	25	120.6	41.7	C + D	E + L	N	Y	N	Y	Y	Y
ESP_025632_2225	50	122.7	42.2	C + D + R	E + L	N	Y	N	N	Y	Y
ESP_046032_2225	25	116.8	42.2	C	E + L	N	Y	N	N	Y	Y
ESP_036366_2235	50	115.4	43	C	E (Tear Drops)	Y	Y	Y	Y	Y	Y
ESP_037223_2235	50	115.8	43	C + R	E (Tear Drops)	Y	Y	Y	Y	Y	Y
ESP_028929_2240	50	117	43.5	C + D	E (Tear Drops) + L	Y	Y	Y	Y	Y	Y
ESP_027821_2245	25	124.7	43.9	C + R	E + L	N	Y	N	N	N	N
PSP_006882_2245	25	112	44	C + D	E + L	N	Y	N	N	N	N
ESP_045610_2245	25	118.5	44.2	C + D	E + L	Y	Y	N	Y	Y	N
ESP_026621_2250	25	123	44.4	C + D + R	E	Y	Y	N	Y	Y	Y
ESP_026410_2250	50	123.3	44.5	C + D + R	E + L	Y	Y	N	Y	Y	Y
ESP_026265_2250	25	122.2	44.7	C + D	E + L	N	Y	N	Y	N	Y
PSP_006618_2250	25	120.9	44.8	C + D + R	E + L	Y	Y	N	Y	Y	N
ESP_027808_2255	25	119.2	45	C + D	E	Y	Y	N	Y	Y	Y
ESP_028072_2255	50	111.5	45.4	C + D	E + L	Y	Y	N	Y	N	N
ESP_034164_2260	25	110.8	45.5	C + D + R	E	Y	Y	N	Y	Y	Y
ESP_027650_2275	50	112.2	46.5	C + D + R	E	Y	Y	N	Y	Y	Y
ESP_026450_2270	50	110.9	46.8	C + D	E	Y	Y	N	Y	Y	Y
ESP_046757_2270	50	122.7	46.9	C + R	E	Y	Y	N	Y	Y	Y
ESP_035614_2280	50	122.3	47.6	R	E + L	N	Y	N	Y	N	N

Table 2.2: Summary of results from our landscape survey. Note that for 'Distribution', **C** corresponds to cluster, **D** corresponds to dispersed, and **R** corresponds to random. For 'Morphology', **E** corresponds to ellipse, and **L** corresponds to labyrinth. The abbreviation of the name of features correspond, respectively, to the following: **LCP** = low-centre polygon, **HCP** = high-centre polygon, **Scallop** = scalloped depressions, **LDM** = latitude-dependent mantle dissection, **CCF** = concentric crater fill, **LVF** = lineated valley fill, and **LDA** = lobate debris apron. With respect to 'CCF/LVF/LDA' column, a 'Y' indicates the presence of at least 1 of these features. In the case of gullies, it may appear that there is no strong spatial correlation since there is more imagery where they are absent than present; however, gullies were found to be strongly correlated with ellipse morphologies on high slopes (i.e., 'tear-drops').

2.4 Discussion

Decameter-scale Rimmed Depression (DRD) is terminology that we have opted to describe objectively the geomorphology of a landform feature observed in Utopia Planitia. DRDs are evident as decameter-scale depressions in the terrain, either entirely or partially encompassed by a rim, no more than a few metres high (e.g., Figure 2.4). These features occur in communities, generally closely-packed together, though they are found with different arrangement distributions (i.e., random, dispersed, clustered) (see Table 2.2). Their overall shape is quasi-circular when distinct from one another (i.e., ellipse morphology), while in instances where they coalesce, they can appear complex, forming labyrinthine channels (e.g., Figures 2.4b and 2.6). Regardless, within a community, DRDs are nearly uniform in size, shape, and long-axis orientation direction.

Topographic lows, such as crater and valley floors, or pitted, pocked, and dissected terrain (e.g., Figure 2.5), appear as favourable areas for aggradation of labyrinth morphologies. On the other hand, ellipse morphologies do not show topographic restrictions in their assembly. In many examples, distinct transitions between these two morphological groups can be observed across an undulating landscape (e.g., Figure 2.6). Notably, on high slopes, ellipse morphologies morph into elongated 'tear-drop' shapes, at times, with rims partially encircling only the lobate portion of the feature (Figure 2.4c).

Geographically, DRDs, alike other potentially periglacial landscape features, occur predominantly in the mid-latitude bands, while more morphologically muted examples can be found in high-latitudes as well (Figure 2.7). Importantly, DRDs always occur spatially associated with patterned ground, specifically polygonised terrain (Table 2.2). As well, their proximity of occurrence to ice-rich remnants, such as LDM, including dissected and degraded instances (e.g., scalloped depressions), and IRFs (i.e., CCF/LDA/LVF), is another notable correlation. In respect to DRD development in craters, 'tear-drops' were always found accompanied by gully presence; although, not all DRD occurrence in craters were accompanied by 'tear-drops' (Table 2.2).

Previous work on Mesoscale Raised Rim Depressions (MRRDs) [*Burr, Bruno, et al.*, 2009], provides some overlap with our observations with respect to DRDs. MRRDs account for a variety of landscape features, coherent in morphology, which either have a hydrovolcanic, sedimentary, or ice-related origin. Considering the overlap in genetics between MRRD features and taking into account the proximity of morphology and spatial statistic parameters of

individual members of MRRDs in respect to DRDs, only a subset of these features that exhibit the most affinity to DRDs, with at least one from each genetic subcategory, will be discussed here. In the case of pseudocraters, modernly referred to as rootless cones, on Mars they possess diameters from 20 to 300 m, and are always found in closely-packed arrangements (i.e., clusters or group distributions) [*Lanagan et al.*, 2001]. More than that, rootless cones on Earth bear the same distributions and identical range of hectometre-scale diameters (roughly between 5 to 250-m), with decameter-scale net-heights [*Chapman et al.*, 2000; *Greeley & Fagents*, 2001]. In comparison, DRDs have diameters that range as low as 6 to as high as 20 m, with heights of, at most, 1 to 2 m, and found in 'isolated' (referred to as 'random' in this study), as well as clustered and group distributions (referred to as 'dispersed' in this study).

Moreover, pingos, which have been an area of research particularly in Utopia Planitia within the recent years [*Burr, Tanaka, et al.*, 2009; *de Pablo & Komatsu*, 2009; *Dundas et al.*, 2008; *Soare et al.*, 2005, 2013], are not known to commonly occur in clustered distributions, with heights that can reach in excess of 60 m and diameters up to 300 m [*Embleton & King*, 1975; *French*, 2013; *Gurney*, 1998; *Mackay*, 1978, 1994; *Porsild*, 1938]. Furthermore, with the exception of collapsed pingos, domal shapes are a common morphology associated with pingos [e.g., *de Pablo & Komatsu*, 2009] and while dome-shaped morphologies were observed within our study area, the lack of correlation and large gap in size and spatial distribution with respect to DRDs, rules out a pingo origin for DRDs. Mud volcanoes share the same distributional predicament as pingos, with basal diameters that can reach tens of kilometres and heights ranging in the hectometre-scale [*Davis & Tanaka*, 1995; *Skinner & Tanaka*, 2007]. Ultimately, given the expansive and intricate volcanic and sedimentary history, and considering the extensive presence of (at least) near-surface ice in Utopia Planitia, the formation of any of the MRRD features within this region cannot (at least currently) be ruled out. However, seeing that the geometric and distribution patterns of these features do not correspond with our observations of DRDs, we do not find them to be a likely candidate to explain DRD formation mechanism.

Considering that aeolian processes are widespread across the planetary surface of Mars, we found it necessary to entertain the possibility that DRDs may have an Aeolian origin. In fact, the 'tear-drop' morphologies can resemble some terrestrial dune examples [c.f. *Hersen et al.*, 2002]. However, we do not see the same latitudinal restrictions that DRDs exhibit, with aeolian processes on Mars. Furthermore, in the case of 'tear-drops', these morphologies are strictly

restricted to high-sloping terrain. Additionally, dunes on Mars, as observed in high-resolution imagery (e.g., HiRISE), typically appear distinct from the surrounding landscape. This is often due to the difference in their spectral signatures, derived by their contrasting mineralogical composition, relative to their encompassing terrain. For instance, many examples of dunes on Mars, appear as some derivation of blue in an enhanced-colour photo of HiRISE, meaning a sharp peak at roughly thein the 500 nm that corresponds to the Blue/Green band of HiRISE [e.g., *McEwen et al.*, 2010]. We did not find DRDs exhibiting such considerable distinction in visible imagery or their spectral signature. In any case, we cannot explain the topographic/latitudinal restrictions observed with DRDs for an Aeolian process, and thus, we find an Aeolian origin to be an unlikely scenario in explaining DRD formation mechanisms. Though, it is more than likely that Aeolian reworking has evolved or altered the preservation state of DRDs to some extent.

Another noteworthy mention, is the striking resemblance of DRDs to what has been commonly referred to as – at least in some variation of the terms – 'brain coral' or 'brain terrain' [e.g., *Levy, Head, & Marchant*, 2009a, 2009b; *Noe Dobrea et al.*, 2007; *Williams et al.*, 2008] which has been identified previously in Utopia Planitia (Figure 2.10). These features remain an active area of research, with multiple hypotheses put forth to explain their formation, including sorted ground [*Noe Dobrea et al.*, 2007], glacial 'veiki' moraine [*Johnsson et al.*, 2016], or modification of glacial-flow [*Levy, Head, & Marchant*, 2009a].
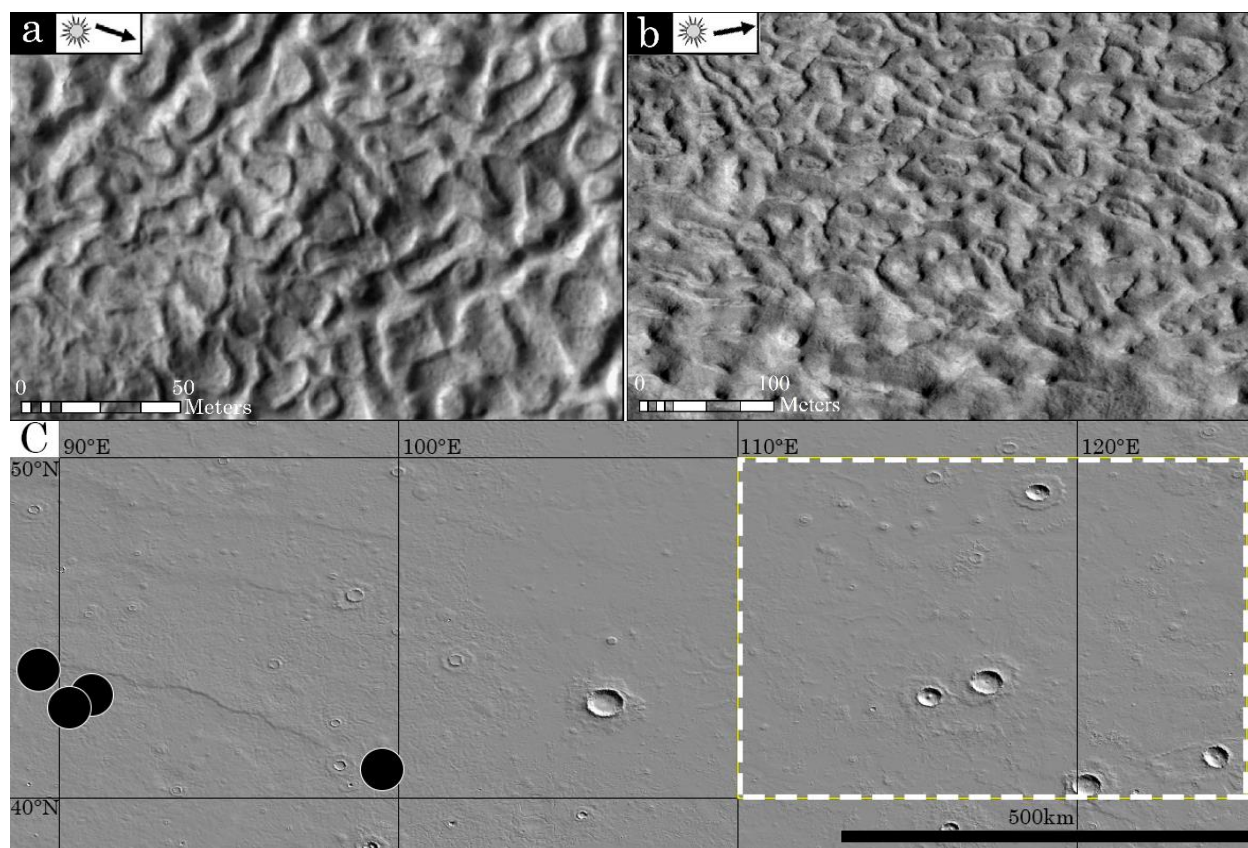
Figure 2.10: **(a)** snapshot obtained from [*Levy, Head, & Marchant*, 2009a] depicting 'brain terrain' **(b)** DRDs on the right for comparison (HiRISE ESP_025632_2225). **(c)** an overview of our study area in the white dotted rectangle, and Levy et al.'s study area as denoted by the black circles (see figure 1 of Levy, Head, & Merchant, 2009a). *Image credit: NASA-Goddard Flight Center/JPL/University of Arizona/MOLA Science Team/PDS Geosciences.*

'Brain' textures have been reported in assortments similar to that of the labyrinth morphology. That is, while at times exhibiting clear distinction of single members, as opposed to interlocking or coalescing 'cells', they are generally bound together within a locality [*Levy, Head, & Marchant*, 2009a]. Spatially, 'brain-terrain' has been reported to occur homogenously with at least one type of IRF [*Levy, Head, & Marchant*, 2009a]. In terms of geometrics, 'brain-terrain' can have widths of 4–20 m, are 10–100 m in length, with heights up to 5 m [*Levy, Head, & Marchant*, 2009a]. In contrast, within our study, we only measured lengths of individual DRDs that showed clear separation from one another. In other words, when DRDs overlap (i.e., labyrinth morphology), they form complex and, at times, long lineations or ring-shaped

landforms, often making it difficult to indicate the number of DRDs that have coalesced to arrive at such a composite landform (e.g., Figures 2.4b, 2.6b and c). This may explain the separation of measurements between DRD and 'brain-terrain' length. It could be argued that our morphology classes represent entirely different landscape features; however, the observed modification and transition between morphologies (e.g., Figure 2.6), along with overlapping geometric measurements and geographic distribution, suggest otherwise.
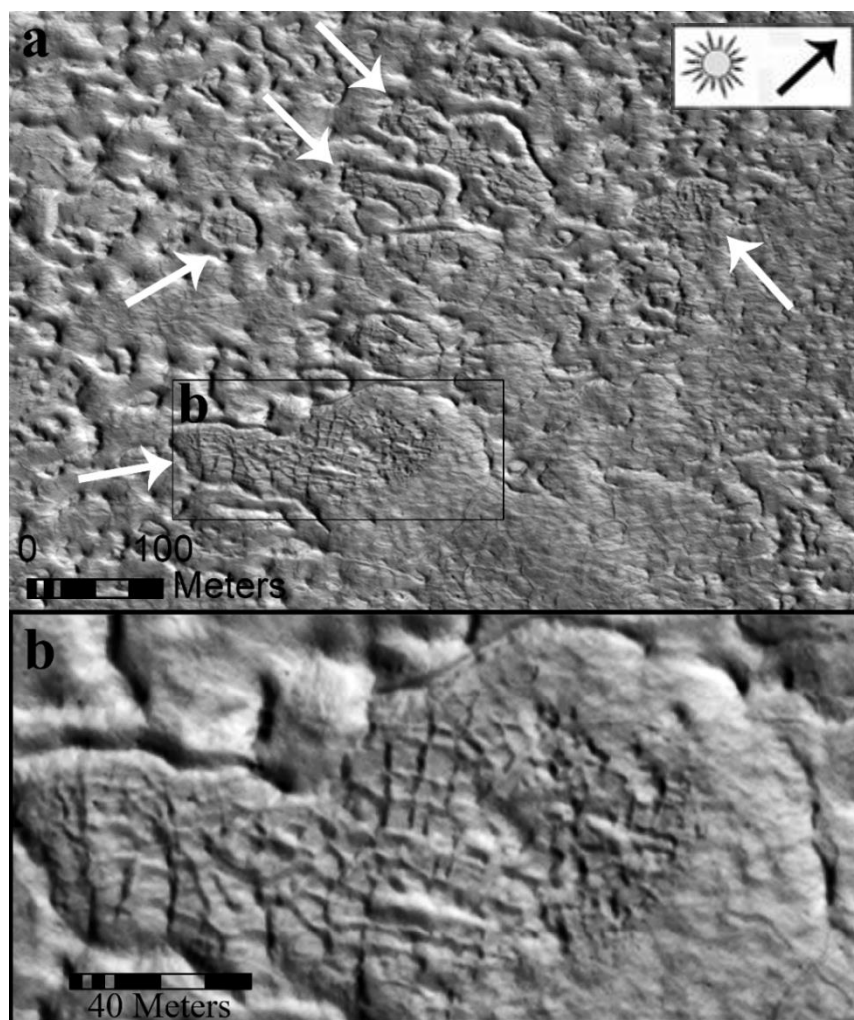
Figure 2.11: **(a)** DRDs with polygonization as pointed out with the white arrows (HiRISE ESP_046322_2230). **(b)** close-up view of the bottom section of **(a)**. *Image credit: NASA/JPL/University of Arizona.*

Moreover, while DRDs show a high geographic relationship with IRFs (Table 2.2), their occurrence is not bound to the confines, or the proximity, of these features. In fact, within our study area, less than 30% of HiRISE images containing DRDs were within crater interiors

(Figure 2.1), and IRFs were completely absent in ~25% of HiRISE images containing DRDs (Table 2.2). Contrary to Levy et al.'s [2009a, 2009b] 'brain terrain', we could not confirm any measurable orientation of DRDs that occurred within crater interiors, that were in concentric formations relative to the crater. Similar to the case of width measurements of labyrinth morphologies, we found it challenging to measure long-axis orientation of DRDs that appear to have coalesced. However, the measurement of the orientation of the long-axis based on DRDs that show clear separation, distinct in morphology (as reported in Figure 2.9), depicted an overall East to West facing orientation. If DRDs and 'brain terrain' are in fact the same landscape feature, it could be that when they occur within craters that contain CCFs, their orientation is biased to the morphology and texture of the antecedent layer on which they are superimposed (i.e., crater fill). Furthermore, similar to what has been reported by Levy et al., [2009a, 2009b], in every case where we observed DRDs, polygonised ground was detected as well (Table 2.2). This is with the difference that, in some cases, we observed polygonization occurring on DRDs, suggesting the superposition of polygons with respect to DRDs (Figure 2.11).

Despite these differences in observation, we recognize that these formation hypotheses are in-tune with the encompassing landscape, morphologic features, and climate history. In addition, the geological and geomorphological evolution of a landscape feature, is almost never due to the sole influence of one processes. Instead, it is commonly a combination of processes that morph an environment and its encompassing landscape features. Thus, we do not reject the possibility that there are ties in the formation mechanisms of DRDs and 'brain' textures. There is the possibility that 'brain terrain' and DRDs are genetically completely different features, but given the similarity in morphology and geographic distribution, we find this unlikely. In fact, our findings are much more in keeping with observations that have been reported in the work of Noe Dobrea et al. [2007]. They emphasize a transition zone between 'circular' and 'labyrinthine' ridges, which we believe is a critical observation in linking ellipse and labyrinth morphologies within our study. This transition is best captured by the model provided by Kessler & Werner [2003] (Figures 2.6 and 2.12). To complement Noe Dobrea et al.'s [2007] hypothesis, the first identification of sorted ground on Mars was reported shortly after [*Balme et al.*, 2009], and specifically in the follow-up work done by Gallagher et al. [2011], they describe observations of a landscape that we have observed to be parallel to what we have found in our study area. In fact, within just one HiRISE image (Figure 2.12a) in our study area, we can observe linear downslope

striations like 'sorted clastic stripes', and horizontal banding/terraces and lobes (i.e., tear-drops) similar to that of 'solifluction lobes'.
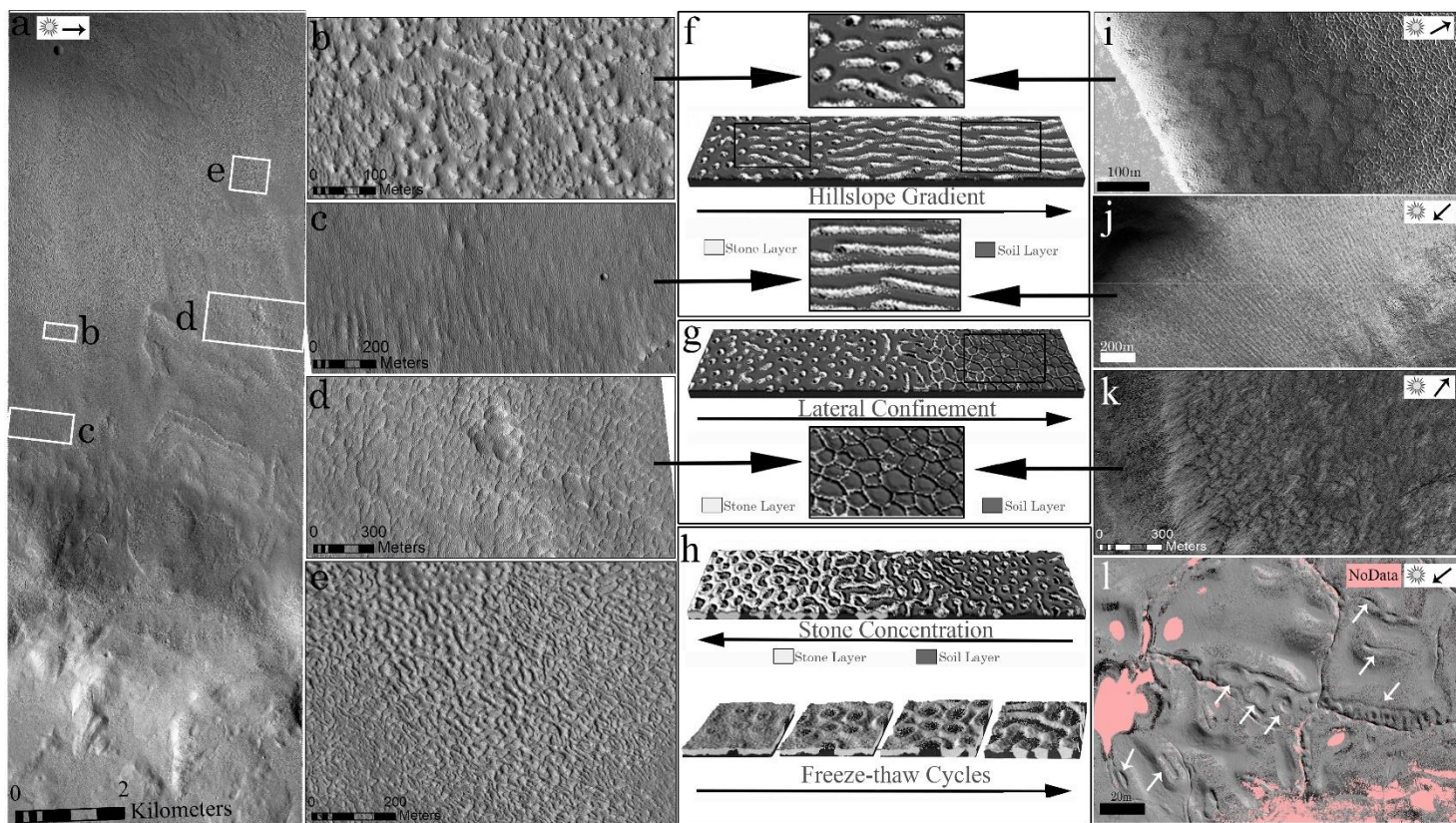
Figure 2.3: **(a)** HiRISE ESP_028652_2210 with 4 close-ups **(b)** 'tear-drops', **(c)** clastic stripes, **(d)** sorted patterned ground, **(e)** Labyrinth and Ellipse DRDs. Note the similarity of **(i)** snapshot from the same HiRISE image used in Gallagher et al. [2011] to outline solifluction lobes and **(b)** tear-drops; as well as **(j)** Gallagher et al.'s [2011] clastic stripes – cf. **(c)**, and **(k)** Gallagher et al.'s [2011] lobes and terraces – cf. **(d)**. **(l)** LiDAR image from Lake Orbiter's (Devon Island) [*Hawkswell et al.*, 2018] sorted circles – cf. **(e)**. **(f)** Data from Kessler & Werner's [2003] model showing an increase in slope gradient from left to right, and its similarity to **(b)** and **(i)** at lower slope gradient, compared to **(c)** and **(j)** at higher slope gradient. **(h)** Data from Kessler & Werner's [2003] model – lateral confinement increasing left to right – noting the similarity between **(d)** and **(k)**. **(h)** Depicts data from Kessler & Werner's [2003] model on top – increase in stone concentration right to left - with data from Kessler et al. [2001] on the bottom – evolution of sorted circles with age. *Image credit: NASA/JPL/University of Arizona/FGI/Teledyne Optec.*

The distribution classes of DRDs, are highly correlated with the erosion pattern observed with periglacial features on Mars. That is, generally with an increase in latitude, the frequency of these features declines. On Mars, the latitude restriction of any potential periglacial feature is mainly explained by the climate history, derived by its periodic shifts in obliquity, during which the appropriate conditions for water/ice stability changes with latitude [*Boynton*, 2002; *Carr*, 1983; *Carr & Head*, 2010; *Head et al.*, 2003; *Hess et al.*, 1977; *Mellon et al.*, 2004]. Throughout times of low obliquity, ice deposits migrate and extend from the poles, where they are currently residing today, to the mid-latitudes [*Levrard et al.*, 2004; *Madeleine et al.*, 2009]. Alternatively, during times of high obliquity, the ice deposits recede and are highly concentrated and confined to lower- and mid-latitude regions [*Carr & Head*, 2010; *Head et al.*, 2003; *Kreslavsky & Head*, 2002]. The range of obliquity shifts of Mars is quite large (i.e., up to 60º) [*Laskar et al.*, 2004; *Levrard et al.*, 2004; *Madeleine et al.*, 2009]; while the projected number of obliquity shifts within the late Amazonian is in the order of a couple of tens of cycles [*Laskar et al.*, 2004; *Levrard et al.*, 2004; *Madeleine et al.*, 2009]. This frequent and large variations in obliquity, and therefore the climate and latitudinal migration of ice would have allowed for mid-latitude zones to periodically host a periglacial environment due to changes in solar insolation [*Laskar et al.*, 2004]. Accordingly, the mid-latitudes are precisely the regions where all potential periglacial landscape features have been reported [e.g., *Hauber et al.*, 2011; *Lucchitta*, 1981; *Mellon et al.*, 2009; *Ulrich et al.*, 2012].

Considering the spatially correlated landscape features in respect to DRDs (Table 2.2), believed to be periglacial in origin, suggests the idea that DRDs have periglacial origins. For instance, the dissection of LDM, proposed to have been triggered by the same processes that derive the formation of gullies (i.e., freeze-thaw cycle erosion), reaches its maximum in the mid-latitudes, roughly where there is the highest frequency of occurrence and where the best-developed gullies appear [*Balme et al.*, 2006; *Bridges & Lackner*, 2006; *Harrison et al.*, 2015; *Head et al.*, 2003; *Heldmann et al.*, 2007; *Heldmann & Mellon*, 2004; *Kneissl et al.*, 2010; *Malin & Edgett*, 1999]. This is also true for scalloped depression distributions [*Head et al.*, 2003; *Kreslavsky & Head*, 2002], as well as IRFs being concentrated along ~35–50º N/S [*Carr & Head*, 2010; *Dickson et al.*, 2010; *Fastook & Head*, 2014; *Squyres*, 1979]. In comparison, within the confines of our study area, DRDs appear from 40º to 47º, with the highest concentration of

DRDs appearing at ~ 45°, where their distribution shifts from clustering at lower latitudes to dispersed distribution and finally to random distributions at higher latitudes within our study area. This is likely an indication of the increase in degradation/erosion and a decrease in the preservation state of DRDs. At around 45°, DRDs appear much more striking and prominent in respect to their surrounding landscape (Figure 2.13a). In contrast, on the northern boundary of where DRDs were observed within our study area (Figure 2.13b), they appear much more muted, eroded and modified. This observation of transition in preservation state is also quite apparent in other landscape features, as well as the overall terrain texture. In images with degraded and isolated DRDs (e.g., Figure 2.13b) the surrounding land surfaces are strikingly heterogeneous in texture, with vast areas covered with patterned ground (e.g., polygons), pitted, with interchanging rough and smoothed plains.
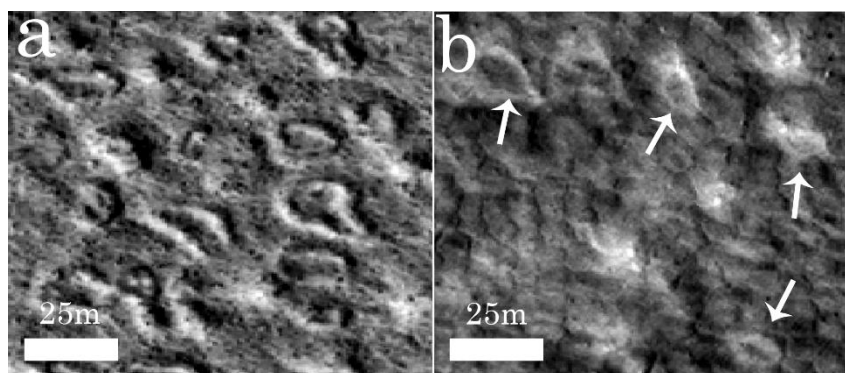
Figure 2.4: **(a)** image exhibits DRDs at 45° (HiRISE ESP_028072_2255), while **(b)** displays DRDs at ~47° (HiRISE ESP_035614_2280) latitude. *Image credit: NASA/JPL/University of Arizona.*

The observations suggest that the process(es) responsible for the formation of DRDs involved a local- to regional-scale mechanism(s). This is because, the overall morphologic uniformity of individual DRDs, regardless of morphology and distribution, and the extensive areas that they cover, suggests that they were all formed via the same process(es) and at relatively the same time. An example of such a scenario is polygonised patterned ground, containing several individual polygons similar in size, shape, and orientation within a locality, which combine to form a polygonised terrain [e.g., *French*, 1993].

The transitions in the morphology of DRDs coincide with changes in slope, and lateral confinement. As DRDs transition from labyrinth morphologies to ellipse morphologies, each individual DRD begins to exhibit clear separation from its neighbours and becomes more morphologically defined from the overall landform and landscape (Figures 2.5 and 2.12). This is observed with changes in slope or the presence of a stratigraphic barrier (e.g., escarpments) between the two morphology types. This transition mirrors the sorting model created by Kessler & Werner [2003] (Figure 2.12h), simulating a decrease in stone concentration from left to right. Naturally, stone concentrations will increase downslope, increasing in accumulation with decreasing slope gradient. Additionally, their concentrations will not always remain constant across stratigraphic barriers, resulting in different morphologies. For instance, over time, a depression in the ground (e.g., impact craters) is likely to accumulate larger quantities of stone, relative to the surrounding terrain outside of the crater, undergoing processes that can result in stone migration across a landscape (e.g., mass-wasting, glacial).

Labyrinth morphologies appear similar to models with high stone concentrations (Figures 2.5, 2.12e), and are respectively found in confined and relatively flat-lying terrain; whereas ellipse morphologies resembling lower stone concentrations (Figures 2.5, 2.12e) are found in areas with relatively higher slope gradients and/or non-confined areas (e.g., outside of a crater, a valley, etc.). Furthermore, as DRDs transition to even steeper slopes (i.e., 'tear-drops'), they become elongated (Figures 2.12c, f, and j) and are likely subject to mass-wasting processes over time (Figures 2.12b, f, and i). In fact, within the bounds of a HiRISE image, in every scenario where 'tear-drops' were observed, gullies were also observed (Table 2.2). Admittedly, DRDs are also in spatial correlation with at least one type of IRFs, when restricted to some type of low-lying terrain (e.g., crater, valley). Nevertheless, we attribute the significance of DRD spatial correlation with IRFs to the fact that, topographically-sourced confinements in an undulating landscape (e.g., a crater), act as large traps for material. As an arbitrary example, if an ice-sheet moves over a crater, a portion of that ice will become entrapped within the confines of the crater walls, as well as the inventory of material that is embedded within that ice (e.g., rocks and boulders). As such, if DRDs are morphologies derived from ground sorting mechanisms, confinements such as craters, valleys, or any low-lying and/or dissected terrains, due to the accumulation and abundance of assortments of deposits, will pose as 'hot-spots' for the rapid

genesis of DRDs.

Simultaneously, our observation of the transition in morphologies of DRDs mirrors the sorting models created by Kessler & Werner [2003] (Figures 2.5 and 2.12h). The evolution of textures in the models provided by Kessler & Werner [2003] are results of fluctuations in geological parameters including, slope, confinement, and supply of material, as opposed to a difference in the inherent formation mechanism. Similarly, the transitions observed within DRDs (see sub-images in Figure 2.12), are likely not a result of a unidirectional change in one variable (e.g., slope). Instead, alike Kessler & Werner's [2003] models, they are a result of a multidirectional change in two or more variables (e.g., slope and confinement) that affect stone concentrations and therefore morphology. In conjunction with the terrestrial examples of sorted ground, in some cases specifically in comparison to Mars, that have been already provided in previous studies [e.g., *Balme et al.*, 2009; *Gallagher et al.*, 2011; *Kessler & Werner*, 2003; *Noe Dobrea et al.*, 2007]; we have observed analogous morphologies on Devon Island (Figure 2.12l). These sorted circles bear similar geometric properties, as well as being encompassed in a landscape, that convey striking resemblance to DRDs.

The challenge in comparing DRDs to the models proposed by Kessler & Werner [2003], is that while patterned ground is a distinct morphologic feature across periglacial landscapes, there is no clear, widely accepted, understanding of how these features form [c.f. *Rowley et al.*, 2015]. Generally, it is believed to be caused by freeze-thaw cycles, triggering frost heave processes, thereby influencing the active layer in permafrost and generating these unique morphologies [e.g., *Marr*, 1969]. In any case, regardless of the specific underlying process, sorted patterned ground, as the name implies, is the product of a size sorting mechanism of surficial deposits, which over multiple freeze-thaw cycles results in distinct division between the stone (i.e., course-grained deposits) and soil (i.e., fine-grained sediment) domains [e.g., *Washburn*, 1956; *Kessler et al.*, 2001]. On Mars, the lack of comparable data (i.e., complete and high-resolution) on stone concentration and grain size distribution across our study area, makes direct comparison difficult. Still, it should be noted that we observed various instances of meter-scale boulder fields in HiRISE images, where we confirmed the presence of DRDs; and based on Viking Lander 2 (VL2) experiments in Utopia Planitia [*Arvidson et al.*, 1989], the presence of both coarse-grained/stone deposits and fine-grained/soils are likely throughout this region. In

past studies, infra-red signatures (e.g., THEMIS data) and spectral signatures (e.g., TES and CRISM) have been used to suggest grain sizes [e.g., *Christensen et al.*, 2001; 2003]. However, as confirmed by this study, resolving decameter-scale features is beyond the resolution capabilities of these datasets. In any case, the subsurface insight required to inform the migration of coarse-grained and fine-grained deposits below the surface, is also currently unfeasible on Mars. On Earth, sorting mechanisms have not been documented to produce a significant change in elevation, when compared to the rim heights of DRDs. However, it must be considered that, due to Mars being in a low mean obliquity period (see Figure 1.2), these potentially periglacial features would have undergone ― hundred-thousand orders of magnitude ― greater freeze-thaw cycles, in comparison to the examples of such features on Earth (e.g., sorted circles in Devon Island). Furthermore, the antecedent topography of the landscape on which DRDs are superimposed, and/or post-depositional processes, may have morphologically altered the state of DRDs to what we see today. As is commonly the case in nature, a landscape feature is a product of multiple processes, that may be separated across geologic time, as opposed to one single process. Thus, here we propose that a similar process to that of ground sorting mechanisms on Earth, has been a prominent influence in shaping these landscape morphologies (i.e., DRDs). It is highly probable that such a mechanism, was combined with others to arrive at the current morphologic state of DRDs. For instance, the DRD orientation pattern observed (Figure 2.9), may be indicative of a regional Aeolian process, or perhaps 'footprints' of previous glacial mechanisms, that have been factors in the morphologic evolution of DRDs.

2.5 Conclusions

Mars appears to be a frozen world today; however, it did not always sustain such conditions. The presence of periglacial features such as patterned ground [e.g., *Balme et al.*, 2009; *Gallagher et al.*, 2011; *Mangold*, 2005] (e.g., polygonised terrain), gullies [e.g., *Malin & Edgett*, 2000], fretted and dissected terrain (e.g., LDM and scalloped depressions) [e.g., *Séjourné et al.*, 2011], and IRFs (i.e., CCF, LVF, and LDA) [e.g., *Levy, Head, Marchant, et al.*, 2009] suggest that within the past few million years, the mid-latitudes were exposed to surface temperatures above the freezing point of water Earth. To complement the periglacial picture, at least specific to Utopia Planitia, here we report the observation of a landscape morphology, dubbed DRD.

Morphologically, DRDs show many areas of overlap, with previously reported features such as collapsed pingos [*de Pablo & Komatsu*, 2009], rootless cones [*Lanagan et al.*, 2001], 'veiki' moraine [*Johnsson et al.*, 2016], and 'brain terrain' [*Levy, Head, & Marchant*, 2009a, 2009b; *Noe Dobrea et al.*, 2007; *Williams et al.*, 2008]. Based on our observations via HiRISE images, geometrics, spatial statistics, geographic correlation with other landscape features, and considering the encompassing landscape and geologic history, we find that DRDs are likely a result of a ground sorting mechanism. In fact, in every HiRISE imagery where DRDs were present, polygons were also observed (see Table 2.2). Several terrestrial examples, in regard to sorted ground, have been already put forth [e.g., *Balme et al.*, 2009; *Gallagher et al.*, 2011; *Kessler & Werner*, 2003; *Noe Dobrea et al.*, 2007]; yet, we complement these previous studies with our observation of sorted circles in Devon Island (Figure 2.12l). Stratigraphically, DRDs appear to superpose scalloped depressions, LDM, and IRFs (though not polygonised ground in all cases), which suggests they are a relatively young feature of this landscape, conveying a worthy, and possibly improved, stratigraphic marker. Ultimately, we advocate that DRDs, considering the formation mechanism suggested in this study, provides additional evidence for cyclic shifts in latitudinal water/ice stability, and ultimately the migration of ice deposits from the poles to mid- and lower-latitudes and vice versa. In respect to the late Amazonian history of Utopia Planitia, and based on the discussion in the previous section, we propose the following scenario extending from ~100Ma to the present:

1. High Obliquity during period of high mean obliquity [*Laskar et al.*, 2004; *Levrard et al.*, 2004]
   a. Migration of regional ice to Utopia Planitia [*Harrison*, 2016]
   b. Terrain enrichment of ice, with possible formation of ice sheets
2. Shift to lower obliquity [*Laskar et al.*, 2004; *Levrard et al.*, 2004]
   a. The retreat of ice-sheet from Utopia Planitia to the poles
      i. Sublimation of surface ice
      ii. Dust-covered remnants preserved [*Harrison*, 2016] (e.g., CCF, LDA, LVF)
   b. Triggering of Interglacial Period [*Head et al.*, 2003] in Utopia Planitia
      i. Sublimation of shallow sub-surface Ice with further atmospheric

instability

    ii. Terrain modification as a result of sublimation of ice [*Shean*, 2010] (e.g., scarps, ridges, hummocks, pits and pocks, etc.)

3. Shift to a higher obliquity with transition to a lower mean obliquity period [*Laskar et al.*, 2004; *Levrard et al.*, 2004]

    a. Seasonal replenishment of the terrain in water-ice through atmospheric deposition [*Madeleine et al.*, 2009]

        i. accompanying seasonal dust storms [*Madeleine et al.*, 2009], as well as volcanic activity producing ash deposits [*Kerrigan*, 2013; *Soare et al.*, 2015], resulting in the formation of layered dust-covered ice (i.e., LDM)

    b. Seasonal changes triggering episodic freeze-thaw cycles

        i. Dissection of LDM resulting in the formation of some scalloped depressions, and gullies

4. Shift to a lower obliquity [*Laskar et al.*, 2004; *Levrard et al.*, 2004]

    a. Incomplete termination of water-ice atmospheric deposition

        i. Accompanied by a temporary halt in sublimation [*Kerrigan*, 2013], Aeolian deposition results in duricrust formation over the terrain

    b. Mass production of Periglacial landforms due to a further decrease in obliquity [*Harrison*, 2016]

        i. Formation of new Gullies and further development of older gullies

        ii. Formation of new Scalloped Depressions

        iii. Formation of patterned ground (e.g., polygons and DRDs)

5. Present-day Obliquity [*Laskar et al.*, 2004; *Levrard et al.*, 2004]

    a. Complete termination of atmospheric water-ice and dust deposition, coupled with Aeolian erosion and reworking

        i. Further dissection and exposition of dust-covered ice deposits (i.e., CCF, LDA, LVF, and LDM) with very limited gully activity still remaining [*Dundas et al.*, 2015]

        ii. Partial erosion of patterned ground (e.g., DRDs, polygons)

2.6 References

Albee, A. L., Arvidson, R. E., Palluconi, F., & Thorpe, T. (2001). Overview of the Mars global surveyor mission. *Journal of Geophysical Research: Planets*, *106*(E10), 23291–23316.

Anderson, J. A., Edmundson, K. L., Sides, S. C., Eliason, E. M., Gaddis, L. R., Torson, J. M., & Edwards, K. (2013). Analysis of Light Time and Stellar Aberration Corrections in ISIS Using Lunar Reconnaissance Orbiter Narrow Angle Camera Images. In *44th Lunar and Planetary Science Conference* (Abstract# 2318).

Arvidson, R. E., Gooding, J. L., & Moore, H. J. (1989). The Martian surface as imaged, sampled, and analyzed by the Viking landers. *Reviews of Geophysics*, *27*(1), 39–60. http://doi.org/10.1029/RG027i001p00039

Baker, V. R., Boothroyd, J. C., Carr, M. H., Cutts, J. A., Komar, P. D., Laity, J. E., … Patton, P. C. (1983). Channels and valleys on Mars. *Bulletin of the Geological Society of America*, *94*(9), 1035–1054. http://doi.org/10.1130/0016-7606(1983)94<1035:CAVOM>2.0.CO;2

Balme, M. R., Gallagher, C. J., Page, D. P., Murray, J. B., & Muller, J. P. (2009). Sorted stone circles in Elysium Planitia, Mars: Implications for recent martian climate. *Icarus*, *200*(1), 30–38. http://doi.org/10.1016/j.icarus.2008.11.010

Balme, M. R., Mangold, N., Baratoux, D., Costard, F. M., Gosselin, M., Masson, P., … Neukum, G. (2006). Orientation and distribution of recent gullies in the southern hemisphere of Mars: Observations from High Resolution Stereo Camera/Mars Express (HRSC/MEX) and Mars Orbiter Camera/Mars Global Surveyor (MOC/MGS) data. *Journal of Geophysical Research E: Planets*, *111*(5). http://doi.org/10.1029/2005JE002607

Boynton, W. V. (2002). Distribution of Hydrogen in the Near Surface of Mars: Evidence for Subsurface Ice Deposits. *Science*, *297*(5578), 81–85.

http://doi.org/10.1126/science.1073722

Bridges, N. T., & Lackner, C. N. (2006). Northern hemisphere Martian gullies and mantled terrain: Implications for near-surface water migration in Mars' recent past. *Journal of Geophysical Research*, *111*(E9). http://doi.org/10.1029/2006JE002702

Burr, D. M., Bruno, B. C., Lanagan, P. D., Glaze, L. S., Jaeger, W. L., Soare, R. J., … Baloga, S. M. (2009). Mesoscale raised rim depressions (MRRDs) on Earth: A review of the characteristics, processes, and spatial distributions of analogs for Mars. *Planetary and Space Science*, *57*(5–6), 579–596.

Burr, D. M., Tanaka, K. L., & Yoshikawa, K. (2009). Pingos on Earth and Mars. *Planetary and Space Science*, *57*(5–6), 541–555.

Byrne, S., Dundas, C. M., Kennedy, M. R., Mellon, M. T., McEwen, A. S., Cull, S. C., … Seelos, F. P. (2009). Distribution of Mid-Latitude Ground Ice on Mars from New Impact Craters. *Science*, *325*(5948), 1674–1676. http://doi.org/10.1126/science.1175307

Carr, M. H. (1983). Stability of streams and lakes on Mars. *Icarus*, *56*(3), 476–495. http://doi.org/10.1016/0019-1035(83)90168-9

Carr, M. H., & Head, J. W. (2010). Geologic history of Mars. *Earth and Planetary Science Letters*, *294*(3–4), 185–203. http://doi.org/10.1016/j.epsl.2009.06.042

Chapman, M. G., Allen, C. C., Gudmundsson, M. T., Gulick, V. C., Jakobsson, S. P., Lucchitta, B. K., … Waitt, R. B. (2000). Volcanism and ice interactions on Earth and Mars. In *Environmental effects on volcanic eruptions* (pp. 39–73). Springer.

Christensen, P. R., Bandfield, J. L., Hamilton, V. E., Ruff, S. W., Kieffer, H. H., Titus, T. N., ... & Jakosky, B. M. (2001). Mars Global Surveyor Thermal Emission Spectrometer experiment: investigation description and surface science results. *Journal of Geophysical Research: Planets, 106*(E10), 23823-23871.

Christensen, P. R., Bandfield, J. L., Bell III, J. F., Gorelick, N., Hamilton, V. E., Ivanov, A., ... & McConnochie, T. (2003). Morphology and composition of the surface of Mars: Mars Odyssey THEMIS results. *Science, 300*(5628), 2056-2061.

Christensen, P. R., Jakosky, B. M., Kieffer, H. H., Malin, M. C., McSween, Jr., H. Y., Nealson, K., … Ravine, M. A. (2004). The Thermal Emission Imaging System (THEMIS) for the Mars 2001 Odyssey Mission. *Space Science Reviews*, *110*(1/2), 85–130.

http://doi.org/10.1023/B:SPAC.0000021008.16305.94

Clifford, S. M. (1993). A model for the hydrologic and climatic behavior of water on Mars. *Journal of Geophysical Research*, *98*(E6), 10973. http://doi.org/10.1029/93JE00225

Clifford, S. M. (2001). The Evolution of the Martian Hydrosphere: Implications for the Fate of a Primordial Ocean and the Current State of the Northern Plains. *Icarus*, *154*(1), 40–79. http://doi.org/10.1006/icar.2001.6671

Costard, F. M., & Kargel, J. S. (1995). Outwash plains and thermokarst on Mars. *Icarus, 114*(1), 93–112.

Davis, P. A., & Tanaka, K. L. (1995). Curvilinear Ridges in Isidis Planitia, Mars--The Result of Mud Volcanism. In *26th Lunar and Planetary Science Conference* (pp. 321–322).

de Pablo, M. Á., & Komatsu, G. (2009). Possible pingo fields in the Utopia basin, Mars: Geological and climatical implications. *Icarus*, *199*(1), 49–74. http://doi.org/10.1016/j.icarus.2008.09.007

Dickson, J. L., Head, J. W., & Marchant, D. R. (2010). Kilometer-thick ice accumulation and glaciation in the northern mid-latitudes of Mars: Evidence for crater-filling events in the Late Amazonian at the Phlegra Montes. *Earth and Planetary Science Letters*, *294*(3–4), 332–342. http://doi.org/10.1016/j.epsl.2009.08.031

Drew, J. V., & Tedrow, J. C. F. (1962). Arctic Soil Classification and Patterned Ground. *Arctic, 15*(2), 109–116. http://doi.org/10.14430/arctic3563

Dundas, C. M., & Byrne, S. (2010). Modeling sublimation of ice exposed by new impacts in the martian mid-latitudes. *Icarus*, *206*(2), 716–728. http://doi.org/10.1016/j.icarus.2009.09.007

Dundas, C. M., Diniega, S., & McEwen, A. S. (2015). Long-term monitoring of martian gully formation and evolution with MRO/HiRISE. *Icarus*, *251*, 244–263. http://doi.org/10.1016/j.icarus.2014.05.013

Dundas, C. M., Mellon, M. T., McEwen, A. S., Lefort, A., Keszthelyi, L. P., & Thomas, N. (2008). HiRISE observations of fractured mounds: Possible Martian pingos. *Geophysical Research Letters*, *35*(4).

Ebdon, D. (1985). *Statistics in geography*. Blackwell.

Embleton, C., & King, C. A. M. (1975). *Glacial and Periglacial Geomorphology* (Vol. 2). Edward Arnold.

Fastook, J. L., & Head, J. W. (2014). Amazonian mid- to high-latitude glaciation on Mars: Supply-limited ice sources, ice accumulation patterns, and concentric crater fill glacial flow and ice sequestration. *Planetary and Space Science*, *91*, 60–76. http://doi.org/10.1016/j.pss.2013.12.002

French, H. M. (1993). Cold-climate processes and landforms. In *Canada's Cold Environments* (pp. 271–290). McGill University Press.

French, H. M. (2013). *The Periglacial Environment* (Third Ed.). Wiley. http://doi.org/10.1002/9781118684931

Gallagher, C. J., Balme, M. R., Conway, S. J., & Grindrod, P. M. (2011). Sorted clastic stripes, lobes and associated gullies in high-latitude craters on Mars: Landforms indicative of very recent, polycyclic ground-ice thaw and liquid flows. *Icarus*, *211*(1), 458–471. http://doi.org/10.1016/j.icarus.2010.09.010

Greeley, R., & Fagents, S. A. (2001). Icelandic pseudocraters as analogs to some volcanic cones on Mars. *Journal of Geophysical Research: Planets*, *106*(E9), 20527–20546.

Gurney, S. D. (1998). Aspects of the genesis and geomorphology of pingos: perennial permafrost mounds. *Progress in Physical Geography*, *22*(3), 307–324.

Harrison, T. N. (2016). Martian Gully Formation and Evolution: Studies From the Local to Global Scale. *Electronic Thesis and Dissertation Repository*, Paper 3980. Retrieved from http://ir.lib.uwo.ca/etd/3980

Harrison, T. N., Osinski, G. R., Tornabene, L. L., & Jones, E. (2015). Global documentation of gullies with the Mars Reconnaissance Orbiter Context Camera and implications for their formation. *Icarus*, *252*, 236–254. http://doi.org/10.1016/j.icarus.2015.01.022

Hauber, E., Reiss, D., Ulrich, M., Preusker, F., Trauthan, F., Zanetti, M., … Olvmo, M. (2011). Landscape evolution in Martian mid-latitude regions: insights from analogous periglacial landforms in Svalbard. *Geological Society, London, Special Publications*, *356*(1), 111 LP-131.

Hawkswell, J. E., Godin, E., Osinski, G. R., Zanetti, M., & Kukko, A. (2018). Comparative Investigation of Polygon Morphology Within the Haughton Impact Structure, Devon Island with Implications for Mars. In *49th Lunar and Planetary Science Conference* (Abstract# 2899).

Head, J. W., Mustard, J. F., Kreslavsky, M. A., Milliken, R. E., & Marchant, D. R. (2003). Recent ice ages on Mars. *Nature*, *426*(6968), 797–802. http://doi.org/10.1038/nature02114

Heldmann, J. L., Carlsson, E., Johansson, H., Mellon, M. T., & Toon, O. B. (2007). Observations of martian gullies and constraints on potential formation mechanisms. *Icarus*, *188*(2), 324–344. http://doi.org/10.1016/j.icarus.2006.12.010

Heldmann, J. L., & Mellon, M. T. (2004). Observations of martian gullies and constraints on potential formation mechanisms. *Icarus*, *168*(2), 285–304. http://doi.org/10.1016/j.icarus.2003.11.024

Hess, S. L., Henry, R. M., Leovy, C. B., Ryan, J. A., & Tillman, J. E. (1977). Meteorological results from the surface of Mars: Viking 1 and 2. *Journal of Geophysical Research*, *82*(28), 4559–4574. http://doi.org/10.1029/JS082i028p04559

Hersen, P., Douady, S., & Andreotti, B. (2002). Relevant length scale of barchan dunes. *Physical Review Letters, 89*(26), 264301.

Johnsson, A., Reiss, D., Hauber, E., Johnson, M., Olvmo, M., & Hiesinger, H. (2016). Veiki-Moraine-Like Landforms in the Nereidum Montes Region on Mars: Insights from Analogues in Northern Sweden. In *47th Lunar and Planetary Science Conference* (Abstract# 1229).

Kerrigan, M. C. (2013). The periglacial landscape of Utopia Planitia; Geologic evidence for recent climate change on Mars. *Electronic Thesis and Dissertation Repository*, Paper 1101. Retrieved from http://www.lpi.usra.edu/meetings/lpsc2013/pdf/2651.pdf

Kessler, M. A., Murray, A. B., Werner, B. T., & Hallet, B. (2001). A model for sorted circles as self-organized patterns. *Journal of Geophysical Research: Solid Earth*, *106*(B7), 13287–13306. http://doi.org/10.1029/2001JB000279

Kessler, M. A., & Werner, B. T. (2003). Self-organization of sorted patterned ground. *Science*, *299*(5605), 380–383. http://doi.org/10.1126/science.1077309

Kneissl, T., Reiss, D., van Gasselt, S., & Neukum, G. (2010). Distribution and orientation of northern-hemisphere gullies on Mars from the evaluation of HRSC and MOC-NA data. *Earth and Planetary Science Letters*, *294*(3–4), 357–367. http://doi.org/10.1016/j.epsl.2009.05.018

Komatsu, G. (2007). Rivers in the Solar System: Water Is Not the Only Fluid Flow on Planetary

Bodies. *Geography Compass*, *1*(3), 480–502. http://doi.org/10.1111/j.1749-8198.2007.00029.x

Kreslavsky, M. A., & Head, J. W. (2002). Mars: Nature and evolution of young latitude-dependent water-ice-rich mantle. *Geophysical Research Letters*, *29*(15), 14-1. http://doi.org/10.1029/2002GL015392

Kress, A. M., & Head, J. W. (2008). Ring-mold craters in lineated valley fill and lobate debris aprons on Mars: Evidence for subsurface glacial ice. *Geophysical Research Letters*, *35*(23). http://doi.org/10.1029/2008GL035501

Lanagan, P. D., McEwen, A. S., Keszthelyi, L. P., & Thordarson, T. (2001). Rootless cones on Mars indicating the presence of shallow equatorial ground ice in recent times. *Geophysical Research Letters*, *28*(12), 2365–2367.

Laskar, J., Correia, A. C. M., Gastineau, M., Joutel, F., Levrard, B., & Robutel, P. (2004). Long term evolution and chaotic diffusion of the insolation quantities of Mars. *Icarus*, *170*(2), 343–364. http://doi.org/10.1016/j.icarus.2004.04.005

Lefort, A., Russell, P. S., Thomas, N., McEwen, A. S., Dundas, C. M., & kirk, R. L. (2009). Observations of periglacial landforms in Utopia Planitia with the high resolution imaging science experiment (HiRISE). *Journal of Geophysical Research: Planets*, *114*(E4).

Levrard, B., Forget, F., Montmessin, F., & Laskar, J. (2004). Recent ice-rich deposits formed at high latitudes on Mars by sublimation of unstable equatorial ice during low obliquity. *Nature*, *431*(7012), 1072.

Levy, J. S., Head, J. W., & Marchant, D. R. (2009a). Concentric crater fill in Utopia Planitia: History and interaction between glacial "brain terrain" and periglacial mantle processes. *Icarus*, *202*(2), 462–476. http://doi.org/10.1016/j.icarus.2009.02.018

Levy, J. S., Head, J. W., & Marchant, D. R. (2009b). Concentric crater fill in Utopia Planitia: timing and transitions between glacial and periglacial processes. *Icarus*, *202*, 462–476.

Levy, J. S., Head, J. W., & Marchant, D. R. (2009c). Thermal contraction crack polygons on Mars: Classification, distribution, and climate implications from HiRISE observations. *Journal of Geophysical Research E: Planets*, *114*(1). http://doi.org/10.1029/2008JE003273

Levy, J. S., Head, J. W., Marchant, D. R., Dickson, J. L., & Morgan, G. A. (2009). Geologically recent gully-polygon relationships on Mars: Insights from the Antarctic Dry Valleys on the

roles of permafrost, microclimates, and water sources for surface flow. *Icarus*, *201*(1), 113–126. http://doi.org/10.1016/j.icarus.2008.12.043

Lucchitta, B. K. (1981). Mars and Earth: Comparison of cold-climate features. *Icarus*, *45*(2), 264–303. http://doi.org/10.1016/0019-1035(81)90035-X

Mackay, J. R. (1978). Contemporary pingos: a discussion. *Biuletyn Peryglacjalny*, *27*, 133–154.

Mackay, J. R. (1994). Pingos and pingo ice of the western Arctic coast, Canada. *Terra*, *106*(1), 1–11.

Madeleine, J.-B., Forget, F., Head, J. W., Levrard, B., Montmessin, F., & Millour, E. (2009). Amazonian northern mid-latitude glaciation on Mars: A proposed climate scenario. *Icarus*, *203*(2), 390–405. http://doi.org/10.1016/j.icarus.2009.04.037

Malin, M. C., & Edgett, K. S. (1999). Oceans or seas in the Martian northern lowlands: High resolution imaging tests of proposed coastlines. *Geophysical Research Letters*, *26*(19), 3049–3052. http://doi.org/10.1029/1999GL002342

Malin, M. C., & Edgett, K. S. (2000). Evidence for recent groundwater seepage and surface runoff on Mars. *Science*, *288*(5475), 2330–2335. http://doi.org/10.1126/science.288.5475.2330

Mangold, N. (2005). High latitude patterned grounds on Mars: Classification, distribution and climatic control. *Icarus 174*(2), 336-359. http://doi.org/10.1016/j.icarus.2004.07.030

Marr, J. W. (1969). Cyclical change in a patterned-ground ecosystem, Thule, Greenland. In *The Periglacial Environment: Past and Present*. McGill-Queen's University Press.

Martínez, G. M., & Renno, N. O. (2013). Water and brines on mars: Current evidence and implications for MSL. *Space Science Reviews, 175*(1–4), 29-51. http://doi.org/10.1007/s11214-012-9956-3

McEwen, A. S., Banks, M. E., Baugh, N., Becker, K., Boyd, A., Bergstrom, J. W., ... & Castalia, B. (2010). The high resolution imaging science experiment (HiRISE) during MRO's primary science phase (PSP). *Icarus, 205*(1), 2-37.

McGill, G. E. (1989). Buried topography of Utopia, Mars: Persistence of a giant impact depression. *Journal of Geophysical Research*, *94*(B3), 2753–2759. http://doi.org/10.1029/JB094iB03p02753

Mellon, M. T., Arvidson, R. E., Marlow, J. J., Phillips, R. J., & Asphaug, E. (2009). Periglacial

landforms at the Phoenix landing site and the northern plains of Mars. *Journal of Geophysical Research E: Planets*, *114*(3). http://doi.org/10.1029/2007JE003039

Mellon, M. T., Feldman, W. C., & Prettyman, T. H. (2004). The presence and stability of ground ice in the southern hemisphere of Mars. *Icarus*, *169*(2), 324–340. http://doi.org/10.1016/j.icarus.2003.10.022

Mischna, M. A. (2003). On the orbital forcing of Martian water and CO2 cycles: A general circulation model study with simplified volatile schemes. *Journal of Geophysical Research*, *108*(E6). http://doi.org/10.1029/2003JE002051

Mitchel, A. (2005). The ESRI Guide to GIS analysis (Vol. 2). In *ESRI Guide to GIS analysis*. ESRI Press.

Mustard, J. F., Murchie, S. L., Pelkey, S. M., Ehlmann, B. L., Milliken, R. E., Grant, J. A., … Wolff, M. J. (2008). Hydrated silicate minerals on Mars observed by the Mars Reconnaissance Orbiter CRISM instrument. *Nature*, *454*(7202), 305–309. http://doi.org/10.1038/nature07097

Nelson, F. E., Anisimov, O. A., & Shiklomanov, N. I. (2002). Climate change and hazard zonation in the circum-arctic permafrost regions. *Natural Hazards*, *26*(3), 203–225. http://doi.org/10.1023/A:1015612918401

Noe Dobrea, E. Z., Asphaug, E., Grant, J. A., Kessler, M. A., & Mellon, M. T. (2007). Patterned ground as an alternative explanation for the formation of brain coral textures in the mid latitudes of Mars: HiRISE observations of lineated valley fill textures. In *7th International Conference on Mars* (p. #3358).

Porsild, A. E. (1938). Earth mounds in unglaciated arctic northwestern America. *Geographical Review*, *28*(1), 46–58.

Séjourné, A., Costard, F. M., Gargani, J., Soare, R. J., Fedorov, A., & Marmo, C. (2011). Scalloped depressions and small-sized polygons in western Utopia Planitia, Mars: A new formation hypothesis. *Planetary and Space Science*, *59*(5–6), 412–422. http://doi.org/10.1016/j.pss.2011.01.007

Shean, D. E. (2010). Evidence for Widespread Removal of Martian Mid-Latitude" Fill" Material. In *41st Lunar and Planetary Science Conference* (Abstract# 1509).

Shean, D. E., Alexandrov, O., Moratto, Z. M., Smith, B. E., Joughin, I. R., Porter, C., & Morin,

P. (2016). An automated, open-source pipeline for mass production of digital elevation models (DEMs) from very-high-resolution commercial stereo satellite imagery. *ISPRS Journal of Photogrammetry and Remote Sensing*, *116*, 101–117. http://doi.org/10.1016/j.isprsjprs.2016.03.012

Skinner, J. A., & Tanaka, K. L. (2007). Evidence for and implications of sedimentary diapirism and mud volcanism in the southern Utopia highland–lowland boundary plain, Mars. *Icarus*, *186*(1), 41–59.

Smith, D. E., Zuber, M. T., Frey, H. V., Garvin, J. B., Head, J. W., Muhleman, D. O., … Sun, X. (2001). Mars Orbiter Laser Altimeter: Experiment summary after the first year of global mapping of Mars. *Journal of Geophysical Research: Planets*, *106*(E10), 23689–23722. http://doi.org/10.1029/2000JE001364

Smith, M. D., Wolff, M. J., Clancy, T., Kleinböhl, A., & Murchie, S. L. (2013). Vertical distribution of dust and water ice aerosols from CRISM limb-geometry observations. *Journal of Geophysical Research E: Planets*, *118*(2), 321–334. http://doi.org/10.1002/jgre.20047

Smith, P. H. (2013). H 2 O at the Phoenix Landing Site. *Science (New York, N.Y.)*, *58*(2009), 2013. http://doi.org/10.1126/science.1172339

Soare, R. J., Burr, D. M., & Wan Bun Tseung, J.-M. (2005). Possible pingos and a periglacial landscape in northwest Utopia Planitia. *Icarus*, *174*(2), 373–382.

Soare, R. J., Conway, S. J., Pearce, G. D., Dohm, J. M., & Grindrod, P. M. (2013). Possible crater-based pingos, paleolakes and periglacial landscapes at the high latitudes of Utopia Planitia, Mars. *Icarus*, *225*(2), 971–981.

Soare, R. J., Costard, F. M., Pearce, G. D., & Séjourné, A. (2012). A re-interpretation of the recent stratigraphical history of Utopia Planitia, Mars: Implications for late-Amazonian periglacial and ice-rich terrain. *Planetary and Space Science*, *60*(1), 131–139. http://doi.org/10.1016/j.pss.2011.07.007

Soare, R. J., Horgan, B., Conway, S. J., Souness, C., & El-Maarry, M. R. (2015). Volcanic terrain and the possible periglacial formation of "excess ice" at the mid-latitudes of Utopia Planitia, Mars. *Earth and Planetary Science Letters*, *423*, 182–192.

Squyres, S. W. (1978). Martian fretted terrain: Flow of erosional debris. *Icarus*, *34*(3), 600–613.

http://doi.org/10.1016/0019-1035(78)90048-9

Squyres, S. W. (1979). The distribution of lobate debris aprons and similar flows on Mars.
Journal of Geophysical Research: Solid Earth, *84*(B14), 8087–8096.
http://doi.org/10.1029/JB084iB14p08087

Stuurman, C., Osinski, G. R., Holt, J. W., Levy, J. S., Brothers, T. C., Kerrigan, M. C., &
Campbell, B. A. (2016). SHARAD detection and characterization of subsurface water ice
deposits in Utopia Planitia, Mars. *Geophysical Research Letters*, *43*(18), 9484–9491.
http://doi.org/10.1002/2016GL070138

Rowley, T., Giardino, J. R., Granados-Aguilar, R., & Vitek, J. D. (2015). Periglacial Processes
and Landforms in the Critical Zone. In *Developments in Earth Surface Processes* (Vol. 19,
pp. 397-447). Elsevier.

Thomson, B. J., & Head, J. W. (2001). Utopia Basin, Mars: Characterization of topography and
morphology and assessment of the origin and evolution of basin internal structure. *Journal
of Geophysical Research*, *106*(E10), 23209–23230. http://doi.org/10.1029/2000JE001355

Ulrich, M., Wagner, D., Hauber, E., de Vera, J. P., & Schirrmeister, L. (2012). Habitable
periglacial landscapes in martian mid-latitudes. *Icarus*, *219*(1), 345–357.
http://doi.org/10.1016/j.icarus.2012.03.019

Washburn, A. L. (1956). Classification of patterned ground and review of suggested origins.
Geological Society of America Bulletin, 67(7), 823-866.

Werner, S. C. (2009). The global martian volcanic evolutionary history. *Icarus*, *201*(1), 44–68.
http://doi.org/10.1016/j.icarus.2008.12.019

Williams, K. E., Toon, O. B., Heldmann, J. L., McKay, C. P., & Mellon, M. T. (2008). Stability
of mid-latitude snowpacks on Mars. *Icarus*, *196*(2), 565–577.
http://doi.org/10.1016/j.icarus.2008.03.017

Chapter 3: Final Discussion, Conclusion, and Future Work

3.1 Research Summary

Investigation of an underrated landform morphology, found in Utopia Planitia, has provided yet another piece of insight to the past environment of this planet. With comparison to Earth, Utopia Planitia is widely accepted to illustrate a periglacial environment, at least at a past and/or present time. Reviews of some of the most prominent landforms (Chapter 1) within this region, believed to be genetically periglacial, and a thorough detailed landscape survey (Chapter 2), provided the stepping stone to infer the evolution of the landform morphology (Chapter 2), dubbed DRDs, and to further suggest a scenario for the late Amazonian climate history specific to Utopia Planitia (Chapter 2).

3.2 Discussion and Major Findings

DRDs, at least within the extent of our study area and with respect to the Northern Plains, are co-located with other potentially periglacial landscape features that prevalently occur in the mid-latitude bands [e.g., *Costard & Kargel*, 1995; *Kreslavsky & Head*, 2002; *Malin & Edgett*, 2000; *Seibert & Kargel*, 2001; *Squyres*, 1979]. That is, the highest frequency and the most morphologically outstanding examples are found above 40º and below 50º, while with an increase in latitude their morphology becomes degraded, muted, dwindling in numbers.

With regards to their geographic proximity to periglacial landforms, they show the most correlation to polygons. In fact, in every HiRISE image that we observed DRDs, polygonised terrain was observed as well (see Table 2.2 in Chapter 2). Interestingly, though our conclusion of DRD formation mechanism was not influenced by their geographic correlation to polygons, it further solidifies our proposal that DRDs are a type of patterned ground. Specifically, we advocate that DRDs, based on classification of morphology, are a combination of sorted circles and clastic stripes.

The factors that control DRD evolution are 1. abundance of stone vs. soil, 2. slope, 3. topographic barriers, 4. number of freeze/thaw cycles [cf. *Kessler et al.*, 2001; *Kessler & Werner*, 2003]. Labyrinth morphology represents DRDs situated in relatively flat low-lying

topography (e.g., crater floor), that arrive at their labyrinthine form through age and multiple freeze/thaw cycles, and given a balance between the concentration of stone and soil [cf. *Kessler et al.*, 2001; *Kessler & Werner*, 2003]. Alternatively, with stone concentrations greater in respect to soil, or visa versa, DRDs will evolve either into stone soil or stone islands respectively, which we have dubbed ellipse morphology [cf. *Kessler & Werner*, 2003]. With increasing slope gradient, ellipse morphologies transition to first solifluction lobes (i.e., teardrops)(see Figure 2.12b in Chapter 2), and a further increase in slope gradient results in cases of sorted stripes (see Figure 2.12c in Chapter 2) [cf. *Kessler & Werner*, 2003]. Given an increase in lateral confinement, for instance within wall terraces of impact craters, ellipse morphology can develop into sorted polygonal shapes (see Figure 2.12d in Chapter 2) [cf. *Kessler & Werner*, 2003].

In comparison to other morphologically similar features, we found DRDs to be distinct (refer to Chapter 2). Notably, in contrast to 'brain' textures [e.g., *Levy et al.*, 2009a, 2009b], we found that the vast majority of DRDs occurred outside of crater interiors, while in many cases they did not occur bound onto any type of IRFs (i.e., CCFs/LDAs/LVFs). While, admittedly, there were areas of overlap, we found that distributionally, geometrically, and orientationally, DRDs and 'brain' textures, based on what has been previously reported, do not match.

Moreover, DRDs superpose LDM, scalloped depression bearing terrain, as well as all IRFs. Stratigraphically, polygonised terrain and DRDs appear to occur co-located with one another; however, in one scenario we did observe polygonization atop of DRDs (see Figure 2.11 in Chapter 2). Regardless, based on our observations, we believe that DRDs are valuable stratigraphic markers, effectively demonstrated by our suggestion of the climate history scenario in chapter 2. Our findings agree with suggestions that Mars, specifically Utopia Planitia, has been subject to numerous freeze-thaw cycles. Based on the observed stratigraphic relationship, and our suggested climate scenario in chapter 2, we believe this landform is quite young, and is, therefore, in complement to other compelling evidence from previous studies discussed in chapter 1, indicative of the presence of a water-ice enriched terrain and a periglacial environment at a past and/or present time.
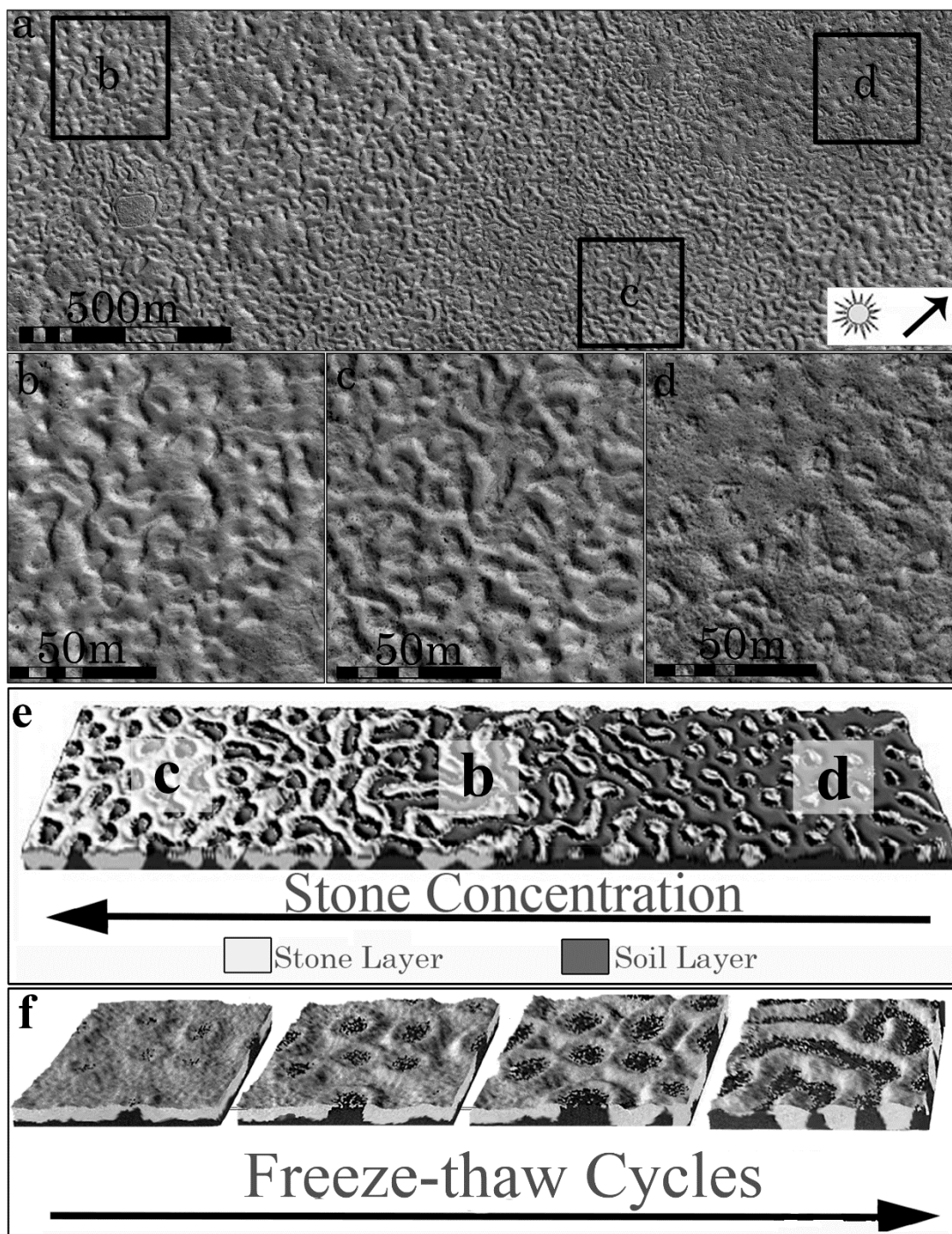
Figure 3.1: **(a)** Overview of a portion of HiRISE PSP_006882_2245 showing an example of transition between labyrinth and ellipse morphologies. **(b)** and **(c)** show changes in labyrinth morphology with concentration of stone vs. soil and transition to **(d)** ellipse morphology. **(e)** model data from Kessler & Werner [2003]. Note high stone concentration and similarity to **(c)**, balance of concentrations vs. **(b)**, and finally low stone concentration vs. **(d)**. **(f)** Diagram and data as inspired by Kessler et al. [2001] model, showing an increase in morphological complexity with cycles. *Image credit: NASA/JPL/University of Arizona.*

3.3 Final Comments and Future Research

While our review of the periglacial landscape of Mars was extensive, one of the more important premises of this research was the small extent of the study area. This was set to effectively focus our investigation, oriented on the genetic nature of DRDs. By zooming-in on our periglacial landform of interest, the large-scale (i.e., planet-wide) influences on landscape evolution, were refined to only include localized controls [cf. *French*, 2013]. This, we believe, is crucial to define accurately the responsible process(es) for the formation of an individual landform feature. However, the trade-off of a fine-scale study such as ours, is the lack of a global context. Historically, studies on periglacial environments and their associated landforms lean onto more qualitative basis to not include in-depth investigations of their correlation to paleoenvironmental conditions and climate history [*Karte*, 1983]. This is except for the broad association suggested between cold climates and periglacial environments. Still, given the spatial limitations of a study such as ours, we accommodated by streamlining our interpretation to infer a climate scenario in respect to Utopia Planitia, as opposed to suggesting one scenario for the entirety of the planet.

The identification and cataloguing of DRDs beyond our study area, specifically in the southern hemisphere, may provide additional insight into the relationship of DRDs to other periglacial features. This requires more high-resolution imagery (i.e., HiRISE stereo-pairs) suitable for DEM production and further geometric analysis. Alternatively, a study of DRDs at a larger scale, one that encompasses both the northern and southern hemispheres, would improve on our observation of geographic distribution, and the correlation between changes in latitude and the frequency and morphology of DRDs.

Earth contains an abundance of sorted circles and clastic stripes; however, locating such features in environments and under climate conditions parallel to that of Mars, is both difficult and valuable for analogous studies. To this end, we briefly introduced similar landforms found in Devon Island on Earth, though we have only scratched the surface. There is still much room for the close comparison of geometrics, distribution, and transition in morphology between DRDs on Mars and sorted circles on Devon Island, yet to be studied.
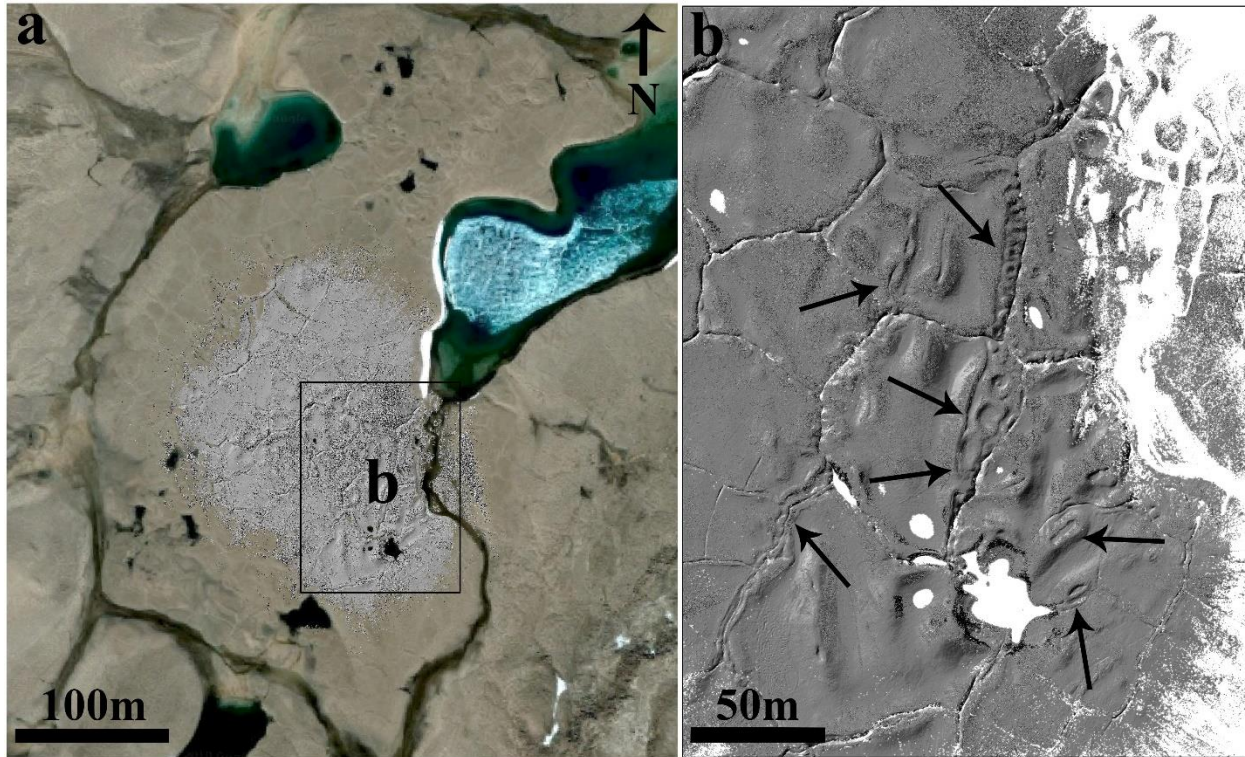
Figure 3.2: **(a)** Overview of Lake Orbiter, an area North of the Haughton impact structure, in Devon Island (Canadian Arctic Circle) with an overlay of LiDAR image obtained via means of LiDAR and Mobile Scene Modeling (mSM) [see *Hawkswell et al.*, 2018; *Osinski et al.*, 2010], specifically using a combination of Polaris LiDAR and the Kinematic Mobile LiDAR scanner (KLS) – funded by the Polar Continental Shelf and the Northern Scientific Training programs. **(b)** A zoomed-in portion of the LiDAR image, with black arrows pointing out a few of the prominent examples of sorted circles (for comparison to Mars, see Figure 2.12 in chapter 2). *Image credit: Google/FGI/Teledyne Optech.*

3.4 References

Costard, F. M., & Kargel, J. S. (1995). Outwash plains and thermokarst on Mars. *Icarus*, *114*(1), 93–112.

French, H. M. (2013). *The Periglacial Environment* (Third Ed.). Wiley. http://doi.org/10.1002/9781118684931

Hawkswell, J. E., Godin, E., Osinski, G. R., Zanetti, M., & Kukko, A. (2018). Comparative Investigation of Polygon Morphology Within the Haughton Impact Structure, Devon Island with Implications for Mars. In *49th Lunar and Planetary Science Conference* (Abstract #2899).

Karte, J. (1983). Periglacial phenomena and their significance as climatic and edaphic indicators. *GeoJournal*, *7*(4), 329–340.

Kessler, M. A., Murray, A. B., Werner, B. T., & Hallet, B. (2001). A model for sorted circles as self-organized patterns. *Journal of Geophysical Research: Solid Earth*, *106*(B7), 13287-13306. http://doi.org/10.1029/2001JB000279

Kessler, M. A., & Werner, B. T. (2003). Self-organization of sorted patterned ground. *Science*, *299*(5605), 380–383. http://doi.org/10.1126/science.1077309

Kreslavsky, M. A., & Head, J. W. (2002). Mars: Nature and evolution of young latitude-dependent water-ice-rich mantle. *Geophysical Research Letters*, *29*(15), 14-1-14–4. http://doi.org/10.1029/2002GL015392

Levy, J. S., Head, J. W., & Marchant, D. R. (2009a). Concentric crater fill in Utopia Planitia: History and interaction between glacial "brain terrain" and periglacial mantle processes. *Icarus*, *202*(2), 462–476. http://doi.org/10.1016/j.icarus.2009.02.018

Levy, J. S., Head, J. W., & Marchant, D. R. (2009b). Concentric crater fill in Utopia Planitia: timing and transitions between glacial and periglacial processes. *Icarus*, *202*, 462–476.

Malin, M. C., & Edgett, K. S. (2000). Evidence for recent groundwater seepage and surface runoff on Mars. *Science*, *288*(5475), 2330–2335. http://doi.org/10.1126/science.288.5475.2330

Osinski, G. R., Barfoot, T. D., Ghafoor, N., Izawa, M., Banerjee, N., Jasiobedzki, P., … Sapers, H. (2010). Lidar and the mobile Scene Modeler (mSM) as scientific tools for planetary exploration. *Planetary and Space Science*, *58*(4), 691–700.

Seibert, N. M., & Kargel, J. S. (2001). Small-scale Martian polygonal terrain: Implications for liquid surface water. *Geophysical Research Letters*, *28*(5), 899–902.

Squyres, S. W. (1979). The distribution of lobate debris aprons and similar flows on Mars. *Journal of Geophysical Research: Solid Earth*, *84*(B14), 8087–8096. http://doi.org/10.1029/JB084iB14p08087

Curriculum Vitae

Name:	Arya Bina

Post-secondary Education and Degrees:	McMaster University Hamilton, ON, Canada 2011-2016 H. B.Sc. Earth & Environmental Science – Minors in Economics & GIS University of Western Ontario London, ON, Canada 2016-2018 M.Sc. Geology & Planetary Science

Honours and Awards:	LPI Career Development Award 2017 University of Western Ontario Graduate Research Scholarship 2016 – 2018 The McMaster Honour Award 2011 – 2016

Related Work Experience:	Research Assistant Department of Earth Science University of Western Ontario 2016-2018 Teaching Assistant Department of Earth Science University of Western Ontario 2016-2018 Visible-Infrared (VISIR) Team Lead CanMars Analogue Mission University of Western Ontario 2016 Co-CIPP HiRISE Mission Operation Western University of Ontario 2016 Research Intern Department of Earth Science McMaster University 2015

Publications:

Osinski, G. R., Battler, M., Caudill, C. M., Francis, R., Haltigin, T., Hipkin, V. J., Kerrigan, M., Pilles,E. A., Pontefract, A., Tornabene, L. L., Allard, P., Bakambu, J. N., Balachandran, K., Beaty, D. W., Bednar, D., **Bina, A.**, ... and Zylberman, W. (2018). The CanMars Mars Sample Return analogue mission. *Planetary and Space Science*.

Soare, R. J., Conway, S. J., Godin, E., Hawkswell, J., Osinski, G. R., and **Bina, A**. (2018). Possible Ice-Wedge Polygonisation in Utopia Planitia, Mars, and Its Poleward Latitudinal-Gradient. In *49th Lunar and Planetary Science Conference* (Abstract# 1084).

Soare, R. J., Conway, S. J., Godin, E., Osinski, G., Hawkswell, J., and **Bina, A.** (2017). Low-Centred Polygons and Alas-Like Basins as Geological Markers of Warming Trends Late in Mars' History. In *AGU Fall Meeting Abstracts* (Abstract #P41C-2844).

Bina, A., Tornabene, L. L., Piatek, J. L., Barlow, N. G., Osinski, G. R., Robbins, S. J., and Watters, W. A. (2017). Visible and Thermophysical Mapping of Craters with Transitional Morphologies: Insights into the Nature and Extent of Crater Degradation on Mars. In *48th Lunar and Planetary Science Conference* (Abstract# 2856).

Bina, A., Cao, F., Li, Y., Poitras, J. T., Tornabene, L. L., Caudill, C. M., and Osinski, G. R. (2017). 2016 CanMars MSR Analogue Mission: Visible/Near-Infrared Spectral and Mineralogical Results based on a "Stand-In" Spectrometer for the Mars 2020 SuperCam-VIS-IR. In *48th Lunar and Planetary Science Conference* (Abstract# 1654).

Osinski, G. R., Battler, M., Caudill, C., Pilles, E., Allard, P., Balachandran, K., Beaty, D., Bednar, D., **Bina, A.**, … and Xie, T. (2017). Overview of the 2016 CanMars Mars Sample Return Analogue Mission. In *48th Lunar and Planetary Science Conference* (Abstract# 2417).

Piatek, J. L., Murphy, I., Tornabene, L. L., **Bina, A.**, Barlow, N. G., Osinski, G. R., and Robbins, S. J. (2017). Thermophysical characteristics of well-preserved Martian craters near the transition diameter. In *48th Lunar and Planetary Science Conference* (Abstract# 2752).